

Copyright
by
Mridula Rani
2009

**The Dissertation Committee for Mridula Rani Certifies that this is the approved
version of the following dissertation:**

Engineering Anti-Infective Antibodies

Committee:

Brent L. Iverson, Supervisor

George Georgiou, Co-Supervisor

Katherine A. Brown

Jennifer A. Maynard

Pengyu Ren

Engineering Anti-Infective Antibodies

BY

Mridula Rani, B.Sc.; M.Sc.

Dissertation

Presented to the Faculty of the Graduate School of

The University of Texas at Austin

in Partial Fulfillment

of the Requirements

for the Degree of

Doctor of Philosophy

The University of Texas at Austin

December, 2009

DEDICATION

To my mom,
&
my brothers, Manish and Tusha,
for their never ending love and support.

Engineering Anti-Infective Antibodies

Publication No. _____

Mridula Rani, Ph.D.

The University of Texas at Austin, 2009

Supervisor: Brent L. Iverson

Co-supervisor: George Georgiou

In the past 15-20 years, advances in antibody engineering have facilitated the generation and isolation of monoclonal antibodies (mAbs) to a wide array of antigens. Consequently, mAbs have become essential therapeutic tools and currently dominate the global protein therapeutics market. The engineering of anti-infective antibodies, however, has proven quite a challenge, despite the fact that antibodies were naturally evolved to fight infections. The identification of suitable antigens, the mode of administration and the high cost associated with the production of antibody therapeutics are some of the major hurdles for the progress of anti-infective antibodies. This dissertation addresses issues concerning the development of anti-infective antibodies against two different pathogens: SARS coronavirus (CoV) and two pathogenic species of Burkholderia bacteria.

To investigate the role of affinity in viral neutralization and evolution of escape mutants, we first sought to isolate an antibody with high affinity towards the receptor binding domain (RBD) of SARS-CoV. Following high-throughput screening of a library of random mutants via the APEX display system, we isolated antibodies with affinities in the range of 0.8 nM - 0.1 nM. The affinity was further improved by additional mutagenesis and DNA shuffling, and a high affinity variant (45pM) with ~300-fold improvement over the parental antibody was isolated. Evaluation of these antibodies in an *in vitro* assay demonstrated that neutralization of wild-type Urbani strain of SARS-CoV correlates well with the affinity of the antibody, with higher affinity leading to greater neutralization. Moreover, the antibody exhibiting the highest affinity could neutralize SARS-CoV escape mutants that evaded neutralization by both parental and lower affinity antibodies.

Another important aspect for the development of anti-infective antibodies concerns the identification of suitable antigen targets to be used in the isolation of antibodies. In an effort to develop a high-throughput screening method for the isolation of antibodies to a wide array of antigens, we used a synthetic antibody (Fab) library constructed by a minimalist approach and displayed on the surface of filamentous bacteriophage. The library was screened against antigens from *Burkholderia pseudomallei* and *Burkholderia mallei*. After only three rounds of selection and enrichment against five different antigens, we obtained Fabs specific to four of the antigens as confirmed by ELISA. These results not only demonstrate the use of a synthetic antibody library for the isolation of antibodies against infectious pathogens, but

also its feasibility, and potential applicability as a high-throughput screen for a variety of antigens.

TABLE OF CONTENTS

| | |
|--|-----|
| List of Tables | xi |
| List of Figures | xii |
| CHAPTER 1: Antibody Engineering..... | 1 |
| Introduction:..... | 1 |
| Antibody structure: | 4 |
| Antigen recognition: | 5 |
| Effector functions of antibodies:..... | 6 |
| Antibody engineering: | 8 |
| Antibody cloning: | 8 |
| Immunogenicity:..... | 10 |
| Antibody Libraries:..... | 11 |
| Library screening technologies:..... | 13 |
| Phage display: | 14 |
| Cell display: | 16 |
| a. Bacterial display..... | 17 |
| b. Yeast display..... | 18 |
| <i>In vitro</i> display technologies:..... | 19 |
| a. Ribosome display:..... | 19 |
| b. mRNA display: | 20 |
| c. Covalent / non-covalent DNA display:..... | 21 |
| d. Antibody arrays:..... | 22 |
| Affinity maturation: | 22 |
| Engineering valency , bispecificity and bifunctionality: | 24 |
| Fc engineering:..... | 25 |
| Production of Recombinant antibodies..... | 26 |
| Antibodies and infectious disease..... | 27 |

| | |
|--|----|
| CHAPTER 2: The Relationship Between Antibody Affinity Against Spike Protein Of SARS-CoV And Viral Neutralization..... | 32 |
| Introduction:..... | 32 |
| Materials And Methods: | 39 |
| Bacterial Strains and Plasmids:..... | 39 |
| Viruses and Cells: | 40 |
| Construction of ScFv Library: | 40 |
| Cloning, Expression and purification of Receptor Binding Domain:.. | 41 |
| Screening and Selection of high affinity ScFv variants by APEX: | 42 |
| Shuffling and random mutagenesis of isolated clones for additional screening: | 44 |
| Expression and purification of single chain antibody fragments (scAbs): | 45 |
| BIAcore analysis for affinity measurement: | 47 |
| Isolation of Escape Mutants:..... | 47 |
| Plaque Reduction Neutralization Assay (PRNT):..... | 49 |
| Results:..... | 49 |
| Expression and purification of the RBD portion of the SARS-CoV S glycoprotein: | 49 |
| Random mutagenesis and affinity maturation of the 80R scFv:..... | 50 |
| Neutralization assay and generation of escape mutants:..... | 61 |
| Discussion:..... | 66 |
| Summary | 69 |
| CHAPTER 3: Isolation Of Antibodies Against <i>Burkholderia mallei</i> And <i>Burkholderia pseudomallei</i> From A Synthetic Antibody Library | 70 |
| Introduction:..... | 70 |
| Materials and Methods:..... | 77 |
| Bacterial strains and antigens: | 77 |
| Synthetic antibody library:..... | 78 |
| Phage Library amplification: | 80 |
| Phage panning using immunotubes: | 81 |
| Phage panning using magnetic beads: | 82 |

| | |
|---|-----|
| Phage ELISA: | 83 |
| Results:..... | 85 |
| Isolation of <i>B. mallei</i> and <i>B. pseudomallei</i> specific antibodies: | 85 |
| Discussion:..... | 92 |
| APPENDIX 1: High-level Periplasmic Expression And Production Of An Antibody Fragment (scAb) Against Anthrax Toxin In <i>Escherichia coli</i> by High Cell Density Fermentation..... | 94 |
| Introduction:..... | 94 |
| Materials and Methods:..... | 96 |
| Bacterial strains and plasmids:..... | 96 |
| Shake flask cultivation..... | 97 |
| High cell density cultivation: | 98 |
| Purification of scAb | 99 |
| Analysis by SDS-PAGE: | 100 |
| ELISAs:..... | 100 |
| Results:..... | 101 |
| Selection of host strain for ScAb expression: | 101 |
| High Cell Density Cultivation with different induction times:..... | 103 |
| Purification and activity assay: | 106 |
| Discussion:..... | 107 |
| References..... | 110 |
| Vita | 129 |

LIST OF TABLES

| | |
|---|-----|
| Table 1.1: FDA approved monoclonal antibodies | 3 |
| Table 1.2: List of anti-infective antibodies in development. | 30 |
| Table 2.1: Rate constants and equilibrium dissociation values for the antibodies isolated from the library as measured by SPR . Standard deviations for the fit as measured by the software are provided..... | 58 |
| Table 2.2: Amino acid differences in the RBD region of the spike protein in different strains of SARS-COV | 62 |
| Table 2.3: Amino acid changes in the RBD of spike protein found in the neutralization escape mutants generated by scAbs..... | 64 |
| Table 3.1: List of antigen targets used for panning experiments..... | 78 |
| Table 3.2: Phage titers from panning experiments using immunotubes..... | 87 |
| Table 3.3: Phage titers from panning experiments using streptavidin beads..... | 89 |
| Table 3.4: CDR sequences of the clones isolated from the library in comparison with the template used for library construction. | 91 |
| Table A 1: List of bacterial strains used in this study..... | 97 |
| Table A.2: Summary of four HCDCs | 104 |

LIST OF FIGURES

| | |
|--|----|
| Figure 1.1: a. Crystal structure of an antibody | 5 |
| Figure 1.2: Effector functions mediated by antibody Fc | 7 |
| Figure 1.3: Schematic representation of different antibody formats | 10 |
| Figure 1.4: Schematic representation of selection and screening of antibodies from the libraries | 14 |
| Figure 1.5: Representation of monovalent display of single chain Fv (scFv) displayed on pIII of M13 phage | 15 |
| Figure 1.6: Representation of cell surface display of single chain Fv (scFv) | 17 |
| Figure 1.7: Representation of ribosome display of single chain Fv (scFv) | 20 |
| Figure 1.8: Representation of mRNA display of single chain Fv (scFv) | 20 |
| Figure 1.9: Representation of DNA display of single chain Fv (scFv) | 21 |
| Figure 2.1: The lifecycle of SARS-COV | 33 |
| Figure 2.2: a- Schematic of the S protein | 34 |
| Figure 2.3: Schematic representation of cross-species transmission of SARS-CoV | 35 |
| Figure 2.4: A- ELISA results for baculovirus purified RBD | 50 |
| Figure 2.5: Comparison of FC histograms | 51 |
| Figure 2.6: BIAcore analysis of scAbs in cell lysates | 52 |
| Figure 2.7: Sequence alignments of clones RS2, RS10, B9 and G5 with 80R | 55 |
| Figure 2.8: Comparison of FC histograms | 56 |
| Figure 2.9: BIAcore analysis | 57 |
| Figure 2.10: Sequence comparison of the high affinity clones RS2, SK4, and RSK with parental 80R clone | 59 |
| Figure 2.11: Interface of structure of the RBD-80R complex | 60 |
| Figure 2.12: Neutralization activity of the four scAbs tested by plaque reduction assay against icUrbani strain | 61 |
| Figure 2.13: Cross neutralization studies of the four scAbs with escape mutants. A. Escape mutant with D480A mutation, B. Escape mutant with D480Y mutation | 65 |
| Figure 3.1: Intracellular lifestyle of B.pseudomallei | 73 |

| | |
|---|-----|
| Figure 3.2: Design of the synthetic antibody library. | 79 |
| Figure 3.3: Purified antigens run on a 4-20% SDS-PAGE | 85 |
| Figure 3.4: Monoclonal phage ELISA | 87 |
| Figure 3.5: Sandwich ELISA for BimA clones | 88 |
| Figure 3.6: Monoclonal phage ELISA | 90 |
| Figure 3.7: Sandwich ELISA for BPSL 2748 clones | 90 |
| Figure 3.8: Monoclonal phage ELISA for two clones from BopE (E2 & G3) and one BipD clone (B3) exhibiting ELISA signal over control GST protein. | 91 |
| Figure A.1: Expression of M18 scAb in E. coli | 102 |
| Figure A.2: Time profiles for cell density (●) and cell specific production yield (mg/L/OD) of M18 scAb (○) during HCDC with induction at four different cell densities: | 105 |
| Figure A.3: SDS-PAGE analysis of samples from each purification step. | 106 |
| Figure A.4: Analysis of solubility and activity of M18 scAb purified from HCDC. | 107 |

CHAPTER 1

ANTIBODY ENGINEERING

INTRODUCTION:

The human immune system plays a crucial role in protecting the human body against infectious diseases. The human body faces a constant onslaught of pathogens from the environment, and as a primary physical barrier, the skin and mucosal membranes prevent the entry of these microbial pathogens into our body. When pathogens cross these formidable barriers, the immune system is activated. The immune system is made up of a complex network of cells, tissues and organs that help the body fight infections by identifying and destroying pathogens. The immune system responds in 2 ways: a nonspecific innate immune response and a specific adaptive immune response.

As a first line of defense, the innate immune responses provide a rapid and non-specific response to microbial challenges. Pathogens are recognized by innate immune cells including macrophages and neutrophils, which help in controlling common infections. However, the innate immune response has a key limitation in that, by itself, it cannot eliminate pathogens once an infection has been established. It is the adaptive immunity activated by the innate immune system that provides a more versatile means of defense against such pathogens. Adaptive immunity also protects against re-infection through immunological memory. The adaptive immune response is highly specific and responds with great precision against specific antigens. The adaptive immune response is

further divided into humoral immunity (B-cell response) and cell mediated immunity (T-cell response)(24, 124).

Antibodies are the key elements of the adaptive immune system, and play a critical role in defense against a wide array of antigens presented by invading microbial pathogens. Being part of humoral immunity, they provide protection through the binding of pathogens (neutralization), promoting phagocytosis by opsonization, and by activation of complement. These elaborate defense mechanisms do fail against certain pathogens, leading to some well-known pandemics (24, 107).

The significance of antibodies in controlling infections has been known for over a century, when serum therapy was used to treat infectious diseases. Serum therapy lost favor with time due to adverse reactions associated with it and the easy access to antibiotics. The development of the hybridoma technology revolutionized antibody therapy by providing an efficient means to generate monoclonal antibodies. With the greater understanding of the structure and function of antibodies, along with the major developments in recombinant DNA technology and protein engineering, it is now possible to modify and fine tune the properties of antibodies for specific applications(23).

Currently, antibodies are a rapidly growing class of biomolecular therapeutics second only to vaccines, with 23 FDA approved antibodies in the market (Table 1.1). About 200 different antibody based therapeutics are in the clinical trials targeting about 70 different molecules (33). In 2008, total sales of antibodies reached nearly \$32 B and has grown rapidly to represent over 30% of the global biologic drug market (171) and is estimated to surpass 50% by 2010. The major driving force for antibody therapeutics in

the future will be improvement in the properties of existing antibodies, identification of novel antibodies, novel targets, and use of novel scaffolds.

This chapter presents an overview of the structure and functions of antibodies, and will give an outline of the current and developing technologies in the antibody engineering field.

| Antibody | Antibody Format | Kd (nM) | Approved Treatment | Year |
|-----------------------|--------------------------|----------------|-------------------------------|-------------|
| Muromonab | Mouse IgG2a | 0.83 | Transplant rejection | 1986 |
| Abciximab | Chimeric Fab | 5 | cardiovascular | 1994 |
| Rituximab | Chimeric IgG1 | 8 | Non Hodgkin's Lymphoma | 1997 |
| Daclizumab | Humanized IgG1 | 0.3 | Transplant rejection | 1997 |
| Basiliximab | Chimeric igG1 | 0.1 | Transplant rejection | 1998 |
| Palivizumab | Humanized IgG1 | 0.96 | RSV infection | 1998 |
| Infliximab | Chimeric IgG1 | 0.22 | Inflammatory disease | 1998 |
| Trastuzumab | Humanized IgG1 | 5 | Breast cancer | 1998 |
| Gemtuzumab ozogamicin | Humanized IgG4, labeled | 0.08 | Acute myelogenous leukaemia | 2000 |
| Alemtuzumab | Humanized IgG1 | 10-32 | Chronic lymphocytic leukaemia | 2001 |
| Ibritumomab tiuxetan | Mouse IgG1, 90Y labeled | 14-18 | Non Hodgkin's Lymphoma | 2002 |
| Adalimumab | Human IgG1 | 0.15 | Inflammatory disease | 2002 |
| Tositumomab I131 | Mouse IgG2a I131 labeled | 1.4 | Non Hodgkin's Lymphoma | 2003 |
| Omalizumab | Humanized IgG1 | 0.17 | Allergy related asthma | 2003 |
| Efalizumab | Humanized IgG1 | 3 | Psoriasis | 2003 |
| Cetuximab | Chimeric IgG1 | 0.2 | Colorectal cancer | 2004 |
| Bevacizumab | Humanized IgG1 | 1.1 | Colorectal cancer | 2004 |
| Natalizumab | Humanized IgG4 | 0.3 | Multiple sclerosis | 2006 |
| Panitumumab | Human IgG2 | 0.05 | Colorectal cancer | 2006 |
| Ranibizumab | Humanized IgG1 Fab | 0.14 | Macular degeneration | 2006 |
| Eculizumab | Humanized IgG2/4 | 0.12 | Inflammatory diseases | 2007 |
| Certolizumab Pegol | Humanized fab | 0.089 | Crohn's disease | 2008 |
| Golimumab | Human IgG1 | 0.017 | Rheumatoid arthritis | 2009 |

Table 1.1: FDA approved monoclonal antibodies (Current as of May 2009)(133)

Antibody structure:

Antibodies are antigen-recognition gamma globulin proteins (immunoglobulins) secreted by plasma B cells (differentiated B cells) that are employed by the immune system to recognize and neutralize pathogens. The antibody molecule is made up of four polypeptide chains - two identical H-heavy (50kDa) and two identical L-light chains (25kDa), with heavy (H) and light (L) chain being covalently linked through disulfide bonds. The immunoglobulins are differentiated into five classes, defined by the structure of the heavy chain. They are IgM, IgD, IgG, IgA and IgE, and their heavy chains are denoted as μ , δ , γ , α & ϵ respectively. IgG is the most abundant immunoglobulin isotype in the plasma. The major differences among these classes are in the hinge and Fc (Fragment crystallizable) regions, which lead to differences in their effector function and in the polymerization state. There are only two types of light chains- kappa (κ) and lambda (λ), and there is no known functional difference between the two (24).

The antibody molecule is divided into two functional regions, the antigen binding region and the Fc region. The antigen binding region varies widely between antibody molecules and is composed of the variable domain (V domain), and constant domain (C domain). The actual antigen binding site is formed by the amino terminal V domain of both the heavy and light chains (VH and VL). The fully folded antibody molecule is comprised of three globular domains linked by a flexible polypeptide chain known as the hinge region to form a Y shaped structure. Papain cleaves the immunoglobulin into two identical antigen binding fragments (Fab – 50KDa) and a crystallizable fragment (Fc- 50KDa). Each domain has the characteristic immunoglobulin fold consisting of two anti-parallel sheets with intra-molecular disulfide bonds. Disulfide bonds are an important

component of IgG structure, in that intra-chain disulphide bonds stabilize each domain, and interchain disulfide bonds reinforce association of H and L chains (antigen binding region) as well as H chains (Fc region) (136) (Fig 1.1).

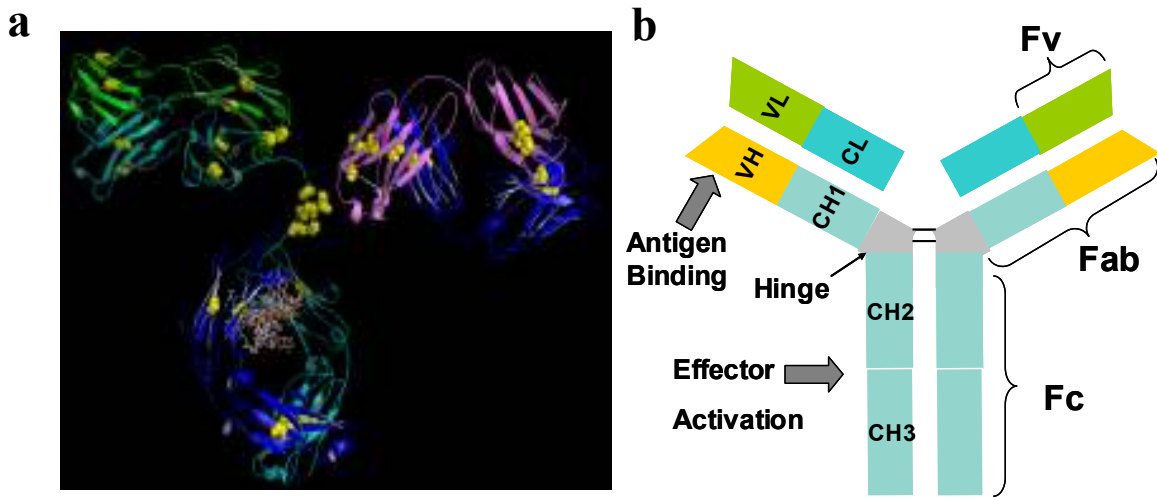


Figure 1.1: a. Crystal structure of an antibody - light chains are in green and pink, heavy chains in light blue and dark blue, disulfide bonds in yellow space fill and carbohydrates in white wireframe.

b. Schematic representation of an antibody

Antigen recognition:

The recognition of antigen is mediated by the contributions of both heavy (VH) and light (VL) chains. Each variable region has three sections of high amino acid sequence divergence or variability, termed hypervariable regions, which are separated by conserved framework regions (FR). The areas of the antibody binding site that contact the antigen as determined by crystallographic studies are referred to as complementary determining regions (CDRs) and the CDRs correspond to the hypervariable regions mentioned above. Crystallography also revealed that FR domains fold into relatively rigid

β strands, with the six CDRs forming loops at the ends of these strands to create the antigen binding site.

Antibody binding depends on the size and shape of the antigen. Smaller antigens such as haptens, small peptides or carbohydrates generally bind in a groove formed at the interface of the heavy and light chain CDR's. Larger protein molecules generally involve larger contact surface areas, which sometime extend into the frameworks. (24).

The antibody recognition site on the antigen is known as the antigenic determinant or epitope. These sites are often discontinuous, meaning the antibody binds to residues that are adjacent to each other on the protein surface, yet are not next to each other in primary sequence (169). The interaction between an antigen and antibody is reversible, being held together through non-covalent interactions including electrostatic forces, van der Waals forces, hydrophobic forces, and hydrogen bonds.

Effector functions of antibodies:

One of the most simple and direct ways antibodies provide immunological protection is through binding to receptor sites on pathogens or released toxins, thereby blocking pathogenic activity. This process is referred to as neutralization. However, neutralization alone does not always provide complete protection as it can fail to hinder pathogen replication. In addition to neutralization, antibodies also contribute to immunity via a process referred to as opsonization as well as through the activation of the complement system, both of which rely on Fc region of the antibody. To combat pathogens that replicate outside cells, antibodies coat the pathogen and stimulate effector functions against the pathogen via cells that recognize antibody Fc regions. This coating

of pathogens by antibodies and the resulting attack by the immune system is known as opsonization. The cells with Fc receptors that recognize these coated pathogens lead the destruction of the pathogen through phagocytosis or release of cytotoxins (Fig 1.2)(107).

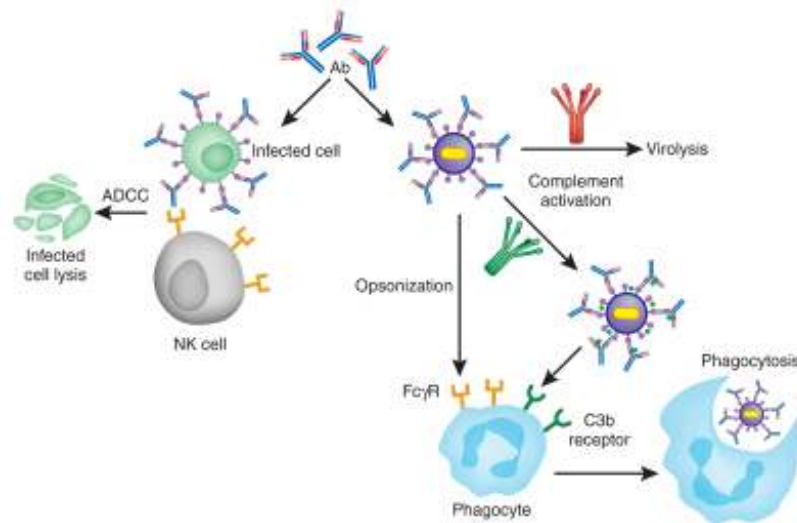


Figure 1.2: Effector functions mediated by antibody Fc. Adapted with permission from Nature Biotechnology (107)

The complement system is a biochemical cascade of more than 20 different proteins that “complements” the function of antibody. The activated complement components can either directly kill bacteria by forming pores in the cell wall, or through opsonization. Since the Fc receptors are isotype-specific, the immune system has greater flexibility to invoke appropriate immune mechanisms for distinct pathogens (107).

ANTIBODY ENGINEERING:

Antibody therapy began a century ago with the discovery that serum from immunized animals can be effective against the disease caused by the same agent in humans. The discovery and development of serum therapy for Diphtheria brought the first Nobel Prize in Medicine to Von Behring in 1901. However, with the intensified competition from widely available antibiotics, serum therapy was abandoned due to problems related to the toxicity and high incidence of allergic reactions. One of the major breakthroughs in the field was the development of the hybridoma technology in 1975, which provided the means to generate large amounts of monoclonal antibodies (23). Moreover, with the advent of recombinant DNA technology, it has been possible to engineer the size, immunogenicity, binding affinity, specificity, pharmacokinetics and effector functions of antibodies (160). Because of antibody engineering, antibody based therapeutics currently enjoy remarkable commercial success. It appears that Paul Ehrlich's concept of "magic bullets" has largely been realized, though it took more than 100 yrs to attain the goal. This introduction provides an update of the field along with the latest technologies that has been radically transforming the field in the last two decades.

Antibody cloning:

The hybridoma technology which was developed in 1975 and relies on the production of antibodies from cell lines formed by the fusion of B-cells from an immunized animal with myeloma cells, still remains as one of the core technologies and established the field of antibody engineering. In the late 1980s, with the help of the recombinant DNA technology, cloning and expression of antibodies in different model

systems became possible with polymerase chain reaction (PCR) simplifying the process of cloning antibody genes. Diverse expression systems including bacteria, yeast, filamentous fungi, insect, plant, or mammalian cells and transgenic animals have been used for the expression of recombinant antibodies. Choice of expression systems usually depends on the form of antibody expressed, but in many cases several different expression systems can be used. Eukaryotic systems are preferred for the expression of full length IgGs since they have the cellular machinery for efficient folding and assembly and also allow glycosylation, which is important for therapeutic purposes(17). Antibody fragments have a simpler structure and do not require glycosylation hence they can be efficiently expressed in bacterial systems.

Antibodies are cloned from mRNA isolated from hybridoma cells, spleen or lymph cells, which are reverse transcribed into DNA and then the antibody genes are amplified by PCR. To amplify the variable domain genes by PCR, degenerate primers are used, comprised of a 3' set complementary to the constant region sequences and a 5' set that are complementary to variable region sequences. Most commonly used primers are based on framework region amino acid sequences from Kabat and V-base databases. IgG is the most abundant immunoglobulin in blood as well as the most commonly used form for antibody therapeutics(24). Heterologous expression in *E. coli* has made it possible to construct a wide variety of functional antibody fragments such as the antigen binding domain (Fab), single-chain Fv (scFv) comprised of the antigen binding site VH & VL joined by flexible linker, single domain antibodies (dAb), the smallest functional binding unit corresponding to either VH or VL alone, and engineering of multivalent

oligomers like diabodies, triabodies or tetrabodies to enhance the functional affinity through avidity (90) (Fig 1.3).

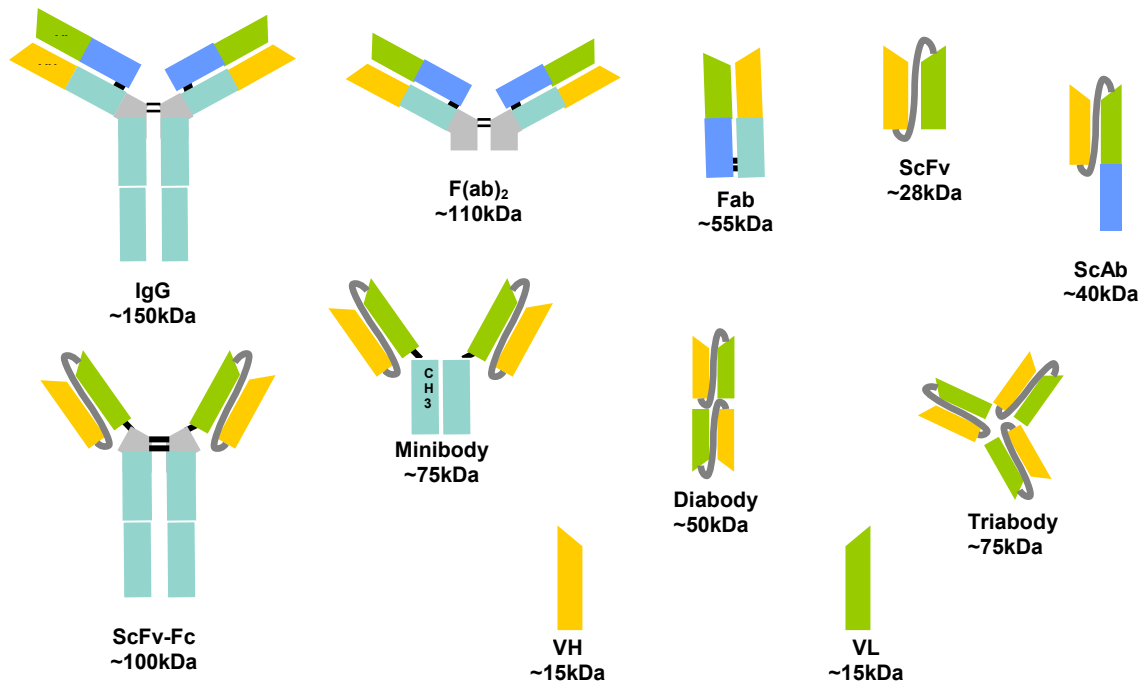


Figure 1.3: Schematic representation of different antibody formats.

Immunogenicity:

In order to be therapeutically effective, antibodies must exhibit high specificity and affinity with minimal immunogenicity. In general, murine mAbs cannot be used as therapeutic agents because of their immunogenicity in humans. Antibody engineering has been used successfully to overcome immunogenicity through a process known as humanization. The most common strategy of humanization is CDR grafting, where

murine CDRs are grafted into human framework scaffold (137). Unfortunately, this method usually lowers the affinity of the humanized antibody (44). In another approach known as resurfacing, only surface residues predicted to be immunogenic are replaced with the corresponding human amino acid (139). More recently, selective humanization strategies that utilize screening of libraries by phage display have been reported (80).

Other than primary amino acid sequence, the presence of misfolded antibody molecules, contaminants, heterogeneity of antibody pool (glycosylation, deamidation), and presence of T cell epitopes can contribute towards immunogenicity of a therapeutic antibody formulation. Clinical parameters like dose, route, frequency of administration, including disease and immune status of patients can also influence the immunogenicity of antibodies(22).

Antibody Libraries:

The progress in antibody engineering generated the necessity of constructing highly diverse libraries to screen for antibodies with high antigen specificity and affinity. Generally, three types of libraries are used (1); immune, naïve or synthetic. Immune libraries are obtained from either B cells of immunized animals or human immune B cells and are the best source for the isolation of high affinity antibodies. These libraries take advantage of the *in vivo* affinity maturation process in the donor and are usually comprised of $<10^8$ clones. Significant limitations of immune libraries include a lack of an immune responses to some antigens, and as well as the unsuitability of some antigens for immunizations. Naïve libraries are isolated from B-cells of non-immune animals or humans. The absence of *in vivo* affinity maturation necessitates the construction of a

large library to increase the odds of finding antibodies specific for a given antigen of interest. It is worth pointing out that the cloning process from isolated B cells involves amplifying the heavy and light chain genes independently, meaning that heavy-light chain pairing information is lost, leading to an unintentional chain shuffling during library construction. This is presumably the reason that antibodies to self-antigens have been isolated from these libraries (8, 39).

Synthetic and semi-synthetic libraries provide an alternative to the reliance on repertoires from animals or humans, and can overcome the problem of diversity and immunological tolerance. Such combinatorial libraries constructed with more than 10^{11} different antibodies of distinct antigen specificities in a small volume can be assumed as an incarnation of a test tube full of Ehrlich's "magic bullets" (97). These libraries are assembled from synthetic oligonucleotides that introduce complete or partial sequence degeneracy mainly into CDR loops, resulting in an overall diversity that bypasses natural biases and redundancies. The first generation of semi-synthetic libraries used a repertoire of VH and VL genes from human germline with synthetic CDR3 with varying CDR3 lengths (32, 120), as CDR3 plays a dominant role in antigen recognition. The second generation of libraries relied more on expression and stability of the frameworks, by using a limited set of variable domain scaffolds (4, 81, 130). One of the most comprehensive libraries yet reported, the so-called "HuCal" library, is a fully synthetic library with about 2×10^9 clones. It was constructed from seven VH and seven VL germline families that covered >95% the presumed human antibody diversity, and was optimized for expression in *E.coli* (88). In a completely different approach, Sidhu and his colleagues have used a minimalistic approach to construct a synthetic library based on the

bias of natural CDR sequences in favor of tyrosine and serine. They constructed a synthetic library with CDR diversity restricted to only four amino acids (Tyrosine, Serine, Alanine and Aspartate), and were successful in isolating high affinity antibodies against VEGF (147). They further simplified the diversity to a binary combination of tyrosine and serines resulting in a highly functional library (42) and introduced additional diversity into CDR3 to enhance the diversity and functionality of the library.

LIBRARY SCREENING TECHNOLOGIES:

Successful isolation of antibodies from large combinatorial libraries that exhibit high specificity towards an antigen of interest relies heavily on the screening technology employed. Because of the large sizes of many antibody libraries (10^6 - 10^{11}), a variety of efficient high-throughput technologies has been developed. There are three major screening methods currently in use, namely phage display, cellular display and *in vitro* display systems. Not surprisingly, it has been demonstrated that different antibodies are isolated from the same library using different screening methodologies, so choosing a suitable method to screen an antibody library is a critical consideration(66).

A common thread that links the various antibody library screening platforms is the requirement for a physical linkage between genotype (encoding DNA) and phenotype (binding activity), thereby allowing a simultaneous isolation of the genes that encode an antibody of interest based on its binding function. This not only allows the enrichment of desired antibodies via application of selection pressure, but also amplification after selection (Fig 1.4)(8).

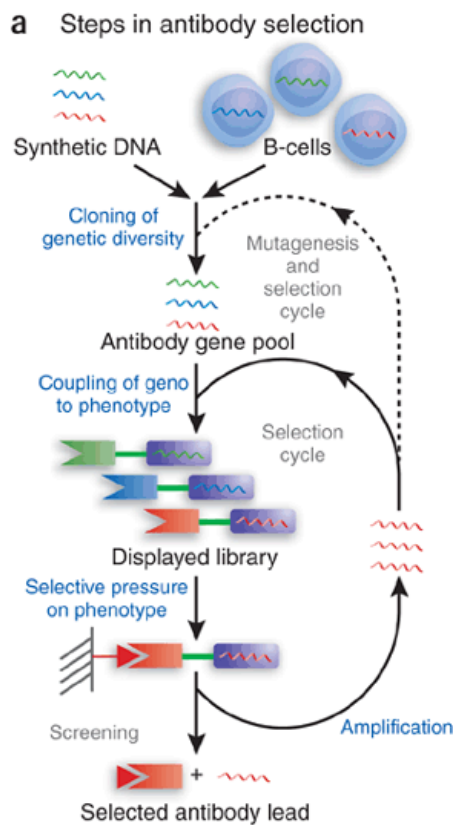


Figure 1.4: Schematic representation of selection and screening of antibodies from the libraries. Adapted with permission from Nature Biotechnology (66)

Phage display:

Antibody phage display is one of the most popular and extensively used selection platforms, and was first reported by McCafferty *et al* in 1990 (114). The display on a filamentous bacteriophage surface is achieved by the fusion of an antibody fragment to a coat protein of the phage particle, such as pIII or pVIII of M13. M13 is the most frequently used filamentous bacteriophage and the pIII coat protein is usually preferred

for display. The display of antibody fragments on a phage particle can either be monovalent or polyvalent(20). Monovalent display is achieved by cloning the antibody fragment gene in frame with the pIII gene in a phagemid vector. Phagemids are plasmid vectors that lack the genes required for packaging into virions. However, subsequent infection of bacteria carrying phagemid vectors with helper phage provides the necessary genes for replication and packaging of phagemid into virions (Fig 1.5). The wild type pIII, encoded by the helper phage, competes with the antibody-pIII fusion encoded by the phagemid, resulting in lower levels of fusion display, often monovalent (20). The advantage of monovalent display is the efficient selection of high affinity antibodies because of the absence of the avidity effect (6, 121). Polyvalent display is achieved by cloning in frame with the pIII of the phage genome, which then displays antibody on all five copies of pIII. Polyvalent display has been used for rapid selection of antibodies as in the case for target discovery (115) and in the Selectively Infective Phage (SIP) system (84, 91).

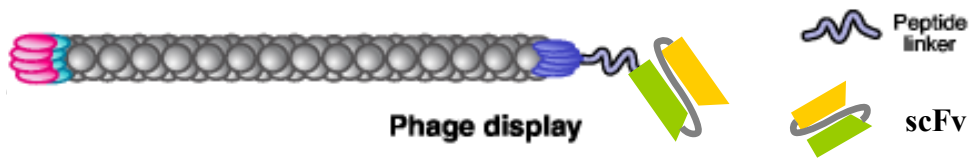


Figure 1.5: Representation of monovalent display of single chain Fv (scFv) displayed on pIII of M13 phage. Adapted from Adv.Drug.Deliv.Rev 2006 (124, 144)

Phage panning is the process of selection, enrichment and amplification used to isolate an antibody specific to a desired antigen via phage display. Antigen-specific antibodies displayed on phage are enriched by selective adsorption onto an immobilized

antigen (immunotube or magnetic bead) and the bound phage is eluted by low pH, which is then amplified through infection of *E. coli* cells (Fig 1.4). Usually 4-6 rounds of panning are necessary to isolate antibodies specific to a desired antigen.

Phage display has been used to isolate antibodies from immune, naïve and synthetic antibody libraries. It also has been successfully applied towards the isolation of antibodies with high affinities or increased resistance to chemical or thermal denaturation, and in the direct selection against whole cells.

Cell display:

Cell surface display of an antibody is a method which utilizes Fluorescence-Activated Cell Sorting (FACS) as a tool for screening the library. This approach has been successfully used to screen antibody libraries by using bacteria, yeast and mammalian cells (Fig 1.6). In this method, cells displaying an antibody library are incubated with a fluorescently-labeled antigen and sorted through flow cytometry, which measures the fluorescence intensity of an individual cell. Cells are then collected depending on their fluorescence as a direct measure of the bound fluorescent antigen. FACS also takes advantage of real-time visualization for optimization of library screening and, in addition, it utilizes multiple fluorescence parameters for specificity or cross-reactivity during screening (30). The successful screening of fluorescent cells relies on factors such as, affinity, expression level and proper folding of the antibody.

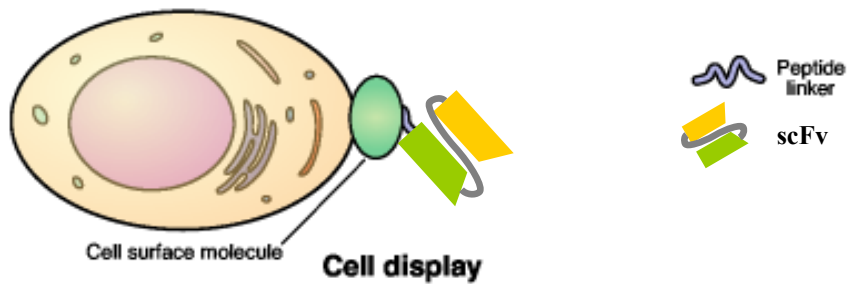


Figure 1.6: Representation of cell surface display of single chain Fv (scFv). Adapted from Adv.Drug.Deliv.Rev 2006 (144)

a. Bacterial display

Escherichia coli (*E. coli*) is one of the most well studied organisms. Its rapid growth rate and ease of genetic manipulation make it a model organism for bacterial display. However, successful display on bacterial cells depends primarily on the size and folding efficiency of the protein. The first method of bacterial display developed, employed the fusion of a scFv antibody gene to Lpp-ompA for display of antibodies on the bacterial surface. This method could enrich scFv-displaying cells from control cells by using FACS (46), and was later used successfully for affinity maturation studies (31). In an effort to combine cell display and phage display, the Lpp-ompA system was also used to capture scFv-displaying phage by antigen displayed on the cell surface(9). However, the method is limited by the size of the antigen that can be bound by the displayed antibody, because lipopolysaccharide (LPS) on the *E. coli* surface interferes with the binding of antigen.

A more versatile system with antibodies displayed on the inner membrane was developed by our group, namely Anchored Periplasmic Expression (APEX). The method utilizes a fatty acylated lipoprotein sequence – NlpA, fused to the antibody fragment to be displayed to facilitate the anchoring of the protein on the periplasmic side of the inner membrane (57). Following the disruption of the outer membrane of the cell by Tris-EDTA-lysozyme treatment, cells are labeled with fluorescently tagged antigen and screened by using FACS. Antibody genes are recovered from sorted cells via PCR and subcloned; the process is repeated until enrichment is achieved. This method has been successfully used for the affinity maturation of scFvs (57, 58) as well as to engineer scFvs that fold in the absence of disulfide bonds (143). A variation of this method the APEX-2-hybrid system, involves an antigen expressed as an epitope -tagged soluble periplasmic protein. The antigen bound to the inner membrane-anchored antibody is detected by fluorescent anti-epitope tag antibody following disruption of the outer membrane(78). This approach has also been used for the engineering of an IgG-display system(113).

b. Yeast display

Display of antibodies on the surface of *S. cerevisiae* is achieved by the fusion to the Aga2p adhesion receptor, which anchors the complex to the cell wall. Yeast cells expressing fusion proteins are then labeled with fluorescent antigens and analyzed by flow cytometry. The eukaryotic expression machinery and the presence of certain post translational modifications give yeast display an added advantage over bacterial display systems. (87). The ability of yeast to form diploids via mating of haploid yeast and to

efficiently recombine homologous DNA sequences has also been exploited to enhance the diversity of libraries (12, 161). One of the most successful applications of yeast display so far, has been in the isolation of high affinity antibodies. Moreover, one of the highest affinity antibodies (48 fM) reported so far was selected through yeast display (13). Yeast display has also been applied for screening of cDNA libraries and epitope mapping (126).

***In vitro* display technologies:**

In vitro display systems have become a valuable tool in the antibody engineering field. This system has made it possible to display libraries with a diversity of $\sim 10^{14}$. In addition, it circumvents the constraints associated with display of toxic proteins. In the last decade, *in vitro* display libraries have been used successfully used to isolate high affinity antibodies, and have become an integral part of the antibody discovery platform.

a. Ribosome display:

Ribosome display is among the first and the most widely used cell-free display systems and was first described by Mattheakis *et al* (111). The system is based on *in vitro* translation of proteins from a DNA library using cell-free expression systems. Following the translation of the antibody, the mRNA–ribosome–antibody complex formed is stabilized by low temperature and high salt concentrations, which stalls the ribosome at the end of mRNA resulting in a display of the antibody outside the ribosome (Fig 1.7).

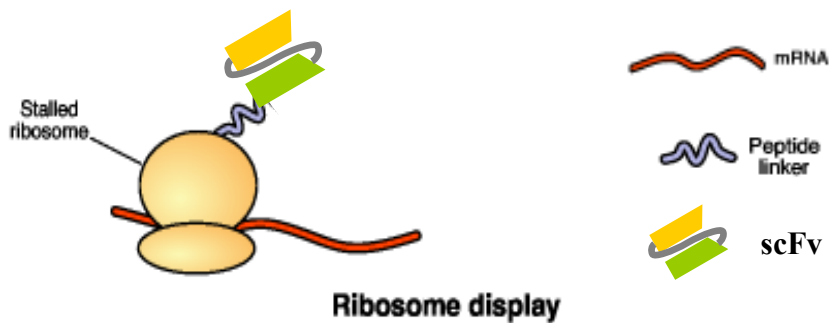


Figure 1.7: Representation of ribosome display of single chain Fv (scFv). Adapted from Adv.Drug.Deliv.Rev 2006 (144)

These mRNA-ribosome-antibody complexes are screened against an immobilized ligand in selection steps and the complexes that bind well are then reverse transcribed to cDNA and amplified by PCR (144, 181). This method has been used for successful isolation of high affinity antibodies (79) and binders from immune libraries(55).

b. mRNA display:

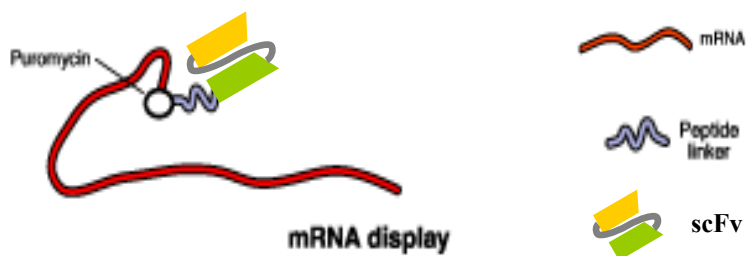


Figure 1.8: Representation of mRNA display of single chain Fv (scFv). Adapted from Adv.Drug.Deliv.Rev 2006 (144)

mRNA display is achieved by the formation of a complex between a polypeptide and its encoding mRNA generated by an *in vitro* translation via a puromycin linkage (138, 162). Puromycin is a peptidyl acceptor antibiotic and an analogue of amino acyl tRNA. It interferes with the translation through entry into the ribosomal A site, and covalently binds to the nascent peptide (Fig 1.8). The mRNA–puromycin-peptide complexes are used for selection over immobilized targets, and are reverse transcribed to cDNA before the consecutive selection process (141). It has been successfully applied for the *in vitro* evolution of single chain antibodies(48).

c. Covalent / non-covalent DNA display:

These methods exploit the *in vivo cis*-activity of replication initiation proteins to bind to its own template DNA. CIS display, described by Odegrip *et al*, uses the bacterial replication initiation protein RepA to bind to its template DNA following *in vitro* translation (122). Translated RepA interacts non-covalently with its origin of replication (Ori) due to the *cis*-element that causes ribosomes to pause during translation, leading to formation of DNA-protein complexes (Fig 1.9).

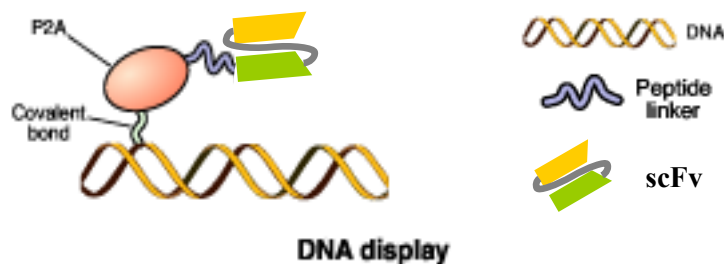


Figure 1.9: Representation of DNA display of single chain Fv (scFv). Adapted from Adv.Drug.Deliv.Rev 2006 (144)

Covalent antibody display (CAD) uses the bacteriophage endonuclease P2A because of its ability to covalently bind 5' phosphate of its own DNA. Antibody libraries fused to RepA / P2A can be used for panning on an immobilized antigen. After enrichment, DNA can be recovered by PCR and used for subsequent cycles of panning (135). DNA display not only provides a direct link between a gene and its protein, but also avoids the use of highly degradable mRNA as in other *in vitro* display technologies. In addition, the system is very well suited for scaling up and automation.

d. Antibody arrays:

Antibody array is a new approach based on immobilized antibodies on an array as a high-throughput screening method to identify interacting antigens. The arrays not only enable the detection of targets in small sample volumes but also allow the multiplexed use of antibodies for efficient screening, where antibody targets can be screened in parallel. It has been successfully applied to cancer research for identification of biomarkers and measure expression of disease related proteins(53).

Affinity maturation:

One way to enhance the therapeutic value of an existing antibody is to improve its affinity, which may allow for a reduced dosage for treatment. The two basic approaches for affinity maturation are random mutagenesis and focused mutagenesis. The selection of a mutagenesis strategy relies on the antibody, type of antigen and information available about their interaction. Random mutagenesis is the method of choice in the absence of structural information about antigen –antibody interaction. It closely mimics

the *in vivo* process of somatic hypermutation without focusing on any particular residue (103). Random mutagenesis can either be applied to an entire variable gene, or can be limited to CDRs. Mutagenesis is commonly achieved through DNA amplification by error prone PCR (19, 47). This method provides a better control over the mutation frequency, and low mutation frequency ($\leq 2\%$ nucleotide substitution per gene) is favored for affinity maturation.

In chain shuffling the light chain of an antibody is initially shuffled with a library of light chains to select for a variant with improved affinity, and then the selected antibody is diversified further by shuffling with heavy chain libraries. This method has been successfully used to improve the binding affinity by 20-200 fold (109) and has been shown to work well when the starting antibody clone displays low-affinity in the micromolar range. In *in vivo* mutagenesis, a bacterial mutant strain with an impaired mismatch repair system is used for propagation of the gene in order to generate a library of random mutants (75, 104)

Focused mutagenesis is a method, where in mutations are concentrated either on CDR residues or residues at the interface of the antigen-antibody complex. Usually either a crystal structure or a homology model of the antigen-antibody complex is used for identification of these residues. In CDR walking, randomization is focused to CDR regions(5, 182), and is accomplished either by error prone PCR or by using degenerate oligonucleotides. In another approach, CDR loops are extended to favor the contact between the antibody and antigen (93).

Finally, DNA shuffling can be used to combine the beneficial mutations of clones isolated from a selection based either on random or focused mutagenesis, since in most cases these can be additive to give rise to a better antibody.

Engineering valency , bispecificity and bifunctionality:

The use of antibody fragments such as Fabs, scFvs and single domain fragments have become an increasingly popular because of the ease with which they can be manipulated, and expressed. However, antibody fragments are monovalent and lack the functional affinity (avidity) exhibited by IgGs. Therefore, various strategies have been used to introduce bivalency or multi-valency to antibody fragments, such as crosslinking of Fabs by an introduction of cysteine in each fragment or creation of multimers by varying the linker length of a scFv(Fig 1.3)(1).

All naturally occurring antibodies are monospecific. Nevertheless, antibodies generated through engineering can be made bi-specific, by introducing two different binding specificities in a single molecule. Bi-specificity can either be towards two adjacent epitopes on a single antigen thereby improving the avidity(34), or by crosslinking two different antigens(127).

Bifunctional antibodies combine the specificity of an antibody with a biological function encoded by either a chemically linked or fused partner (1). These include; (i) Antibodies conjugated to radioisotopes such as Ibritumomab and Tositumomab (both anti CD20 mAbs), which target B-cell tumors and induce cellular damage in the target and neighboring cells. (ii) Antibodies conjugated or fused to a bacterial toxin. For example, Gemtuzumab which targets CD33 expressed in 90% cases of acute myeloid leukemia

(AML) is linked to a cytotoxic agent from the class of calicheamicins. (iii) Antibodies conjugated to a polyethylene glycol (PEG) molecule as in the case of Certolizumab pegol – a humanized tumor necrosis factor (TNF) specific Fab, which increases the serum half life and reduces the immunogenicity (26).

Fc engineering:

Engineering the Fc region (constant region) of an antibody has gained momentum in recent years, and is focused either on elimination or enhancement of the effector functions. In order to eliminate effector functions, human IgG4 (3) or human IgG1 with either specific mutations (71) or removal of Asn297 – a conserved Fc glycosylation site (131, 163) have been pursued.

To enhance the effector functions by improving the affinity of Fc to Fc receptors (FcγRs), either mutagenesis and screening or computational design approaches has been used. By screening such Fc variants Lazar *et al* (95) isolated Fc that displays 100-fold better affinity towards FcγR, and two-three fold better antibody dependent cell mediated cytotoxicity (ADCC). Mutations that result in either 100-fold enhanced ADCC by improving FcγR binding (152), or improved CDC and C1q binding (72) have also been identified. In an entirely different approach, studies have been performed to change the composition of the carbohydrate moiety of IgG, which is essential for maintaining a functional Fc structure (160). It has been shown that absence of fucose results in efficient ADCC without affecting other FcγRs interactions (145) and absence of sialic acid in a murine IgG display enhanced affinity for FcγR111 resulting in better effector function

(85). Finally, a number of Fc variants have been identified that exhibit enhanced affinity towards neonatal Fc receptors (FcRns) (170), which enhances the serum half life.

So far, Fc glycosylation has been deemed important for effector functions. However, attempts are being made to introduce effector functions to an aglycosylated antibody. For example it was shown that modifications in the aglycosylated Fc domain result in the engagement of Fc gamma receptors (142). These results offer hope that it will be possible to produce full length IgGs with enhanced effector functions in bacterial systems, thus reducing the cost of antibody therapeutics. Nevertheless, these Fc modifications might also impact the immunogenicity of the antibody.

PRODUCTION OF RECOMBINANT ANTIBODIES

Production scale of an antibody is determined by the intended application, which can range from grams per annum for diagnostics to 1,000s of kilograms per annum for therapeutics. In addition, the purity of an antibody required for therapeutics is highly stringent driving up its cost. The most challenging aspect of therapeutic antibody development in comparison to other biologics is that often high doses are required, resulting in a high cost to the patient. At present, all the monoclonal antibodies that are in the market are produced by mammalian cell culture. Thanks to recent developments, yields of antibodies in bioreactor of 5 g/l or higher are now routine (17). Advances in cell line generation, including expression vectors, transfection technologies and new cell lines have given a significant boost to the productivity of antibodies in mammalian culture.

Nonetheless, production costs are still high, leading researchers to seek out alternative expression systems such as yeasts, filamentous fungi, transgenic plants and *E. coli*.

Transgenic plants present an attractive and economical system for production of antibodies, as proteins produced in plants are regarded as safe (105). Even though plant expression systems can assemble functional full length immunoglobulins, they differ in their ability to glycosylate proteins relative to mammalian cells. Since the antibody glycans are quite heterogeneous, research is in progress to develop mutant plants with a humanized glycosylation pathway (172).

Yeast and filamentous fungi are attractive options for cost-effective large scale production of antibody fragments and antibody fusion proteins and are generally regarded safe. However, active proteases present in the yeast cells degrade antibodies, thereby reducing the yield (83).

E. coli expression systems so far have been limited to the production of antibody fragments, but research is underway in making the system more suitable for expression of full length IgG antibodies. The extensive knowledge of *E.coli* based protein expression and the ease of genetic manipulation makes it a desirable host for antibody production. Though expression levels exceeding 1-2g/L of scFv in fermentor has been observed (21), the system is limited by its unreliability and reproducibility as the expression may vary from batch to batch, and difficulty in producing functional antibodies.

ANTIBODIES AND INFECTIOUS DISEASE

High specificity and recruitment of the immune system make antibodies excellent candidates to treat infectious diseases. However, of the 23 mAbs approved by the FDA

only one is an anti-infective (the anti-RSV antibody) (Table 1.1). The slow pace of the progress of antibody therapeutics towards infectious disease is due to the high cost and the necessity for early and precise diagnosis of the pathogen. With the emergence of novel viruses, antibiotic resistant micro-organisms, threat of bioterrorism, and fear of rapid spread of infection as a result of globalization interest in anti-infective antibody therapy has increased. (134).

Anti-viral antibodies have so far been clinically more successful in comparison to antibodies against other infectious diseases. Such antibodies can prevent infection through a variety of mechanisms. Antibodies can inhibit infection either by blocking various steps that virus takes to enter the cell, or by interfering with the internalization or release of virions (Fig1.10).

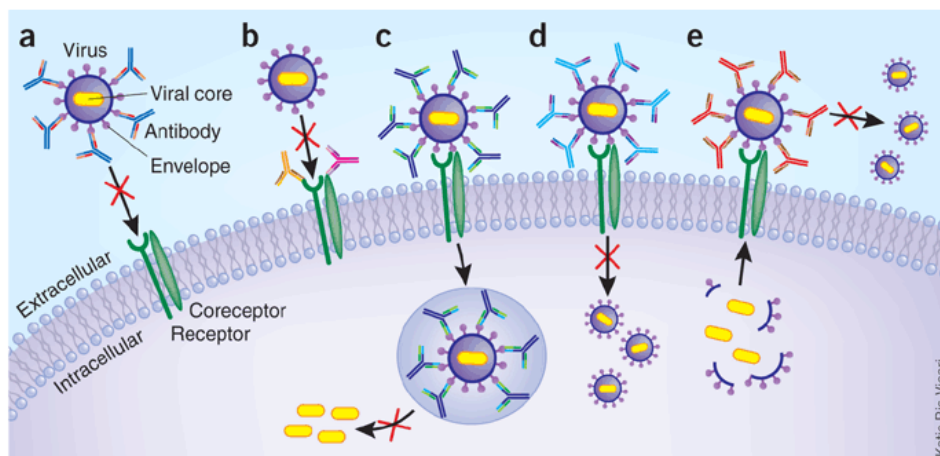


Figure 1.10: Mechanisms of viral neutralization by antibodies a- Blocking receptor engagement by binding to spike, b-Blocking viral entry by binding to viral receptor, c and d – Blocking internalization of virus, e- Inhibition of release of virions. Adapted with permission from Nature Biotechnology (107)

However, the exact mechanism of viral neutralization and the role of Fc-mediated effector function in clearance of viruses are still not clear and seem to be virus dependent (107, 124). Two different models for neutralization have been proposed: The occupancy model and the critical binding site model. According to the occupancy model, successful neutralization depends on the proportion of epitopes that are bound by the antibody on the virion in a linear fashion. Hence, the larger the virion, the higher the concentration of antibody required for neutralization. This model has been supported by neutralization studies of West Nile Virus (WNV), which showed efficient neutralization at higher concentrations, whereas antibody dependent enhancements (ADE) of infection at a lower concentration of antibody(129). Alternatively, the critical binding model focuses on the epitopes that are more critical for neutralization than the coating of the virus by antibody.

Many antiviral mAbs are currently under clinical development and some of them are listed in Table 1.2. Since one of the major challenges for developing successful anti-viral antibody is rapidly evolving viruses that generate variants which escape neutralization; treatments with cocktails of mAb are also being pursued. Their synergistic effects may help to cover a majority of circulating strains and prevent neutralization escape.

| | Infectious Agent | Targets | Antibody |
|------------------------------|-------------------------|---|---|
| Virus | RSV | Glycoprotein F | Humanized – IgG1 |
| | Rabies | Glycoprotein antigenic site I / II / III | Transgenic HuMab-mouse |
| | West Nile Virus | Envelope protein Domain III | Humanized / human -IgG1 |
| | SARS | S1- RBD | Human IgG1 |
| | CMV | Envelope glycoprotein gb | Human –IgG1 |
| | EBV | CD20 | Chimeric- IgG1 |
| | VZV | Envelope glycoprotein III | Human –IgG1 |
| | HIV | CD4 CCR5 Gp120-V3 tip Amino phospholipids | Humanized –IgG1 / IgG4 |
| | HCV | Amino phospholipids Envelope protein E2 | Chimeric- IgG1 Human hybridoma –IgG1 |
| Bacteria / Toxins | B. anthracis | Protective antigen | Humna / humanized mAb |
| | B. pertussis | Pertussis toxin | Human |
| | E. coli | Shiga toxin 1 and 2 | mAbs |
| | C. difficile | Toxins A & B | Human |
| | S. Aureus (MRSA) | Staph cell adhesion molecules ABC transporter Clumping factor Lipoteichoic acid Protein A | Polyclonal human immune sera Antibody fragment Humanized igG1 Chimeric monoclonal HP antibody |
| Fungal | Candida | Anti-hsp90 | Human scFv |

Table 1.2: List of anti-infective antibodies in development. (Information from literature(107, 124))

As bacterial toxins have a direct role in the pathogenesis of bacterial infections, they form excellent candidates for antibody therapy. Anti-toxin antibodies neutralize toxin activity by either competing with the cellular receptor, or by blocking the substrate access (124)(Table 1.2). These antibodies generally do not to require effector functions, as antibody fragments have been shown to be effective in the absence of Fc domain(106).

The development of anti-bacterial and anti-fungal antibodies is faced with many challenges and is less advanced in comparison to anti-viral and anti-toxin antibodies. For a viable therapeutic strategy and its success, identification of suitable targets is very important(124). Targeting cell surface antigens that are either essential for the cell survival or for the recruitment of the host immune response are ideal candidates. However, variability among clinical isolates necessitates the development of isolate-specific therapeutics raising the costs. It also exerts evolutionary pressure on the cells, potentially leading to the emergence of resistant isolates. On the other hand, targeting extracellular virulence factors and signaling molecules may prove to be a attractive approach(7). Several monoclonal antibodies are currently under development for treatment of both bacterial and fungal diseases (Table 1.2).

Limitations

Even with the tremendous progress in the development of therapeutic antibodies, their role in prevention and treatment of infectious disease has been slow compared to other diseases. Antigenic variance and the emergence of antibody resistant variants have all played a role in hampering the development of antibody based therapeutics for infectious diseases. Furthermore, a major hindrance for the success of anti-infective antibodies has been the cost associated with antibody therapeutics. To have an advantage over other therapeutic approaches it is crucial for antibody therapeutics to be cost-effective. We hope that with better understanding of pathogenesis combined with advances in antibody engineering will help in lower the costs, making antibody therapeutics more accessible in the future.

CHAPTER 2

THE RELATIONSHIP BETWEEN ANTIBODY AFFINITY AGAINST SPIKE PROTEIN OF SARS-COV AND VIRAL NEUTRALIZATION

INTRODUCTION:

Severe acute respiratory syndrome (SARS) is an infectious disease that set off an epidemic in late 2002 and early 2003, and turned out to be the first new infectious disease of the twenty first century. It is characterized by a rapidly progressive atypical pneumonia and its causative agent was identified after a concerted effort from researchers all over the world led by WHO, to be a novel coronavirus (CoV) termed SARS-CoV (110). The virus first appeared in Guangdong province of China in November of 2002, and spread swiftly around the world. The ease of international travel due to globalization has been held responsible for the rapid spread resulting in more than 8000 cases across 33 countries, with a mortality rate close to 10% (149, 175) The epidemic was effectively brought under control by July of 2003 by quarantine measures and travel restrictions (36, 125). Since then only a few sporadic cases have been reported, which were caused by different isolates of SARS-CoV (101). The SARS epidemic has been divided into zoonotic, early, middle and late phases and refers to the timeline of the emergence of the disease (187).

SARS-CoV is an enveloped, single-stranded positive sense RNA virus, whose structural proteins consist of the spike(S), envelope (E), membrane (M), and nucleocapsid (N) proteins (92, 110, 140). It is a zoonotic virus, considered to have originated from bats (94, 100) that crossed the species barrier and then spread mainly through respiratory secretions and by a person to person contact. SARS-CoV is known to primarily target cells in the respiratory system that express an abundant Angiotensin-Converting Enzyme 2 receptor (ACE2)(99). After infection the virus enters and replicates in these cells, and the released matured virions infects new target cells (Fig: 2.1). SARS-CoV has also been shown to target mucosal cells of the intestine, tubular epithelial cells of kidneys, epithelial cells of renal tubules and immune cells.

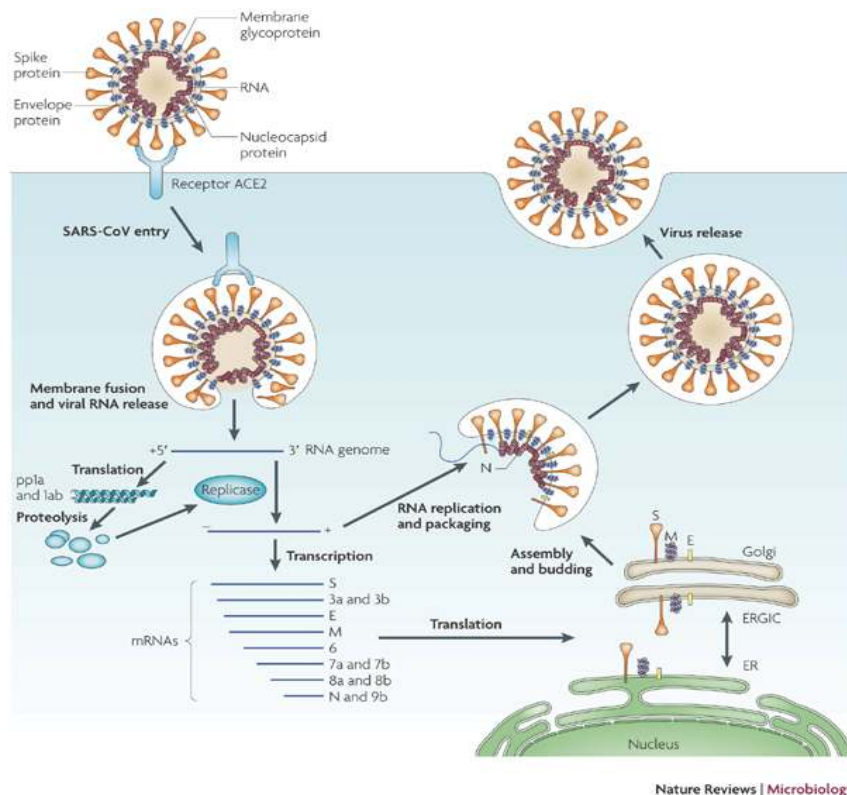
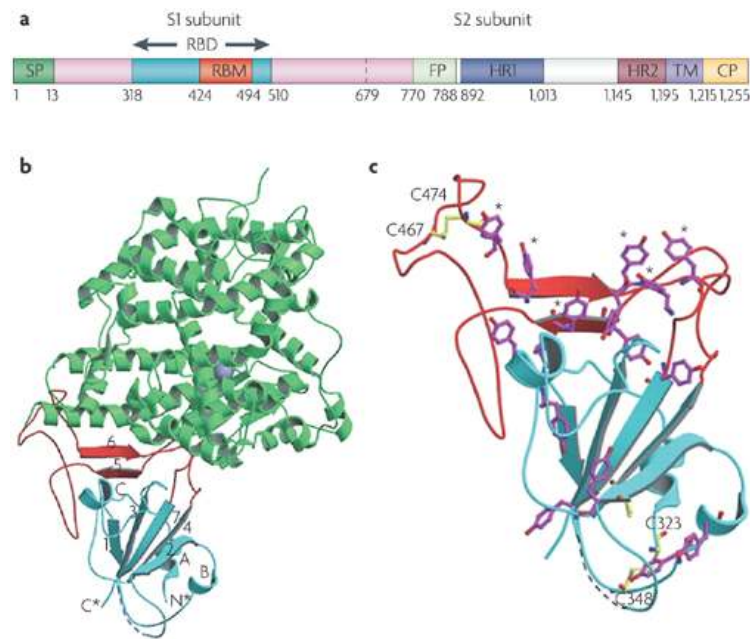


Figure 2.1: The lifecycle of SARS-COV (adapted with permission from Nat Rev. Microbiology)

The spike (S) protein of SARS-CoV is a ~180 kDa type 1 transmembrane glycoprotein that trimerizes to form the spike. The S protein has two functional domains: The N-terminal S1 domain that contains the receptor binding domain (RBD- 318-510 amino acids) and the membrane anchored C-terminal S2 domain, which contains two heptad repeat regions (HR1 and HR2) (98) (Fig:2.2). The entry of the virus into the host cell is mediated by binding of the RBD to ACE2 on host cells and subsequent conformational changes in S2 that facilitate membrane fusion (94). Genome analysis of different isolates of SARS-CoV revealed a high rate of evolution in the S protein with amino acid changes in the RBD region. These amino acid changes in RBD have played a major role in its ability to overcome species barrier, initially allowing animal-to-human transmission, and subsequently human-to-human transmission (Fig 2.3)(186).



Nature Reviews | Microbiology

Figure 2.2: a- Schematic of the S protein, b- Crystal structure of RBD complexed with the receptor ACE2, c- Structure of RBD. Adapted with permission from Nat. Rev. Microbiol (36)

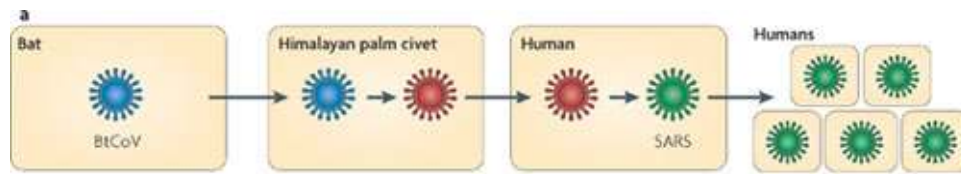


Figure 2.3: Schematic representation of cross-species transmission of SARS-CoV.
Adapted with permission from Nat Rev Microbiol (128)

The S protein is a highly immunogenic antigen and is responsible for inducing neutralizing antibodies and protective immunity against virus infection. It also has determinants for host specificity, cell tropism and pathogenesis. Because of its immunogenicity and its crucial role in infection by recognition of the host receptor, the S protein has become an important target for both vaccine and therapeutic development. Researchers have used both full length S protein and recombinant RBD to develop vaccines. The full length S protein when used as a vaccine has been shown to provide protective immunity *in vivo*, both as a DNA vaccine (183) and as a highly attenuated modified vaccinia virus Ankara(MVA) vaccine(11). Vaccination by the purified full length protein in the form of S trimer has been shown to induce neutralizing antibodies against different SARS-CoV isolates in a mouse model (61). The use of recombinant RBD either by immunization as a RBD-Fc or following *in vivo* expression from an adeno-associated virus (AAV) vector - (RBD-rAAV) has been shown to elicit neutralizing antibodies and to confer protection against SARS-CoV challenge (35, 37, 62). Although most of these vaccines induced neutralizing antibody responses against infection, vaccination of ferrets with rMVA-spike (recombinant vaccinia Ankara)

exhibited increased inflammation and vaccine-linked hepatitis, raising concerns over the safety and efficacy of these vaccines (29).

Different approaches have been taken to develop spike protein-based therapeutics. Peptides having either the RBD sequence (aa 471-503) (68), or RBD-binding motifs of ACE2 (aa 22-44 & aa 351-357)(54) have been shown to disrupt the RBD-ACE2 interaction and to exhibit inhibitory activity towards SARS-CoV infection *in vitro* (36). *In vitro* inhibition of infection was also seen with peptides that either interfere with the cleavage of S protein (188), or block the HR1-HR2 interaction, thus inhibiting the fusion of the viral envelope with the host membrane (15).

The use of monoclonal antibodies (mAbs) that block S protein from binding to the receptor is an attractive approach for passive immunization and for short-term protection against infection. Even though highly potent neutralizing mouse mAbs to RBD have been generated, the risk of human-anti mouse antibody (HAMA) responses prevents these from being an effective human therapeutic. To avoid this problem, a wide range of neutralizing human mAbs have been isolated from B cells of patients infected with SARS-COV(118, 167), from transgenic mice encoding the human immunoglobulin locus immunized with S protein(28), or from a non-immune human antibody library screened by phage display (158). Most of the isolated antibodies were successful in preventing the binding of SARS-CoV to ACE2 receptor and thereby neutralizing the infection *in vitro*. Some of these antibodies like 80R, m396 (189), 201 and 68 (51) have been shown to exhibit protection against infection in the mouse model. Specifically, the 80R antibody was isolated from a non-immune human antibody library by phage display. The scFv form of 80R was reported to exhibit an affinity of 32nM to S1 protein, as measured by

Surface Plasmon Resonance (158). Marasco *et al.* found that the neutralizing epitope of 80R overlaps the ACE2-RBD domain and that not only it neutralizes SARS-CoV *in vitro*, but also effectively reduces the viral titers *in vivo* (159).

Even though there have been no reported cases of SARS after 2004, threat of re-emergence is still present because of the presence of coronavirus in animal reservoirs. Antibody therapy provides an attractive approach for both prophylaxis and treatment. It is known that the potency of an antibody in viral neutralization is dictated by its epitope specificity, the dose (concentration) and half life in the blood stream. Both antibody affinity and valency have a strong influence on biological activity, with increasing affinity often resulting in higher neutralization potency (112). The concentration of antibody can also have an impact on viral neutralization, and the number of antibodies required for neutralization may be directly correlated to the size of the virus (16). In their study, Pierson *et al.* observed that neutralization is a function of both affinity and epitope accessibility, and lower concentration of weak neutralizing antibody might lead to antibody-dependent enhancement (ADE) of infection (129). However, recent studies with antibodies against RSV reported high affinity related non-specific tissue binding that led to very poor bio-distribution *in vivo* (180). This study suggests that functional improvement observed *in vitro* because of high affinity may not always translate to improvements *in vivo*. The mechanisms of viral neutralization vary among viruses, and a high affinity neutralizing antibody (nAb) directed towards a critical epitope constitutes an attractive strategy in designing therapeutic anti-viral antibody.

One of the major obstacles in treating RNA-viruses is the random mutations that drive the antigenic drift. As described before, amino acid changes in the spike protein

have been found to be responsible for the ability of SARS-CoV to cross the species barrier. The generation of neutralization escape mutants from studies with nAbs, and the presence of zoonotic strains that evade neutralization signifies the need for broad neutralizing antibodies (BnAbs) for protection against a range of viral strains. In their efforts towards isolating BnAbs, Dr. Marsaco and his group sought to isolate improved variants of the 80R antibody by utilizing structural information from 80R-RBD complex to guide the construction of mutant libraries targeting the light chain. Screening of these libraries by phage display against RBD protein containing the dominant mutations found in escape variants (D480A and D480G) led to the isolation of antibody variants exhibiting broad neutralizing ability(157). However, the broadly neutralizing antibodies reported in this work exhibited only about 3-fold higher affinity for the Urbani strain RBD protein to which the starting antibody, 80R had been raised. The above findings raise the question, whether antibody variants of 80R displaying greatly improved affinity might elicit broader neutralization. In one scenario, high affinity might result from increased binding energy to multiple residues within the binding epitope. If so, a single mutation of the spike protein within that epitope might be sufficient to allow escape. Alternatively high affinity might arise from more favorable interaction to a single residue or “hot spot” and thus mutations in the hot spot or in other residues within the binding epitope might result in escape.

In this research, we explore the relationship between affinity towards the viral antigen and the evolution of escape mutants. The 80R antibody was affinity matured by random mutagenesis and screening using the bacterial display technology Anchored Periplasmic Expression or APEx (57). After just one round of random mutagenesis and

screening by APEX, we isolated antibodies with 140-fold higher binding affinity. DNA shuffling and mutagenesis of the best clones followed by additional screening resulted in a further increase in antigen affinity to ~ 300-fold relative to the parental scFv antibody, 80R. These high affinity antibodies were shown to exhibit increased neutralization potency *in vitro* against the wild-type Urbani strain compared to the parental antibody 80R, validating the critical role of affinity in viral neutralization. However, the affinity matured antibody fragments were ineffective against zoonotic strains of SARS-CoV, suggesting that a high affinity towards RBD alone is not sufficient to provide broad protection against different isolates of SARS-CoV. On the other hand SK4, our highest affinity antibody fragment could neutralize SARS-CoV mutants that either evaded neutralization by 80R or could escape other lower affinity antibodies.

MATERIALS AND METHODS:

Bacterial Strains and Plasmids:

Escherichia coli Jude 1 [DH10BF::Tn10] cells were used for all the cloning and protein expression experiments reported here. Plasmid pAPEX 1 was used for N-terminal APEX display of scFv, and the construction of scFv libraries (57). pMopac 16 encodes a pelB leader followed by Sfi 1 sites and the Skp chaperone that helps in soluble expression of protein into periplasmic space, a C-terminal constant human kappa light chain for scAb expression and C-terminal 6 x Histidine tag for easy purification (59).

Viruses and Cells¹:

Recombinant viruses' icUrbani (AY278741), icGD03-MA and icHC/SZ/61/03 were propagated in Vero E6 cells. Vero E6 was maintained in MEM media (Invitrogen, Carlsbad, CA) supplemented with 10% Fetal Clone II (Hyclone, South Logan, UT) and gentamycin / kanamycin (UNC Tissue Culture Facility). Growth curves were performed in Vero E6 with the different wild type or mutant recombinant-derived escape mutant viruses at a MOI of 0.1 for 1 hour and overlaid with medium. Virus samples were collected at various time points post infection and stored at -70°C until viral titers were determined by plaque assay.

Virus titers were determined as plaque forming units (pfu) by plating 6-well plates with 5×10^5 Vero E6 cells per well and inoculating cultures with 200 μ l from the 10-fold serial dilutions. Cells were incubated with the virus for 1 h at 37°C and overlaid with 3 ml of 0.8% agarose in complete media. Plates were incubated for 2 days at 37°C and plaques were visualized by staining with neutral red for 3-6 h. Virus concentration was calculated as pfu /ml. All virus work was performed in a Class II biological safety cabinet in a certified bio-safety level 3 laboratory containing redundant exhaust fans while wearing Tyvek suits and Powered Air Purifying Respirators.

Construction of ScFv Library:

The 80R single chain antibody gene (158) was constructed by overlap extension PCR (153). The heavy and light chain variable regions of the antibody were amplified by PCR, and a flexible (Gly₄ Ser)₄ linker introduced by overlap PCR. The amplified 80R

¹ All *in vitro* viral neutralization experiments were conducted by Dr. Ralph Baric (UNC).

scFv PCR product was digested with Sfi1 and cloned into the Sfi1-digested pAPEx 1 vector (57) for bacterial display. The 80R scFv gene was subjected to random mutagenesis by error-prone PCR using standard protocols. A library of 1.6×10^8 independent transformants was obtained. Sequencing of 10 random clones revealed a nucleotide substitution rate of 1.3% (47).

Cloning, Expression and purification of Receptor Binding Domain:

A gene encoding the S protein of the SARS-CoV Urbani strain (AY278741) was generously provided by Dr. S. Makino (UTMB-Galveston), and used to amplify the receptor binding domain (RBD) consisting of amino acids 318 to 518. The RBD was cloned into pFastbac vector (Invitrogen) with the N-terminal Honeybee Mellitin signal sequence (164) for secretion in insect cells and a C-terminal Flag tag for screening and N-terminal 6 x Histidine tag for purification. Bacmid DNA was prepared and transfected into SF9 cells (Invitrogen) according to the manufacturer's (Invitrogen – Bac-Bac system) instructions to generate and amplify baculovirus particles, and the titers were determined by following the Bac-Bac protocol. High five cells (Invitrogen) were cultured in Insect Xpress media (Cambrex, Walkersville, MD) supplemented with 10% fetal bovine serum (Sigma) and Penicillin/Streptomycin (Sigma) at 27°C as a monolayer. To produce RBD, insect cells were seeded at a density of 10^6 /ml in 250 ml of media and infected at a multiplicity of infection of 5 with recombinant RBD baculovirus. Media were harvested after 90 hours, and the culture supernatant was dialyzed against 1x IMAC buffer at 4°C. Following dialysis, the culture supernatant containing the RBD protein was incubated with 1ml of nickel-nitrilotriacetic acid (Ni-NTA) agarose (Qiagen, Hilden,

Germany) for 2 hours at 4°C. The mixture was then loaded onto a 5 ml column, and washed with 10 column volumes of 1x IMAC buffer (10mM Tris. 0.5M NaCl pH 8.0). Protein was eluted with 3 column volumes of 1 x IMAC buffer with 300 mM imidazole. The protein eluate was further purified on a superdex-200 (GE Healthcare) size exclusion column via FPLC. Protein samples were analyzed for purity on a 4-20% polyacrylamide gel (NuSep, Lawrenceville, GA) and stained with coomassie blue stain.

Screening and Selection of high affinity ScFv variants by APEX:

E. coli strain Jude 1 cells transformed with the 80R scFv library in the pAPEX 1 vector, were used to inoculate shake flask containing 20 ml of terrific broth (TB) media (Difco, Sparks, MD)) supplemented with chloramphenicol (Cm) at 35 µg/ml to an OD₆₀₀ of 0.1. Cells were grown at 37°C with shaking until the OD₆₀₀ reached 0.5, at which point cultures were transferred to a 25°C shaker for 30 min. Protein synthesis was induced with IPTG to a final concentration of 1mM, and incubation was continued for 3 hours at 25°C with shaking. 2-3 ml of cells equivalent to an OD₆₀₀ of 10 were collected by centrifugation and resuspended in 350 µl of ice-cold Tris- sucrose (0.75 M Sucrose and 0.1 M tris-HCl pH 8.0) solution with 30 µl of 40 µg /ml lysozyme. An additional 700 µl of ice-cold 1 mM EDTA was added drop-wise and the mixture was incubated at 4°C on a rotary shaker for 15 min. 50 µl of 0.5M MgCl₂ was then added and incubated for another 10 min at 4°C on a rotary shaker. Cells were then gently pelleted and resuspended in 1 ml 1x PBS with purified RBD (100 nM for the first round) and incubated for 40 min at room temperature on a rotary shaker. Subsequently, the cells were pelleted again and resuspended with 1x PBS containing 200 nM anti-FLAG-PE (Phycolink – Prozyme, San

Leandro, CA), at room temperature for 40 min. After labeling, the cells were pelleted to remove the excess label, resuspended in 1ml 1x PBS and analyzed on a FACS ARIA (BD Biosciences) flow cytometer using 488 nm for excitation. The spheroplasted cells were gated based on forward scatter (FSC) and side scatter (SSC) parameters, 5% of the most fluorescent cells were collected and the sort population was resorted immediately. scFv genes in the resort solution were amplified by PCR, cloned into the pAPex 1 vector, the ligation mixture was transformed into *E. coli* strain Jude 1 cells and plated on LB agar plates containing chloromphenicol at 35 µg/ml. Cells were scraped from the agar plates, and was used for inoculation into liquid media and then subjected to additional three rounds of sorting as above, with decreasing concentration of RBD to increase the stringency of sorting as follows 100 nM in the first round; 50 nM in the second; 25 nM in the third and 20 nM in the final round.

After the fourth round of sorting via FACS, genes were rescued by PCR and cloned into pMopac16 (60) for soluble expression. For high throughput screening based on off-rates, colonies were inoculated into 96 well seed plate containing 200 µl of TB with 2% glucose and 200 µg/ml ampicillin per well. After overnight growth at 37°C with shaking, 20 µl of the culture from each well was used to inoculate fresh 96 well plates with same growth media as above. The seed plate was stored with 15% glycerol at -20°C for future use. After overnight growth at 37°C with shaking, cultures were pelleted by centrifugation at 4,500 rpm for 10 min. The media were discarded and cell pellets were resuspended in 200 µl of expression media (TB with 200 µg/ml ampicillin and 1 mM IPTG), and incubated at 25° C for 3 h. The cells were pelleted again by centrifugation at 4,500 rpm for 10 min, resuspended in 200 µl of lysis buffer (20% bugbuster HT-Novagen

in HBS-EP buffer) and incubated with shaking at room temperature for 2 hours. The lysates were centrifuged to precipitate the insoluble fraction, and the lysate supernatant was transferred to a 96 well Multi screen HTS filter plate (Millipore, Billerica, MA) set on a collection plate, centrifuged for 10 min and clarified filtrate was collected in a 96 well collection plate. The clarified filtrate was used for off-rate (k_{off}) analysis by SPR using a BIAcore 3000 instrument (GE Healthcare, Uppsala, Sweden) as follows: Purified RBD was first Covalently immobilized in 10mM Sodium acetate, pH 5.9 on to a CM5 sensor chip (carboxymethylated dextran matrix-GE Healthcare, Uppsala, Sweden) by using 1-ethyl-3-(3-dimethylaminopropyl) carbodiimide / *N*-hydroxy succinimide chemistry to the level of 300RUs (Response units). BSA was similarly coupled to the chip as an in-line subtraction standard. Kinetic analysis was performed in HBS-EP buffer (GE Healthcare, Uppsala, Sweden) at a flow rate of 25 μ l/min at 25 °C. Samples were injected over the immobilized RBD for 2 min followed by a 5 min dissociation phase. The surface was regenerated by injection of 10 μ l of 4 M $MgCl_2$ at a 50 μ l/min flow rate. Dissociation kinetics were calculated using BIA evaluation software, and clones with slowest dissociation rate compared to 80R were selected for further analysis.

Shuffling and random mutagenesis of isolated clones for additional screening:

The four highest affinity scFv genes (B9, F10, RS2 & RS5) isolated from the off-rate analysis above along with the 80R scFv gene were chosen for DNA shuffling. The four isolated genes were first amplified individually by PCR and the DNA products were pooled with a 4 molar excess of 80R scFv and then digested with 0.125 U of DNase I (Roche, Germany) per 3 μ g of DNA at room temperature for 30 min. The reaction was

stopped by heat inactivation at 80°C for 10 min and DNase I digest fragments of 50–100 bp were gel-purified using the QIAEX II (Qiagen) gel extraction kit. The DNA fragments were re-assembled by PCR for first few rounds without primers, and then full length DNA was amplified using outside primers encoding Sfi1 site. DNA was separated by gel electrophoresis and a band ~750 bp in length was excised and gel-purified using the Qiagen gel extraction kit (Qiagen), then digested with Sfi1 and ligated to Sfi1 digested pApex 1 vector. Following electroporation 5.4×10^7 transformants were obtained. Ten clones were chosen at random and sequenced to evaluate the presence of mutations from different templates, suggesting that DNA shuffling had been successful. PCR product after the assembly was also used as a template for error prone PCR as above, and the DNA product from that reaction was cloned into pApex 1 vector to generate a library of 1.5×10^7 transformants.

The shuffled library and the shuffled + error prone libraries above were combined for FACS screening, and three rounds of sorting were performed as described above. The concentration of RBD used for labeling was reduced in successive rounds as follows: 20 nM for the first round; 10 nM for the second round and 5 nM for the final round. After the final round of sorting, scFv genes were PCR amplified and sub cloned into pMopac 16. Subsequently, 96 colonies were inoculated for high throughput screening, and cell lysates were prepared and analyzed by BIAcore for off-rates as described before.

Expression and purification of single chain antibody fragments (scAbs):

Antibody fragments were expressed as scAbs by inserting the scFv genes into pMopac16 vector, a pAK400 derivative in which the scFv is fused in frame to a C-

terminal human constant kappa domain. pMopac16 also co-expresses the Skp periplasmic chaperone which aids in the expression of soluble antibody fragments (60). ScAbs are expressed as fusions with a C-terminal 6x his tag for easy detection and purification.

Antibody fragments were expressed in *E. coli* Jude1 [DH10BF::Tn10]. Individual colonies were inoculated into 50 ml TB media with 200 µg/ml ampicillin and 2% glucose, and were grown overnight at 37°C. The overnight cultures were used to inoculate 500 ml of TB media with 200 µg/ml ampicillin and the cells were grown at 37°C for 3 hours. Cultures were transferred to 25°C for 30 min and protein expression was induced with 1 mM IPTG. After a 4 h incubation at 25°C, cells were collected by centrifugation and protein was purified from the osmotic shock fraction (60,). Briefly, cells were resuspended in 12 ml of ice cold Tris-sucrose solution (0.75 M sucrose, 100 mM Tris pH 8) with the addition of 1 ml of 30 µg/ml lysozyme in Tris-sucrose buffer. Cells were gently mixed for 10 min at 4°C, 24 ml of 1 mM EDTA was added dropwise and was allowed to mix for an additional 20 min at 4°C. 1.7 ml of 0.5 M MgCl₂ was added and incubated for further 10 min. The samples were centrifuged at 12,000 rpm for 15 min, and the resulting supernatant was dialyzed against 1x IMAC buffer (10 mM Tris. 0.5 M NaCl pH 8.0). ScAbs were purified from the supernatant using IMAC (immobilized metal affinity chromatography) column, by using Ni-NTA agarose according to manufacturer's protocol (Qiagen, Hilden, Germany), followed by size exclusion FPLC on Superdex 200 (GE Healthcare) as explained earlier. The purity of isolated scAb was verified by gel electrophoresis on a 4-20% SDS-PAGE gel (NuSep, Lawrenceville, GA) stained with coomassie blue.

To remove the endotoxin from the purified scAbs for *in vitro* neutralization assays, the purified protein samples were passed three times through Detoxi-gel endotoxin removal columns (Pierce, Rockford, IL) according to the manufacturer's instructions. The endotoxin levels in the samples were measured by the Limulus Amoebocyte Lysate (LAL) assay (Associates of Cape Cod, East Falmouth, MA) as described by the manufacturer.

BIAcore analysis for affinity measurement:

The purified RBD protein was immobilized on CM5 chip as described above and BSA was used as in-line subtraction. Kinetic analysis was performed in HBS-EP buffer at a flow rate of 50 μ l/min at 25°C. The affinity of the FPLC-purified scAbs was analyzed by injecting the samples over the chip for 2 min for the association phase followed by 5 min dissociation. Five different concentrations of antibodies from 9 nM-36 nM were analyzed in duplicate, along with a blank as a reference. The surface regeneration was performed with a 12 sec injection of 4 M MgCl₂. Binding kinetics were calculated using BIA evaluation software (GE Healthcare, Uppsala, Sweden). Calculated fits were based on the Langmuir 1:1 model, with chi² values below 1.

Isolation of Escape Mutants:

Recombinant icUrbani used as seed stocks for deriving RS2, RSK, SK4 and 80R escape mutants. Briefly, 1×10^6 pfu of icUrbani were incubated with 20 μ g of a neutralizing scAb (RS2, RSK, SK4 or 80R) for 30 mins and then inoculated onto cells in the presence of scAb at a concentration of 20 μ g/ml. The development of cytopathic

effect (CPE) was monitored over 72 hrs and progeny viruses harvested. Antibody treatment was repeated two additional times and more rapid CPE noted with each passage. The viruses from passage four were plaque purified in the presence of antibody and neutralization resistant viruses were isolated. The S glycoprotein genes from four individual plaques for each neutralization experiment were sequenced and the neutralization titers between wild type and antibody-resistant viruses were determined as described below.

In the experiment above, the SK4 scAb resulted in the extinction of parent viruses on three separate occasions. Therefore, we incubated 1×10^6 PFU of icUrbani with 15, 10, 5 and 1 μg of SK4 for 30 mins, and then infected cultures in the presence of 5 $\mu\text{g}/\text{ml}$ SK4 antibody. Depending on treatment conditions, cytopathology was evident either within 48 h (5, 1 μg doses) or was minimal after 4 days (15 and 10 μg). Low dose SK4 treated progeny viruses (1 and 5 μg doses) were treated with 5 μg of SK4 for two passages, and then selected with one additional treatment of 10 and 15 μg doses, resulting in highly antibody resistant viruses that produced extensive CPE in cultures within 24-36 hours. High-dose treated stocks were passaged once in the absence of antibody (pass 2) to restore virus titers, and then reselected two times in the presence of 5 μg antibody. Two final treatments of 10 and 15 μg of SK4 antibody resulted in highly resistant populations that rapidly produced CPE in culture. Two to four plaques were isolated from each treatment regimen (10 plaques total) in the presence of 20 μg SK4 antibody and the S glycoprotein gene was sequenced.

Plaque Reduction Neutralization Assay (PRNT):

30 µg of each scAb in the panel (80R, RS2, RSK, and SK4) were diluted into 50 µl and diluted 1:2 into PBS. Wild-type icUrbani, icGD03-MA and icHC/SZ/61/03 and various recombinant viruses were diluted and approximately 100 PFU of each in 175 µl was added to the scAb dilution series for 30 mins at 37°C. The percentage neutralization was calculated as $1 - (\text{number of plaques with antibody} / \text{number of plaques without antibody}) \times 100$.

RESULTS:**Expression and purification of the RBD portion of the SARS-CoV S glycoprotein:**

Marasco and coworkers had shown that recognition of RBD by the 80R antibody is glycosylation independent. Therefore, initially we made efforts to express the aglycosylated RBD in bacteria. We cloned RBD in various expression vectors either as a fusion protein with MBP or GST or alone. Though we were successful in expressing and purifying the RBD polypeptide, it was found to not bind to the 80R scFv. Therefore, we chose to express RBD in the Baculovirus system (Fig 2.4). The expression yield of RBD in High Five cells was around 1.2 mg/L of insect cell culture. Following purification the RBD domain was found to be >95% pure as determined by SDS-PAGE and gave a strong signal on ELISA with 80R scFv.

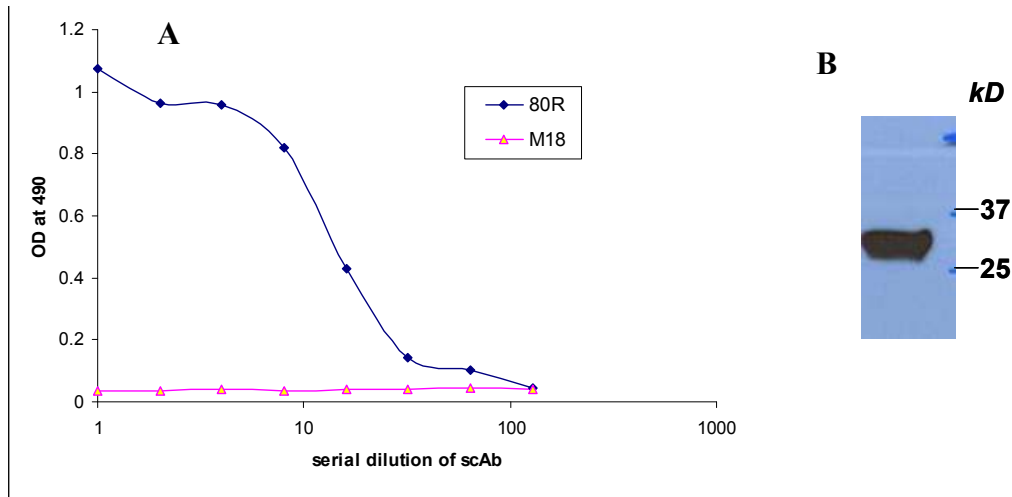


Figure 2.4: A- ELISA results for baculovirus purified RBD protein detected by 80R scAb. M18scAb was used as negative control. B- Western blot analysis for baculovirus expressed RBD .The protein was detected by anti-spike polyclonal antibody.

Random mutagenesis and affinity maturation of the 80R scFv:

Random mutagenesis by error-prone PCR was employed to construct a library of variants of the 80R scFv. Following transformation of the ligated DNA by electroporation a total of 2×10^8 transformants were obtained with an average of 1.3% nt substitutions per gene. Cells were grown in liquid culture, and after the protein expression was induced for 4 h, the cells were harvested and converted to spheroplasts. The spheroplasts were incubated with 100 nM RBD for 40 min, followed by labeling with 200 nM anti-FLAG -PE. A total of 4×10^8 cells were sorted and 5% of the spheroplasts with the highest fluorescence were collected and resorted. The scFv genes from the sorted cells were rescued by PCR amplification and were re-cloned into pApex 1. Following transformation, the cells were subjected to three additional rounds of sorting. For these successive rounds, the stringency of sorting was increased by reducing

the concentration of antigen from 100 nM RBD in the first round to 20 nM in the final round. An increase in the percentage of fluorescent cells was observed after 3 rounds of sorting (Fig 2.5). After round four, scFv genes were rescued by PCR and cloned into pMopac 16 for soluble expression.

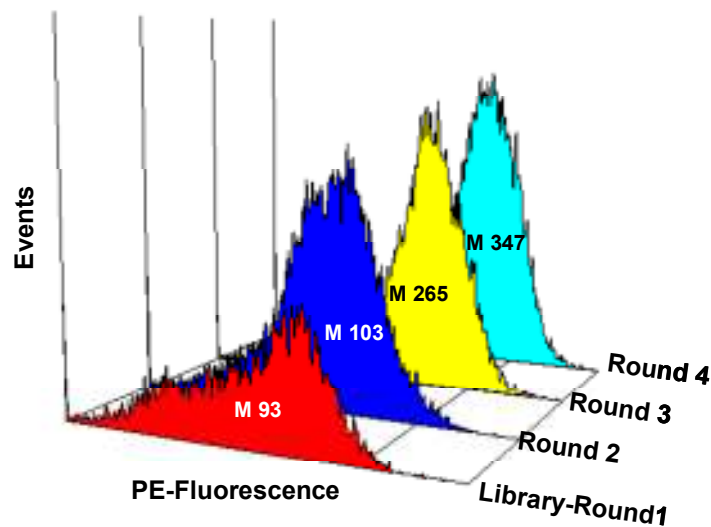


Figure 2.5: Comparison of FC histograms of library with the 3 successive rounds of sorting, showing enrichment in the fluorescence. M= Mean fluorescence intensity

Since the enrichment of high affinity clones by the Apex screening method presumably relies on relative dissociation rates, antibodies with higher affinity can generally be identified by measuring off-rates (k_{off}) by Biacore. As k_{off} is *not* concentration dependent, it was possible to set up a high throughput screen to measure k_{off} without purifying the antibody fragments. A total of 88 randomly picked colonies from the round 4 and 8 colonies of 80R scAb as a control was grown in a 96-well plate. Expression of antibody fragments was induced with IPTG and the soluble fraction was isolated by treating the cells with the lysis solution prepared in BIACORE running buffer

(HBS-EP) to reduce the effects on the refractive index during analysis. Lysates were filtered using a 96-well filter plate, to remove the cell debris which may interfere with SPR measurements. The filtered lysates were used for SPR analysis, and the k_{off} was calculated using the BIACORE software. The k_{off} values were compared to the parental clone 80R, and rank-ordered.

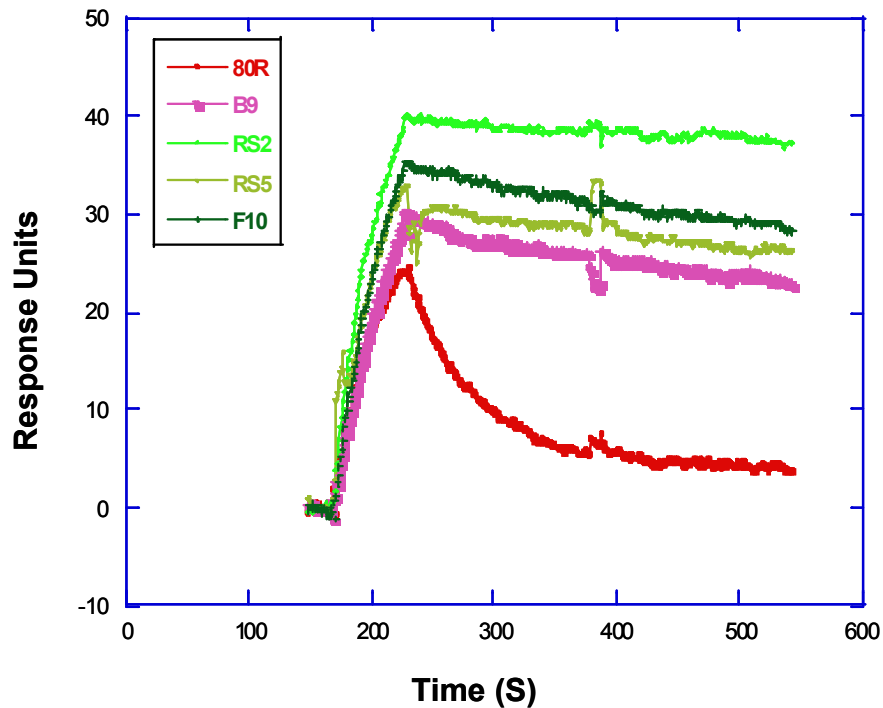


Figure 2.6: BIAcore analysis of scAbs in cell lysates. Data for four clones exhibiting slower dissociation rates compared to parental 80R clone are shown

The four clones with the slowest antigen dissociation kinetics were produced in large scale (500 ml), and were purified by Ni NTA chromatography followed by gel-

filtration FPLC to remove any scAb dimers. SPR analysis of the purified proteins revealed that they all exhibit significantly lower K_D values for RBD binding compared to the parental 80R antibody and that the improvement in K_D values are primarily from slower k_{off} , as anticipated (57)(Fig 2.6). The affinities of the scAb variants ranged from 0.78 nM to 0.103 nM, with the highest affinity clone RS2 exhibiting a K_D of 103 pM and a k_{off} of $1.7 \times 10^{-4} \text{ sec}^{-1}$ which corresponds to a RS2-RBD complex half life of 1 h (Fig 2.7). This represents a > 140 -fold improvement compared to the parental antibody 80R ($K_D = 15.9 \text{ nM}$).

Sequence analysis of the isolated clones revealed the presence of 5-8 amino acid substitutions per scFv gene, with RS2 possessing 8 amino acid substitutions (Fig 2.7). Most of the amino acid substitutions were present in the framework regions, with only one consensus mutation, S167N, observed in the CDR1 light chain of all four clones (data not shown). S167 is located at the interface of the co-crystal of 80R-RBD complex (70) indicating its possible involvement in RBD binding. The significance of this mutation was recently highlighted by Marasco and coworkers (157) who reported that S167N is important for broad neutralization of SARS-CoV Urbani strain variants containing a D480A/G mutation that renders them resistant to neutralization by the 80R IgG.

```

-----FR1----- -CDR1 -FR2----- -CDR2-----
80R EVQLVQSGGGVVPQPKSLRLSCAASGFAFS SYAMH WVRQAPGKGLEWVA VISYDGSNKYYADSVKG RFTI
RS2 .....D.....Q.....T.....S.....
B9 .....D.....
RS10 .....R.....T.....G.....P.....
G5 .....G.....S.....

```

```

-----FR3----- -CDR3-- -FR4----- LINKER -----
80R SRDNSKNTLYLQMNSLRAEDTAVYYCAR DRSYYLDY WGQGLTVTVSS GGGGSGGGGSGGGGSGGGGS TTL
RS2 .....R.....A.....A.....P..SD...
B9 .....A.....A..R.....P..SD...
RS10 .....P..SD...
G5 .....SG.....~...

```

```

-----FR1----- -CDR1----- -FR2----- -CDR2-- -----FR3-----
80R TQSPATLSLSPGERATLSC RASQSVRSNLA WYQQKPGQAPRPLIY DASTRAT GIPDRFSGSGSGTDFTLT
RS2 .....N.....N.....
B9 I.....N.....
RS10 .....N.....
G5 .....D.....N.....

```

```

----- -CDR3-- -----FR4-----
80R ISRLEPEDFAVYYC QQRSNWPPT FGQGTKVEVKSASGAEFAAA
RS2 .....
B9 .....
RS10 .....
G5 .....

```

| | $k_a(1/Ms)$ | $k_d(1/s)$ | $K_D(nM)$ |
|-------------|-----------------------------|--------------------------------|-----------|
| 80R | $8.20 \pm 0.04 \times 10^5$ | $1.30 \pm 0.04 \times 10^{-2}$ | 15.9 |
| RS9 | $1.16 \pm 0.04 \times 10^6$ | $9.14 \pm 0.11 \times 10^{-4}$ | 0.78 |
| RS2 | $1.66 \pm 0.02 \times 10^6$ | $1.70 \pm 0.01 \times 10^{-4}$ | 0.10 |
| RS10 | $1.52 \pm 0.03 \times 10^6$ | $7.40 \pm 0.05 \times 10^{-4}$ | 0.48 |
| RS5 | $1.51 \pm 0.02 \times 10^6$ | $5.20 \pm 0.03 \times 10^{-4}$ | 0.34 |

Figure 2.7: Sequence alignments of clones RS2, RS10, B9 and G5 with 80R Affinity data for the four clones in comparison to parental 80R along with the standard deviations for the fit are provided in the table.

To investigate if other amino acid substitutions, in addition to S167N, have a beneficial role in improving the antigen affinity and also to eliminate neutral mutations, clones B9, RS2, RS5, F10 and the parental 80R were subjected to DNA shuffling followed by random mutagenesis by error-prone PCR. The 80R scFv was used in 4 molar excess for DNA shuffling in order to reduce the number of neutral mutations. Two libraries were constructed: A shuffled library with 5.4×10^7 members and an error-prone library of 1.5×10^7 members. Ten random clones from both libraries were sequenced to verify the shuffling between the templates in the shuffled library and to calculate the approximate nucleotide substitution in the second library, which was 0.5%. Both the libraries were pooled for screening and the combined library was sorted by FACS. The stringency of screening was further increased by reducing the concentration of antigen from 20 nM in the first round to 5 nM in the third round. After the third round of sorting, scFv genes were rescued by PCR and cloned into pMopac16 for soluble expression as scAbs. The antigen dissociation rate constants of 80 scAbs from clones picked at random from the 3rd Round were analyzed by SPR analysis and two clones with slower off-rates were identified (data not shown). Both clones were further produced in a preparative scale from 500 ml liquid cultures, and purified proteins were used to measure K_D values. Antibody variant SK4 exhibited a K_D value even lower than RS2, equal to 45 pM, and a k_{off} of $8.05 \times 10^{-5} \text{ sec}^{-1}$, resulting in an antigen: antibody complex half-life of 2.2 h (Fig

2.9, Table 2.1). Overall, the SK4 antibody fragment is more than 300-fold affinity enhanced compared to the parental fragment 80R. Sequence analysis of SK4 revealed 12 mutations including three mutations in common with RS2: N57S, S167N and S188N (Fig 2.10)

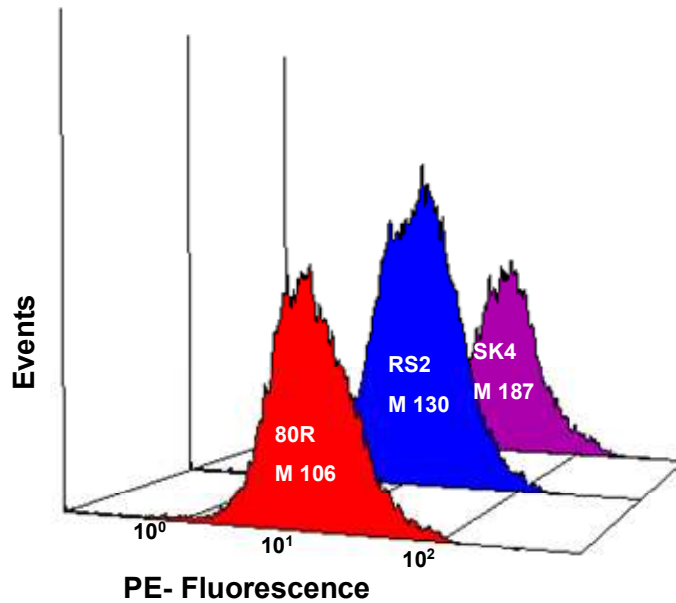


Figure 2.8: Comparison of FC histograms depicting the mean fluorescence intensity (M) of the selected high affinity clones RS2 and SK4 with 80R.

To determine the role of the N57S, S167N and S188N amino acid substitutions in affinity enhancement, the respective mutations were introduced into 80R scFv by site directed mutagenesis to construct a variant referred to as RSK (Fig 2.11). SPR analysis of RSK revealed a K_D value equal to be 220 pM, which is lower than 80R, indicating a role for some or all of these three amino acid substitutions (N57S, S167N and S188N) in affinity improvement (Fig 2.9, Table 2.1). Clearly, however, this is not the whole story as other framework mutations must be contributing to higher affinity in the case of RS2 and SK4.

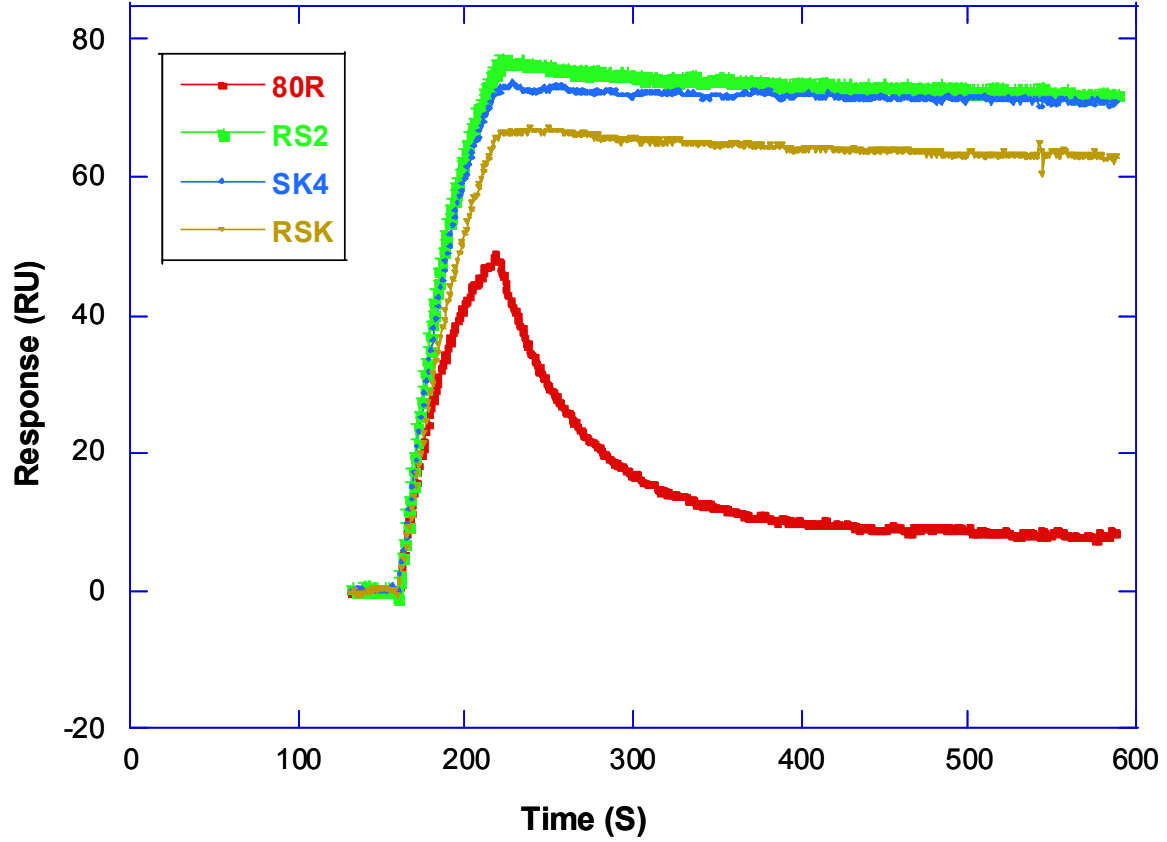


Figure 2.9: BIAcore analysis of purified anti-RBD scAb proteins on immobilized RBD. Comparison of the sensograms of the highest affinity clones isolated from the library with 80R.

| Clone | k_a (1/Ms) | k_d (1/s) | K_D (nM) |
|------------|-----------------------------|--------------------------------|------------|
| 80R | $8.20 \pm 0.04 \times 10^5$ | $1.30 \pm 0.04 \times 10^{-2}$ | 15.9 |
| RS2 | $1.66 \pm 0.02 \times 10^6$ | $1.70 \pm 0.01 \times 10^{-4}$ | 0.10 |
| SK4 | $1.77 \pm 0.02 \times 10^6$ | $8.05 \pm 0.14 \times 10^{-5}$ | 0.045 |
| RSK | $7.89 \pm 0.01 \times 10^5$ | $1.76 \pm 0.02 \times 10^{-4}$ | 0.22 |

Table 2.1²: Rate constants and equilibrium dissociation values for the antibodies isolated from the library as measured by SPR . Standard deviations for the fit as measured by the software are provided.

² Affinity values for clones 80R, RS2 and SK4 are from two independent measurements. Affinity value for RSK is from a single measurement.

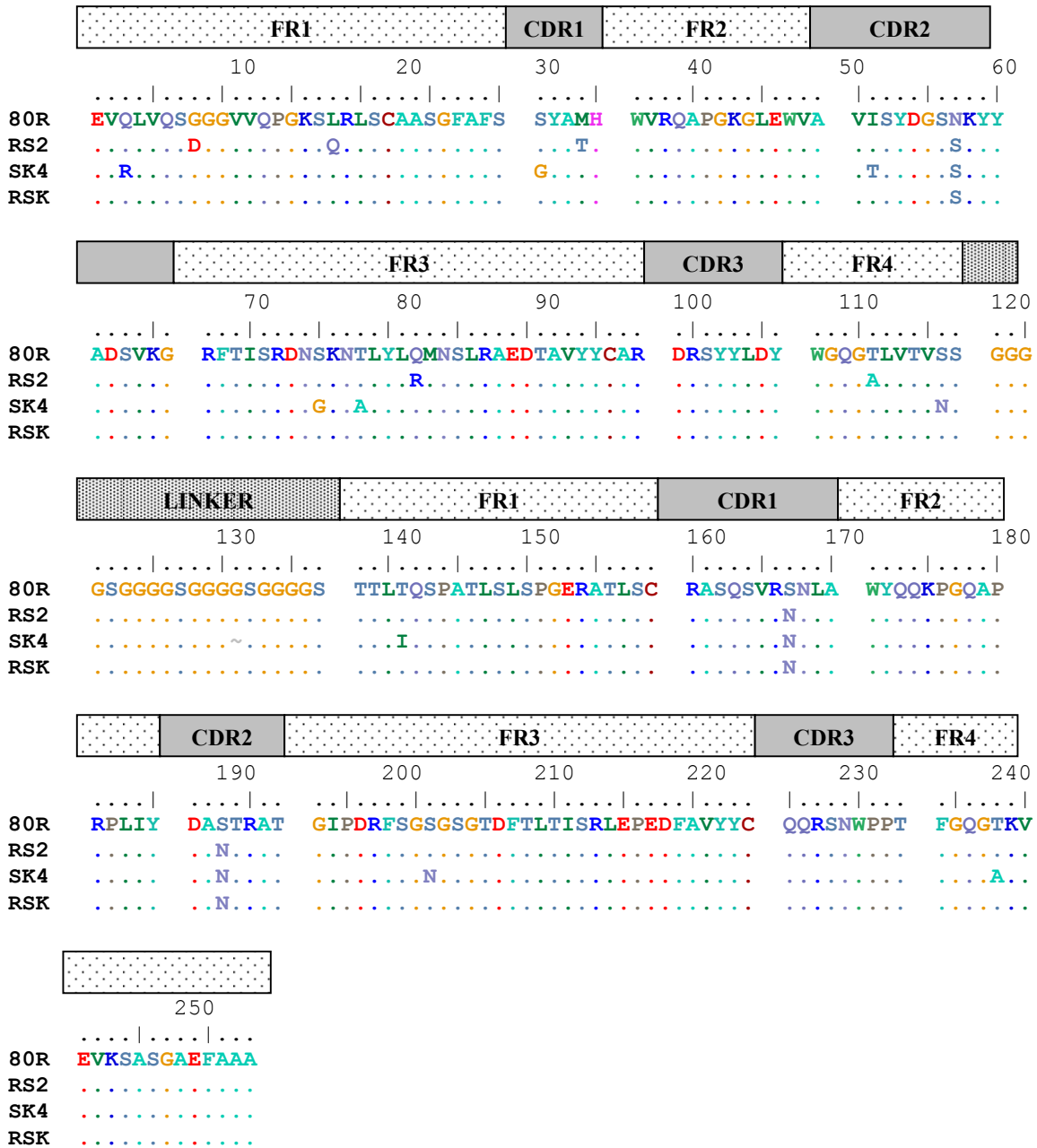


Figure 2.10: Sequence comparison of the high affinity clones RS2, SK4, and RSK with parental 80R clone.

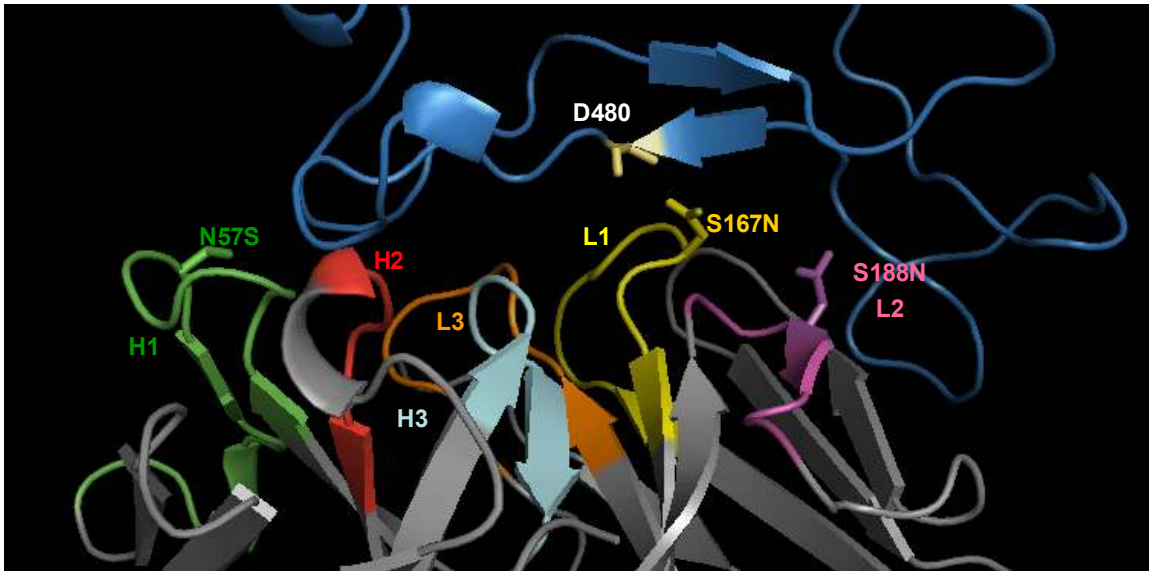


Figure 2.11: Interface of structure of the RBD-80R complex . S1-RBD is in blue, CDR loops (H1-H3 and L1-L3) of 80R, mutations N57S, S167N, S188N from high affinity clones RS2 & SK4, and 480D of S1-RBD are colored as shown.

Neutralization assay and generation of escape mutants:

The neutralizing ability of the purified 80R, RS2, SK4 and RSK scAbs against SARS CoV (Urbani strain) was tested by plaque reduction assay. Approximately 100 PFUs of wild type icUrbani strain were incubated at 37°C for 30 min with a serial dilution of each of the 4 scAbs using a starting concentration of 30 µg in 200 µl. The number of plaques present in each dilution of antibody was determined.

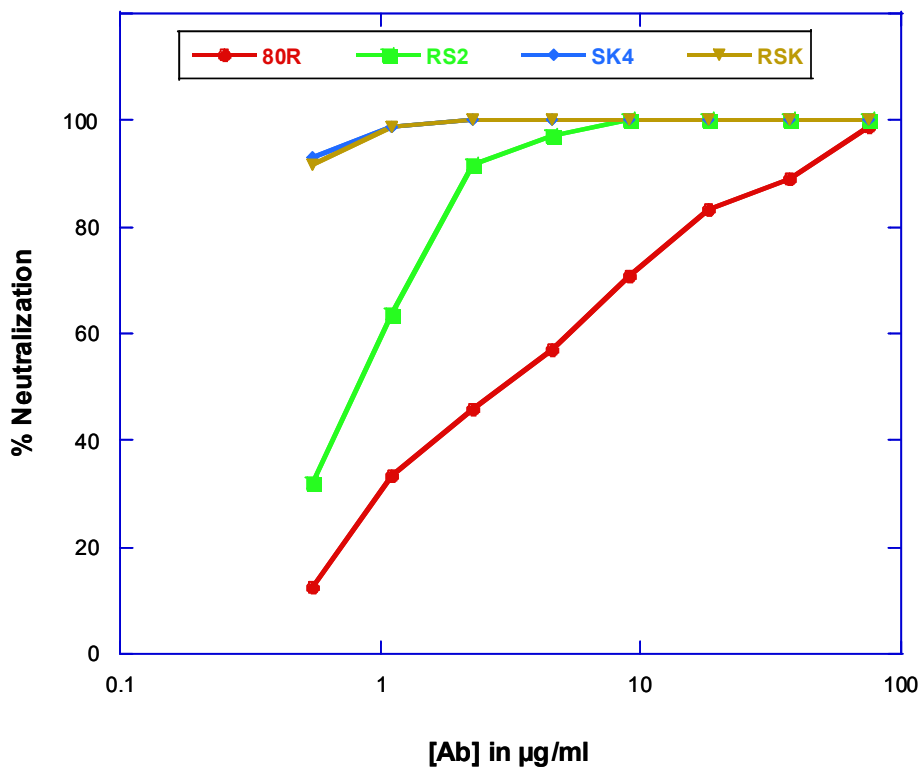


Figure 2.12: Neutralization activity of the four scAbs tested by plaque reduction assay against icUrbani strain

These experiments revealed that, as expected, the neutralization potency of the antibodies increased with affinity with SK4 and RSK exhibiting higher neutralization potency (Fig 2.12). However, none of the scAbs could neutralize icHC/SZ/61/03 (a Civet strain) or icGD03MA (a mouse adapted human 03/04 strain, data not shown). The spike protein of these strains differs from that of the icUrbani strain at 6 amino acid positions within the RBD region (Table 2.2). Evidently, these mutations play a crucial role in escape from neutralization.

| Strain | 344 | 360 | 436 | 472 | 479 | 480 | 487 |
|--|-----|-----|-----|-----|-----|-----|-----|
| Urbani (Human 02/03) | K | F | Y | L | N | D | T |
| HC/SZ/61/03 (Civet) | R | S | Y | P | R | G | S |
| GD03MA (Mouse adapted Human 03/04) | R | S | H | P | N | G | S |

Table 2.2: Amino acid differences in the RBD region of the spike protein in different strains of SARS-COV

In vitro neutralization escape mutants of the icUrbani strain that emerged following incubation with each of the four scAbs mentioned above were obtained. After 3 passages in cell culture with antibody, 4 plaques were picked for analysis. RNA isolated from the plaques was used to amplify the RBD cDNA by RT PCR and sequenced. All the four escape mutants of 80R and RS2 had a single amino acid mutation at position 480. Three of the four 80R-escape mutants carried a mutation from aspartic acid to alanine at position 480 (D480A), and one had a mutation of aspartic acid to tyrosine

(D480Y). The four RS2 escape mutants had the D480Y mutation. In the case of the RSK antibody, three of the four escape variants had the D480Y mutation and one had mutation at position 436 with an amino acid change from tyrosine to histidine (Y436H) (Table 2.3).

The SK4 antibody exhibited a very high neutralizing potency and did not generate any escape variants, unlike the other three antibodies. Therefore, conditions were modified by decreasing the initial concentration of SK4 scAb used for incubation. The cytopathic effect (CPE), as observed by detectable morphological changes in the host cell due to infection with icUrbani strain was evident and robust in the virus treated with lower concentration (5 µg, 1 µg) of antibody in the initial passage . Virus treated with the higher concentration (15 and 10 µg) of antibody in the initial round showed minimal CPE after 4 days, and therefore viral titer had to be restored in the absence of the antibody in the second passage.

A total of nine out of ten plaques that were isolated from different treatment regimens with SK4 were sequenced. All the 9 escape mutants of the SK4 antibody had two mutations: N479I and D480Y (Table 2.3). The presence of mutations at position D480 in most of the escape mutants was not surprising, since it has been shown to have a critical role in the binding of the parental antibody 80R to the RBD (70). D480 is the most common residue to undergo mutation as has been observed before (159), and substitution to a Tyrosine does not affect the binding of the RBD (and therefore the virus) to the human ACE2 receptor (178).

Cross-neutralization studies with mutant virus particles encoding either D480A or the D480Y that mediated escape from 80R and its derivatives were performed with all

four antibodies (Fig 2.13). Only the SK4 antibody successfully neutralized both escape mutants, suggesting a role of high affinity in overcoming the effect of D480 substitutions.

| scAb | Mutations (Number of clones) |
|-------------|---|
| 80R | D480A (3/4) D480Y (1/4) |
| RS2 | D480Y (4/4) |
| RSK | D480Y (3/4) Y436H (1/4) |
| SK4 | N479I (9/9) D480Y (9/9) |

Table 2.3: Amino acid changes in the RBD of spike protein found in the neutralization escape mutants generated by scAbs.

The number of clones in which mutations are found is shown in parenthesis.

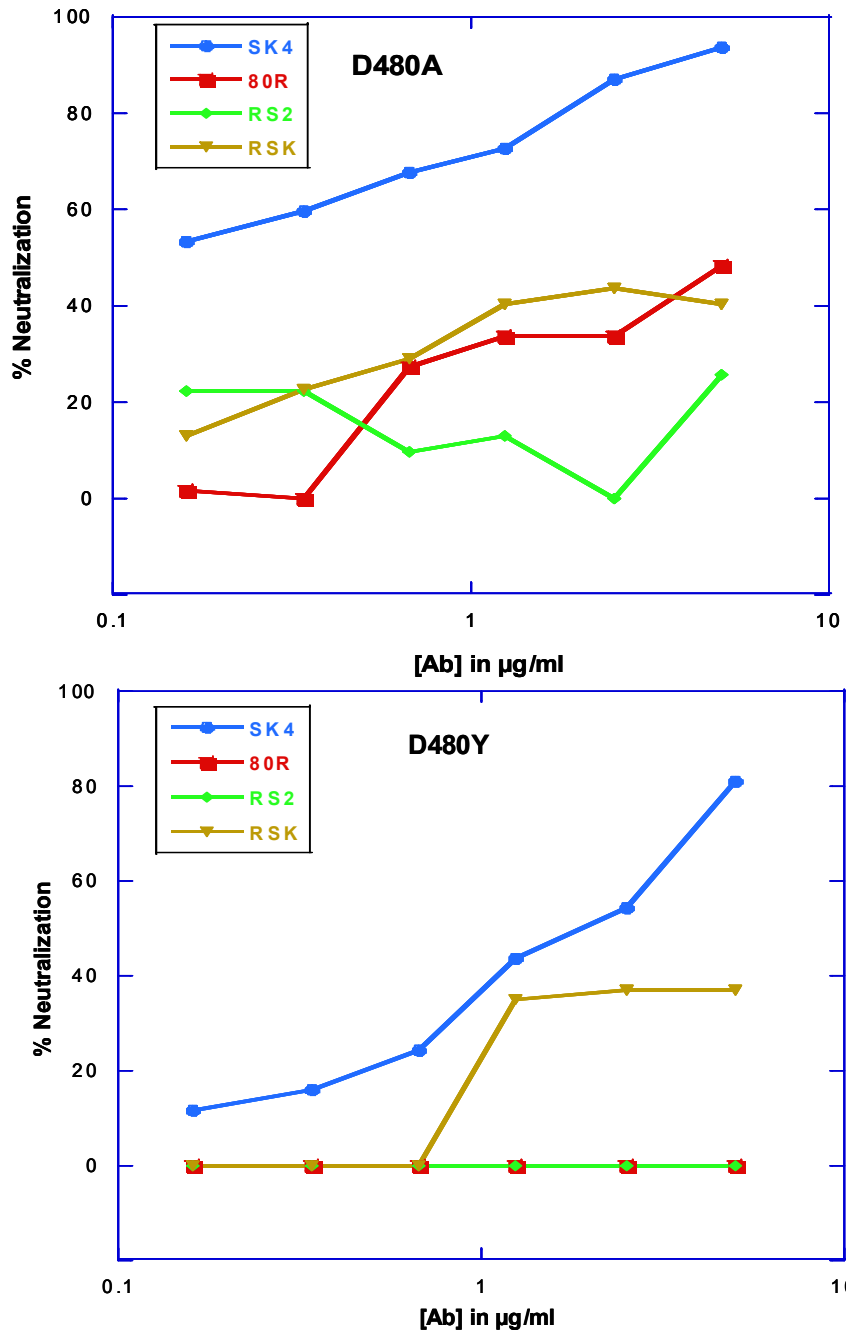


Figure 2.13: Cross neutralization studies of the four scAbs with escape mutants. A.

Escape mutant with D480A mutation, B. Escape mutant with D480Y mutation

DISCUSSION:

SARS was the first new major infectious disease to challenge the world population in the twenty first century. Though the number of deaths resulting from the disease was smaller compared to previous pandemics such as plague, influenza, or the mortality of other infectious diseases such as HIV, malaria or tuberculosis, the widespread fear and resulting travel restrictions eventually resulted in a global economic loss of about 59 billion dollars (187), emphasizing the role of globalization in the spread of the disease and also its effect on the global economy. Collaborative efforts from researchers all over the world were successful in controlling the epidemic in a short period of time. One of the main focuses of research efforts has been to develop neutralizing antibodies that could be used for both prophylaxis and therapy. Of the many neutralizing antibodies that have been developed, the one against the RBD region of the spike protein has been shown protective by blocking its binding to the host cell receptor in both *in vitro* and *in vivo* studies(158, 159, 189). However, the use of neutralizing antibodies for the prevention and treatment of infectious diseases, especially in the case of possible pandemics, is restricted by the related issues of production limitations and cost. One way to tackle these problems is to improve the neutralization potency of the antibody; thereby reducing the dosage required and thus making it more cost-effective while simultaneously easing production requirements.

In the present study, we investigated the role of affinity in enhancing the neutralization potency of the 80R antibody. For affinity maturation, we employed the APEX bacterial display system for the screening of libraries of random mutants. The screening of a large library of random mutants resulted in the isolation of antibody

variants that bind to the RBD region of the spike protein with affinities ranging from 0.78 nM to 0.1 nM, the latter corresponding to a 140-fold improvement in affinity. We were able to further improve the binding affinity of the best clones from the random mutagenesis library by additional mutagenesis via DNA-shuffling combined with a round of random mutagenesis. Screening of the resulting library led to the isolation of the SK4 antibody which exhibits a monovalent antigen affinity of 45 pM (Table 2.1), representing a roughly 300-fold improvement over wild-type 80R. Only one consensus mutation, S167N in the CDR1 of the light chain, was observed in all the isolated affinity-improved antibodies. In addition, two more common mutations, N57S and S188N, were observed in the high affinity antibody clones RS2 and SK4 (Fig 2.7). We introduced these three consensus mutations into the 80R parental antibody to generate construct RSK. RSK displayed a substantial affinity improvement indicating that these three amino acid substitutions play a significant role in decreasing the dissociation rate of the antigen:antibody complex, without affecting the association rate. Clearly, other mutations present in RS2 and SK4 are making contributions as well.

In vitro neutralization studies revealed that as expected, higher affinity leads to greater neutralization. The high affinity antibody SK4 along with RSK exhibited the highest neutralizing potency against the icUrbani strain (Fig 2.8). It has been shown previously that the 80R antibody fails to neutralize SARS-CoV strains with the D480A/G mutation in their RBD (158). In their recent study, Dr. Marasco and coworkers screened and isolated antibodies based on a criterion of broad neutralizing ability of SARS-CoV strains with D480A/G mutation, and observed the presence of the S167N mutation in all the isolated antibodies suggesting it has possible role in broad neutralization (157).

In order to determine if high affinity along with the presence of S167N mutation will help in neutralization of various strains, our antibodies were tested against strains HC/SZ/61/03 and GD03MA (Table 2.2). All the antibodies failed to neutralize these strains (data not shown) suggesting that neither high affinity nor the S167N mutation was sufficient for neutralization of these strains.

To further understand the potential role affinity might play during simulated infection, the anti-RBD antibodies were used at sub-neutralizing concentrations in order to generate viral escape mutants. Sequencing revealed that the most common RBD mutation observed in the escape mutants generated by all four antibodies was D480Y. A D480A mutation in RBD was observed in the case of 80R, and a Y436H mutation in RBD was seen in the case of the RSK antibody. For SK4, the highest affinity antibody in the study, all the escape mutants generated had an N479I mutation combined with D480Y. Cross neutralization studies revealed that SK4 successfully neutralized the escape mutants generated with either the D480A or D480Y mutation, suggesting a critical role of N479I in escape of neutralization from SK4 antibody. It remains to be seen whether this result is due to overall enhanced affinity, wherein more RBD mutations are required to inhibit SK4 binding below a critical neutralization threshold affinity, or whether N479I is specifically counteracting a unique SK4 interaction with RBD.

On an entirely different level, it is important to point out that the mutations present in the escape mutants could very well represent mutations that might appear in future viral strains. It is therefore of value to catalogue these changes, as well as develop strategies to develop neutralizing antibodies against them.

SUMMARY

Consistent with expectations, enhanced antibody affinity was correlated with neutralizing potency against the wild-type Urbani SARS strain. However, our studies indicate that high affinity on its own is not enough to protect against other viral strains and escape mutants. It is important to keep in mind that all of our studies were conducted with antibody fragments, and it is likely that bivalent IgG's will increase the potency of neutralization. Studies with whole IgG's are currently in progress and will be reported in due course.

All of the high affinity antibodies used in this study were isolated after just one round of random mutagenesis using our bacterial display system. As such, the results have affirmed the reliability of the bacterial display system for antibody affinity enhancement in general, and in particular, for the production of neutralizing antibodies to RBD protein. In the future, one can imagine creating a panel of high affinity antibodies using RBD antigens from different strains of virus. Cocktails of these high affinity antibodies might be sufficient to provide protection against multiple viral strains encountered in future SARS outbreaks.

Acknowledgements:

I would like to acknowledge our collaborator Dr. Ralph Baric (University of North Carolina) for conducting the *in vitro* viral neutralization experiments.

CHAPTER 3

ISOLATION OF ANTIBODIES AGAINST *BURKHOLDERIA MALLEI* AND *BURKHOLDERIA PSEUDOMALLEI* FROM A SYNTHETIC ANTIBODY LIBRARY

INTRODUCTION:

Burkholderia pseudomallei and *Burkholderia mallei* are non-spore forming, rod shaped, pathogenic Gram-negative bacteria that belong to the Burkholderia genus. They are the causative agents for the diseases melioidosis and glanders, respectively. At present, there are no vaccines available and both species are resistant to many antibiotics (86); hence treatment is limited to few antibiotics and requires a long-term regimen. Moreover, the potential for the pathogens to cause disease through inhalation of aerosols has resulted in classifying them as a category B agent (potential bio-threat agent) by the Center for Disease Control (CDC)(14).

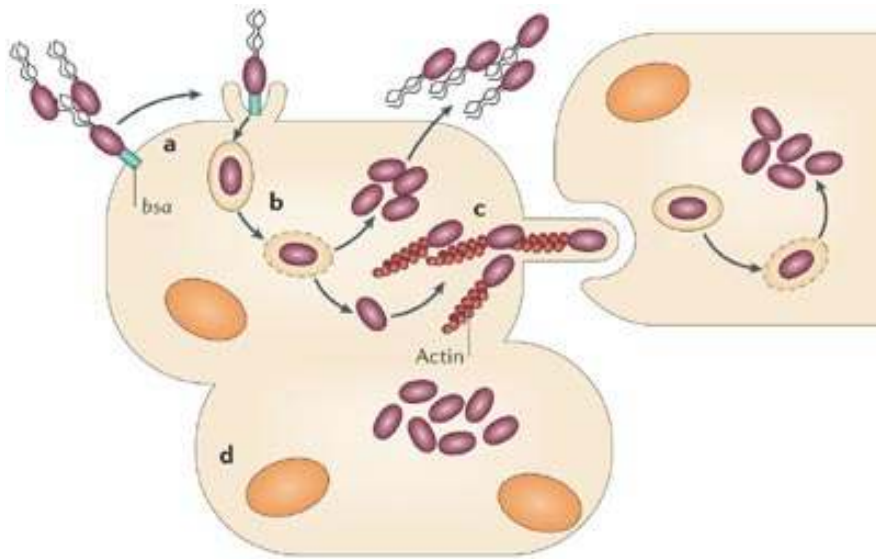
B. pseudomallei is a natural saprophyte and is found in soil and water, which are the natural reservoirs of the bacteria. It is the causative agent of melioidosis in humans, and is endemic in Thailand, parts of Southeast Asia, northern Australia and South America (74). Although a rare disease in the developed countries, the number of cases that have been diagnosed has been increasing, due to rise in travel to endemic areas. The spectrum of infection in humans varies from the sub-clinical to fatal septicemia and

immunocompromised individuals were more susceptible to the disease. Currently, the isolation of the bacteria from clinical samples is the only reliable method for diagnosis. However, a delay in identification of the organism due to its slow growth can prove fatal in cases of acute infection, especially septicemia. Hence for an adequate onset of therapy, rapid and reliable diagnosis is required. The diagnostic value of serological based testing like ELISA, immunoblot, hemagglutination and immunofluorescence have so far been limited is unreliable in endemic areas (73). In addition, the application of PCR based testing has been limited due to lack of appropriate controls and the high incidences of false positives (190). Furthermore, the disease cannot be readily diagnosed by clinical manifestations alone due to flu-like symptoms(173) (176). Though melioidosis can be treated with an aggressive regimen of antibiotics, relapse rates are very high and mortality rate associated with septicemia is 40%.(14)

B. mallei is a non-motile, obligate mammalian pathogen that causes the zoonotic disease glanders. It usually infects solipeds, such as horses and mules. Human infections are rare, and only people in direct contact with the infected animals were found to be at most risk. A person to person spread of *B. mallei* is extremely rare (155). *B. mallei* is highly infectious as an aerosol, and inhalation can lead to septicemia, pulmonary infection or chronic infections of the muscle, liver and spleen. The disease has a mortality rate of 50% when treated with antibiotics, and 95% when untreated (174). As with melioidosis, diagnosis is made primarily through culture detection. In addition, the mallein test is a specific clinical test used in animals(116). Other serological tests and PCR detection are also used, but have not been validated yet.

The genomes of both Burkholderia species have been sequenced and each organism has two chromosomes (64, 119). The large chromosome carries genes associated with cell growth and metabolism, whereas the smaller chromosome carries genes associated with adaptation and survival (64). Both species have a highly homologous genome, and *B.mallei* is not only a deletion derivative but also a clone of *B. pseudomallei* as revealed by MLST analysis (49). Both organisms are facultative intracellular bacteria, and exploit the host cell to promote their intracellular replication and survival. Since they reside within the cytosol of the bacteria, it provides them with a means of protection from the humoral immune system, thus making it difficult to overcome an established infection.

Though the pathogenesis of Burkholderia is not well understood, some of the mechanisms are deduced because of its similarity to other intracellular organisms. The life cycle of cytosolic bacteria can be divided into three stages: escape from the vacuole, replication within the cytosol and manipulation of the innate immune responses triggered in the cytosol (132). The invasion of non phagocytic cells by *B. pseudomallei* have been found to be dependent on a type III secretion system (TTSS)(156). Following their entry into the eukaryotic target cells, intracellular survival becomes crucial for bacteria as they can be destroyed by autophagy- a pathway by which lysosomes destroy the intracellular pathogens. To promote their survival, cytosolic bacteria interact with and modify the autophagy pathway. It has been observed that *B. pseudomallei* mutants lacking TTSS effector BopA (homologue of Shigella IcsB) are preferentially targeted to autophagosomes and show reduced survival indicating that this bacterial protein is involved in escape from autophagy (132).



Copyright © 2006 Nature Publishing Group
Nature Reviews | Microbiology

Figure 3.1: Intracellular lifestyle of *B.pseudomallei* adapted with permission from Nature Reviews Microbiology (176)

- a. Invasion of cells with the help of Burkholderia secretion apparatus (bsa) system
- b. Endosome escape and intracellular proliferation
- c. Cell to cell spread using actin based membrane protrusions
- d. Cell fusion – multinucleated giant cells

Bacteria escape from the endocytic vacuoles into the cytoplasm after internalization. Once in the cytoplasm, polymerization of actin at one pole of the bacterium drives its intracellular motility. The motility of these bacteria leads to the formation of protrusions on the host cell membrane that project into adjacent cells, which are engulfed and lysed by neighboring cells. This results in the intracellular spread of the infection, and evasion of immune surveillance. In *B. pseudomallei* the actin-based motility in murine macrophages was eliminated by a *bimA* mutation and was restored by transient expression of the gene *in trans* indicating a crucial role of BimA in actin tail formation (154).

Many putative virulence factors have been listed for Burkholderia, and are mainly identified based on their role in virulence of similar pathogens. Genes associated with the quorum sensing, type III secretion system, capsular polysaccharide, lipopolysaccharide, flagella and siderophore are some of the putative candidates that are under investigation for their relevance to the disease (176).

The surface molecules of the bacteria not only form the interface between the organism and the host, but also play an important role in its pathogenicity. Several surface immunogenic proteins of *B. pseudomallei* have been identified by a proteomics based approach, in which a biotinylation approach was used to detect surface proteins, which were later screened with immune human sera to identify immunogenic proteins (56, 179). The highly immunodominant Hep_Hag autotransporter proteins have also been identified through screening of bacteriophage expression libraries from both species (166). Recently, microarray technology has been used to screen and identify immunogenic antigens from *B. pseudomallei* (40).

The intracellular lifestyle of the bacteria makes both antibiotic treatment and vaccine development challenging. There are several approaches that have been taken towards developing vaccines, which include using killed whole cells, live attenuated cells, LPS and capsular polysaccharide and recombinant proteins (14). However none of these agents could provide full protection from challenge in an animal model of infection. Passive protection using mAbs has been evaluated and was shown to delay the death of BALB/c mice infected with *B. mallei* (168) or with *B. pseudomallei* (82). However, these antibodies could provide protection only at the initial stage of the infection, and failed at later stages presumably due to the intracellularization of the bacteria. The role of

LPS and capsular polysaccharides as subunit vaccine candidates against *B. pseudomallei* have also been evaluated and were found to delay the time of death in mice but did not provide protection against challenge via the aerosol route (117). Several other mAbs against LPS of *B. pseudomallei* have been used for immunological detection, but they have not been specific enough to discriminate between different species (190)

Antibiotic therapy is usually successful with early diagnosis of melioidosis, but the relapse rate is very high. The use of antibodies for either diagnosis or therapeutics of melioidosis and glanders has so far been limited. Antibodies which are bactericidal or promote phagocytosis can play an important role in the initial clearance of the organism. In addition, antibodies to other bacterial components or cellular mechanisms may also contribute to protective immunity as the infection progresses (63).

In general, the success of anti-bacterial antibodies so far has been limited primarily to anti-toxin antibodies. Identifying suitable candidate targets for passive immunization has been a major limitation in developing effective antibody therapies. In the case of *Burkholderia*, many surface-associated immunogenic proteins and virulence factors have been identified, and we sought to isolate antibodies against some of these targets. By screening for antibodies to a wide array of antigens, we hope to be able to select suitable candidate antibodies that can be used for either diagnostic or therapeutic purposes. These antibodies can also be used as tools for understanding the pathogenesis of these bacteria.

For decades, the traditional approach for the generation of antibodies has been the use of the hybridoma technology, which relies on immunization of animals. In the past 15 years, there has been a considerable progress in the field of antibody engineering, with

the development of *in vitro* immune repertoires and selection platforms that can be used to isolate antibodies. These technologies provide with an attractive alternative to hybridoma technology.

Highly diverse synthetic antibody libraries where diversity is introduced into the CDRs via degenerate synthetic DNA into a selected highly stable and well-expressed framework have been developed. Considerable progress has been made in constructing highly functional synthetic antibody libraries. One such attempt was made by restricting the CDR diversity to amino acids serine and tyrosine, because of the bias towards these amino acids found in natural CDRs (10, 42, 89). By introducing additional diversity in a stepwise manner to the above mentioned binary coding library, Dr. Sidhu and his colleagues have constructed a rationally designed synthetic Fab antibody library with more than $>10^{10}$ members(41, 43). They have used phage display as a selection platform, and have successfully isolated antibodies with low nanomolar affinity against a wide range of protein antigens.

In our efforts to isolate antibodies to a broad range of antigens from both *B. pseudomallei* and *B. mallei*, we used the above mentioned synthetic antibody library in combination with phage display. In this chapter, the successful isolation of antibodies by phage display to a range of antigens from *B. pseudomallei* and *B. mallei* is presented.

MATERIALS AND METHODS:

Bacterial strains and antigens:

Escherichia coli XL1 Blue Strain (Stratagene, La Jolla, CA) was used for all the phage amplification and panning experiments and was grown in 2x TY media (BD Difco, Sparks, MD).

All the purified antigens used for screening experiments were provided by Dr. Annie Gnanam, Dr. Omar Qazi, and Dr. K. A. Brown, University of Texas –Austin. List of the antigens and the respective expression vectors are summarized in Table 3.1. All antigens with a histidine tag were purified using Ni-NTA followed by size-exclusion FPLC. Antigens fused to glutathione-S-transferase (GST) were purified using a glutathione agarose resin as described by the manufacturer.

| Antigens | Function | Size kDa | Cloning/Expression |
|---|--|---------------------|---------------------------|
| BPSL1549 (<i>B. pseudomallei</i>) | Hypothetical protein (64) | 25.6 | pET15B / N- 6x His tag |
| BPSL2748 (<i>B. pseudomallei</i>) | Putative oxidoreductase (64) | 26.15 | pET15B / N- 6x His tag |
| BMA_A0749 (BimA) (<i>B. mallei</i>) | Intracellular motility protein A (119) | 26.2 | pET28a / N- 6x His tag |
| BPSS1525 (BopE) (<i>B. pseudomallei</i>) | G-nucleotide exchange factor(156) | 42.5 | pGEX-4T1/ GST Fusion |
| BPSS1529 (BipD) (<i>B. pseudomallei</i>) | type III effector protein IpaD/SipD/SspD (64) | 59.12 | pGEX-4T1/ GST Fusion |

Table 3.1: List of antigen targets used for panning experiments.

Synthetic antibody library:

A synthetic Fab phage display library, which expresses a bivalent Fab₂ by virtue of a disulfide linkage at the hinge region, was obtained from Dr. S. Sidhu (University of Toronto). The library was constructed using a single highly stable Fab framework from a humanized MBP specific Fab with diversity introduced only in the Complementary

determining Regions (CDRs)(41). The diversity introduced in all the heavy chain CDRs and light chain CDR3 as shown in Fig 3.2. The theoretical diversity of the library is 1×10^{29} , but actual diversity of the library is 3×10^{10} .

Phage Library amplification:

The Fab synthetic antibody library was provided in the form of 6 sub-libraries of frozen phage stock with a titer of $\sim 10^{11}$ /ml per sub-library. Each sub-library consists of varying loop lengths in CDRH3. In order to amplify the library for the panning experiments, 0.5 ml of each sub library was diluted with 0.5 ml of PBS with an addition of $\frac{1}{4}$ volumes of PEG/NaCl (20% PEG 6000, 2.5M NaCl) for precipitation and was left on ice for 30 min. The samples were centrifuged for 15 min at 13,000rpm. The phage pellet was resuspended in 1 ml PBS, and all the six phage sub-libraries were pooled and used to infect 5 L of exponentially growing XL1 Blue cells in 2x YT media. After a 30 min incubation at 37°C, the culture was co-infected with M13K07 (NEB, Ipswich, MA) helper phage at 1:20 bacteria / phage ratio and the cells were incubated for 30 min at 37°C. Following co-infection, carbenicillin (carb) at 50 $\mu\text{g/ml}$ and kanamycin (kan) at 35 $\mu\text{g/ml}$ was added and cells were grown overnight at 30°C at 250 rpm for phage propagation. The following day cells were harvested by centrifugation at 10,000 rpm, and the phage from the media supernatant was rescued by precipitation with an addition of $\frac{1}{4}$ volume of PEG/NaCl. Following incubation on ice for 1 h, the phage precipitate was collected by centrifugation. The phage precipitate was resuspended in 40 ml of PBS, and precipitated again with the addition of PEG/NaCl. Following the second round of precipitation, phage precipitate was resuspended in 20 ml of PBS. Finally, the

supernatant containing the bacteriophage particles was filtered (pore size, 0.45 μm) prior to storage with the addition of 15% glycerol at -80°C . The phage titer was determined by serial dilution of infected *E. coli* (XL1 Blue) plated on 2x YT agar supplemented with 50 $\mu\text{g}/\text{ml}$ of carbenicillin. The phage titer was calculated from the number of colonies and found to be around 10^{14} cfu /ml. Aliquots of the amplified phage were stored in -80°C .

Phage panning using immunotubes:

Purified protein antigens (BPSL1549, BPSL2748 and BimA) were used at 100 nM concentration (50 nM for 2nd round and 25 nM for 3rd round) to coat NUNC maxisorp immunotubes, in a 50 mM sodium carbonate buffer pH 9.6 overnight. Immunotubes were blocked with 2% milk PBS for 2 h at room temperature. A depletion step was performed before each panning round by incubating the phage library (10^{12} - 10^{13} cfu) in 2% milk PBS in a BSA (10 $\mu\text{g}/\text{ml}$) coated immunotube. Following the depletion step, the phage library in 2% milk PBS was added to the immunotube coated with the appropriate antigen and incubated for 2 h at room temp. Immunotubes were washed five times with PBST (PBS+ 0.05% Tween 20) and five times with PBS to remove the non-specifically bound phage (10 washes each for 2nd round and 15 washes each for 3rd round). Bound phages were eluted by incubating with 1 ml of 0.1 M triethylamine (TEA) for 15 min while rotating and were neutralized with 0.5 ml of 1 M Tris-HCl, pH 7.5. 0.75ml of the eluted phage was used to infect 10 ml of XL1 Blue cells in mid-log phase for 30 min at 37°C without shaking. Phage titers were determined as before, and the infected cells were then transferred to 40 ml 2x YT media with 50 $\mu\text{g}/\text{ml}$ carb and were grown overnight at 30°C with shaking. The next day, cells were collected by centrifugation and resuspended in 5

ml 2x YT +50 µg/ml carb+ 15% glycerol, and were stored in -80°C. For phage amplification, cells were inoculated to an OD₆₀₀ of 0.3 and infected with helper phage M13KO7 and grown overnight, and phage was precipitated by PEG/NaCl as described before. For each antigen target, library was panned for three rounds before screening for binders by ELISA.

Phage panning using magnetic beads:

Purified protein antigens (BPSL1549, BPSL2748, BopE and BipD) were biotinylated using Biotin-NHS-SS (Pierce, Rockford, IL) according to the manufacturer's instructions.

A depletion step to remove phage that bind to biotin was performed for each round of panning using streptavidin dynabeads (M-280, Invitrogen, Carlsbad, CA) as follows. 100 µl of streptavidin beads were washed twice with 1 ml of PBS, followed by a single wash with 1 ml of PBST (PBS + 0.05% Tween 20). Beads were then blocked with 2% milk PBS for 30 min while rotating. To avoid the enrichment of biotin specific phage antibodies, biotinylated DsbC protein was added at a concentration of 5 µg/ml to the blocked beads and incubated for 30 min while rotating. The blocked beads were then washed once with PBS, and incubated with around 2×10^{12} phage particles from the library in 2% milk PBS for 1h while rotating. For depletion of glutathione S-transferase (GST) specific phage antibodies, purified GST at 10 µg/ml was added to the above mixture. This phage was used for the following panning procedure.

The phage from the depletion step was incubated with 20 µg/ml biotinylated antigen (BPSL1549, BPSL2748, BopE and BipD) for 1 h in 2% milk PBS while rotating.

The phage – protein mixture was then added to a fresh batch of blocked 100 μ l of streptavidin beads for 30 min while rotating. Following incubation, beads were washed 6 times with PBST and 3 times with PBS to eliminate non-specific and weak binders. The bound phages were eluted by incubation with 1 ml of 100 mM triethylamine (TEA) for 15 min, and neutralized by the addition of 0.5 ml of 1 M Tris pH7.4 buffer. 0.75 ml of eluted phage was incubated with 10 ml of XL1 Blue cells in mid-log phase at 37°C for 30 min without shaking. Following infection, a cell aliquot was plated in serial dilution for titer determination. The remainder of the cell solution was inoculated into 40 ml of 2x TY with 50 μ g/ml carb, and was grown overnight at 30°C. The following day, cells were harvested by centrifugation and resuspended in 5 ml of 2x TY with 50 μ g/ml carb and 15% glycerol. Aliquots of cells were stored at -80°C. Phage amplification was performed as described above.

For the successive round of panning, the concentration of antigen was decreased from 5 μ g/ml for the 2nd round to 1 μ g/ml for the 3rd round. All incubation steps were performed at room temp. During washing and elution steps, beads were collected using a magnet. Typical yield of phage after each round of amplification following a panning round were 10^{13} cfu/ml, and around 10^{12} phage particles were used for successive round of panning.

Phage ELISA:

Monoclonal phage ELISAs were performed with individual clones to identify target specific binders. Single colonies from round 3 titer plates were inoculated in 96-well plates (Costar-3790 Corning, Lowell, MA) containing 200 μ l of 2x YT with 50

$\mu\text{g/ml}$ carbenicillin and grown overnight at 37°C . $30\ \mu\text{l}$ of the overnight cultures were used to inoculate fresh 96-well plate containing $200\ \mu\text{l}$ of $2\times\ \text{YT} + 50\ \mu\text{g/ml}$ carb + M13KO7 (10^{10} phage/ml), and grown overnight at 30°C for phage propagation. $50\ \mu\text{l}$ of the culture supernatant containing the phage was used for ELISA.

$100\ \mu\text{l}$ of $20\ \mu\text{g/ml}$ of antigens (BPSL1549, BPSL2748, BimA, BopE and BipD) in PBS buffer, and BSA at $10\ \mu\text{g/ml}$ as control used to coat 96 well ELISA plates (Corning) overnight at 4°C . Plates were blocked with 2% milk PBS for 2 h at room temp, and washed once with PBS. $50\ \mu\text{l}$ of the culture supernatant containing phage diluted with $50\ \mu\text{l}$ of 2% milk PBS was added to each well. Each phage solution was tested for binding to both specific antigen and to the negative control BSA. After a 2 h incubation at room temperature, wells were washed 3x in PBST and once with PBS. $100\ \mu\text{l}$ of anti-M13 HRP antibody (Pharmacia) in 1:1000 dilution in 2% milk PBS was added to each well, and incubated for 1 h at room temperature. Following incubation, wells were washed 3x PBST and 1x with PBS. For detection, $100\ \mu\text{l}$ of TMB substrate (Dako, Carpinteria, CA) was added to each well, and incubated for 20-30 min, until the color developed. The reaction was stopped by the addition of $100\ \mu\text{l}$ of $4.5\ \text{M}\ \text{H}_2\text{SO}_4$, and was read at 450 nm in a microtiter plate reader.

For sandwich ELISAs, phage antibody was prepared by growing phagemid containing cells in 30 ml of $2\times\ \text{YT} + 50\ \mu\text{g/ml}$ carbenicillin to exponential phase, and infected with M13KO7 helper phage. Infected cells were grown overnight and phage was purified by PEG/NaCl precipitation and resuspended in 2 ml PBS. A $100\ \mu\text{l}$ solution was used to coat 96-well ELISA plate at 4°C overnight. After blocking the wells with 2% milk PBS for 2 h, serial dilution of each antigen was added with a starting concentration

of 40 µg/ml and incubated at room temperature for 2 h. Following washing as described before, 100 µl anti-His HRP(Sigma) in 1:5000 dilution for the detection of his tagged proteins (BPSL2748 and BimA). Following incubation for 1 h, wells were washed and detected by the addition of TMB substrate as described before.

RESULTS:

Isolation of *B. mallei* and *B. pseudomallei* specific antibodies:

A total of five protein antigens were selected for antibody isolation (Table 3.1). The protein BimA is a *B. mallei* protein, whereas the other four proteins BPSL1549, BPSL2748, BipD and BopE were from *B. pseudomallei*. All the proteins were provided by Dr. Annie Gnanam and Dr. Omar Qazi (University of Texas), and were >90% pure as determined by SDS-PAGE (Fig: 3.3).

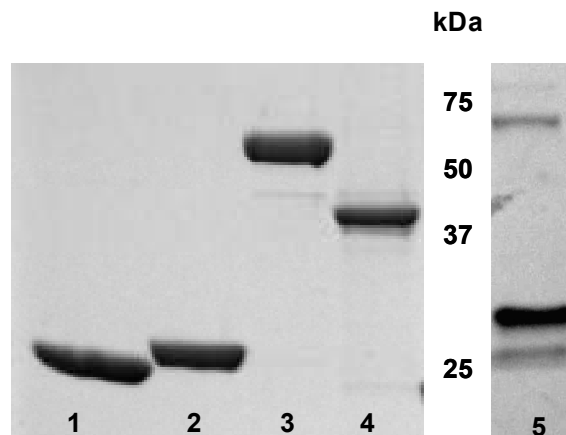


Figure 3.3: Purified antigens run on a 4-20% SDS-PAGE

Lanes1-BPSL1549, 2-BPSL2748, 3- BipD, 4-BopE, 5-BimA

The synthetic antibody library provided by Dr. S. Sidhu (University of Toronto) was used for panning experiments. The library contains $> 3 \times 10^{10}$ members (Fig 3.2). The library was panned against select antigens from both *B. mallei* and *B. pseudomallei* using two different selection strategies, either by immobilization on immunotubes or in suspension following biotinylation and capture by streptavidin beads.

For panning experiments using immunotubes, three antigens BPSL1549, BPSL2748 and BimA were immobilized on immunotubes (1st round-100 nM, 2nd round-50 nM and 3rd round -25 nM). After 3 rounds of panning, enrichment was observed as shown in Table 3.2. Monoclonal phage ELISA for 40 clones each from the round 3 populations was performed. However, no binders were obtained with phage isolated by panning against BPSL1549 or BPSL2748. 13 out of 40 clones screened for BimA showed specific binding, with some clones exhibiting more than 10-fold ELISA signal over the BSA control (Fig 3.4). Three clones exhibiting the highest ELISA signals (clones C7, D3 and E8) were shown to bind specifically to antigen in a concentration-dependent manner in a sandwich ELISA (Fig 3.5). These clones were sequenced, and each one was found to have a distinct CDR amino acid sequence (Table 3.4).

| | BPSL1549 | BPSL2748 | BimA | Conc. of Antigen nM |
|---------|-------------------|-------------------|-------------------|---------------------|
| Round 1 | 1.8×10^7 | 6×10^8 | 6×10^6 | 100 |
| Round 2 | 2.1×10^8 | 1.2×10^8 | 1.2×10^8 | 50 |
| Round 3 | 3×10^9 | 2×10^8 | 2.4×10^9 | 25 |

Table 3.2: Phage titers from panning experiments using immunotubes

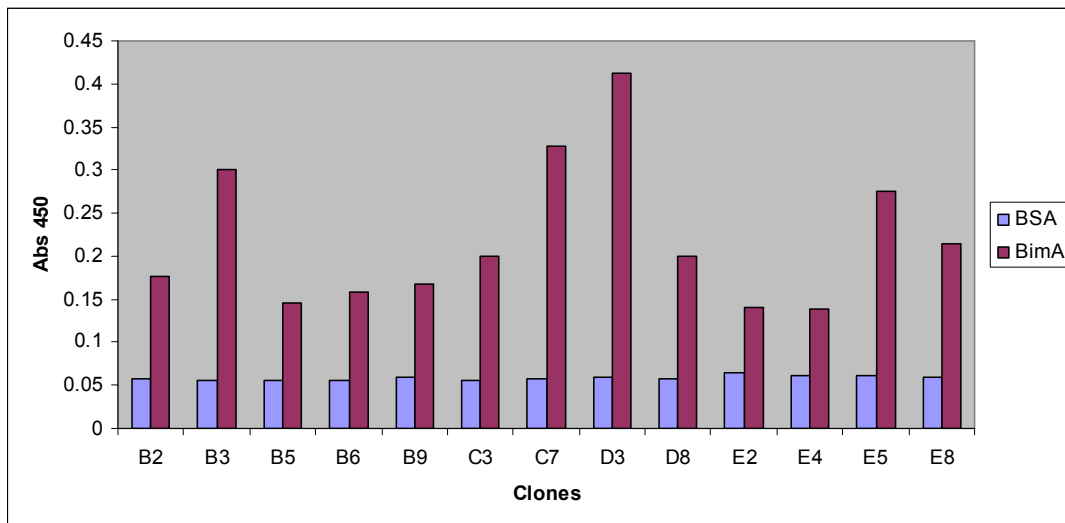


Figure 3.4: Monoclonal phage ELISA results for BimA clones isolated from panning experiments exhibiting >2-fold ELISA signal over control BSA.

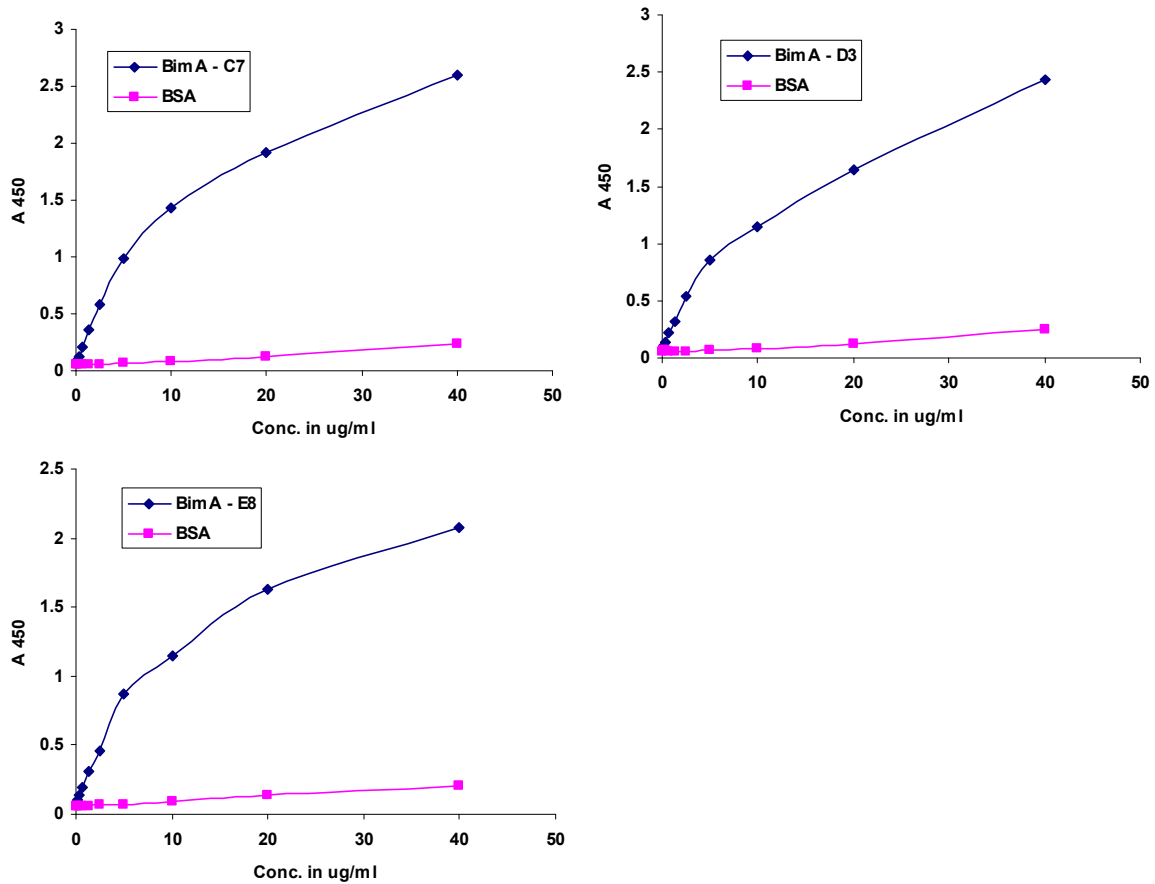


Figure 3.5: Sandwich ELISA for BimA clones C7, D3 and E8
 Phage antibodies were incubated with serial dilution of BimA protein, and specific binding was detected by anti-His antibody. BSA was used as control.

For panning experiments using streptavidin beads, BPSL1549, BPSL2748, BipD and BopE were first biotinylated and used at a concentration of 10 µg/ml, 5 µg/ml and 1 µg/ml for panning rounds 1, 2 and 3 respectively. A significant enrichment was observed in all the panning experiments as given in Table 3.3. 30 clones each for BPSL1549, BPSL2748, BopE and BipD were screened by monoclonal phage ELISA. Four clones that gave ELISA signals at least two-fold above background were obtained for BPSL2748, 3 clones for BopE and one for BipD (Fig 3.6, 3.8). We did not find any specific binders for BPSL1549. The specificity two clones from BPSL2748 (B5 and B8) was tested by sandwich ELISA, and it was found to be antigen concentration dependent, (Fig 3.7). Two clones from the BPSL2748 selection, two clones from BopE (E2 and G3) and the one clone (B3) from the BipD selection were sequenced (Table 3.4).

| | BPSL1549 | BPSL2748 | BipD | BopE | Conc. of Antigen µg/ ml |
|---------|-------------------|-------------------|-------------------|-------------------|-------------------------|
| Round 1 | 9.6×10^5 | 9.6×10^5 | 1.1×10^5 | 2.2×10^6 | 20 |
| Round 2 | 4.4×10^5 | 3.8×10^5 | 1×10^6 | 2×10^6 | 10 |
| Round 3 | 4.4×10^8 | 3.3×10^8 | $> 10^9$ | $> 10^9$ | 5 |

Table 3.3: Phage titers from panning experiments using streptavidin beads

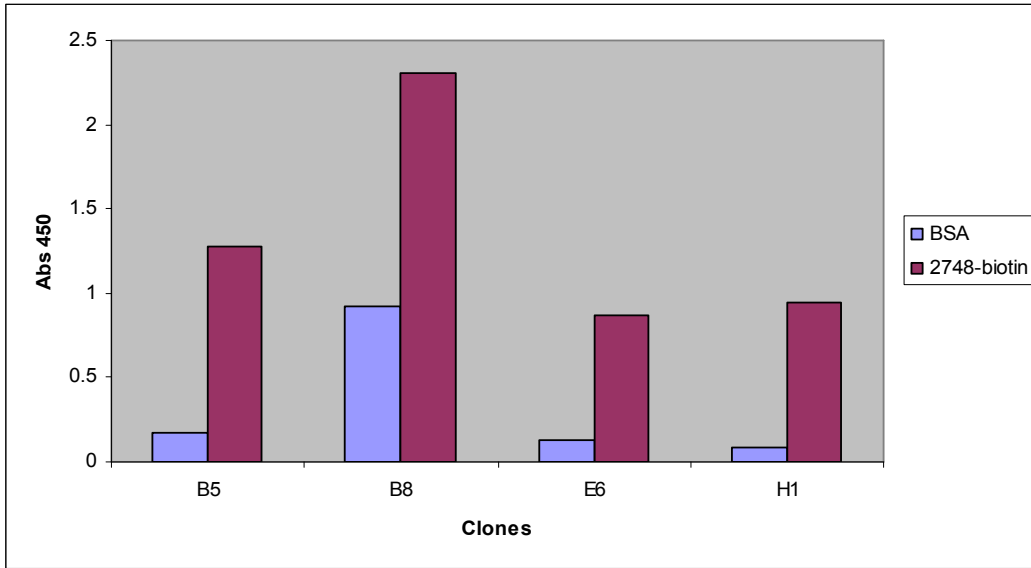


Figure 3.6: Monoclonal phage ELISA results for BPSL2748 clones isolated from panning experiments exhibiting >2-fold ELISA signal over control BSA.

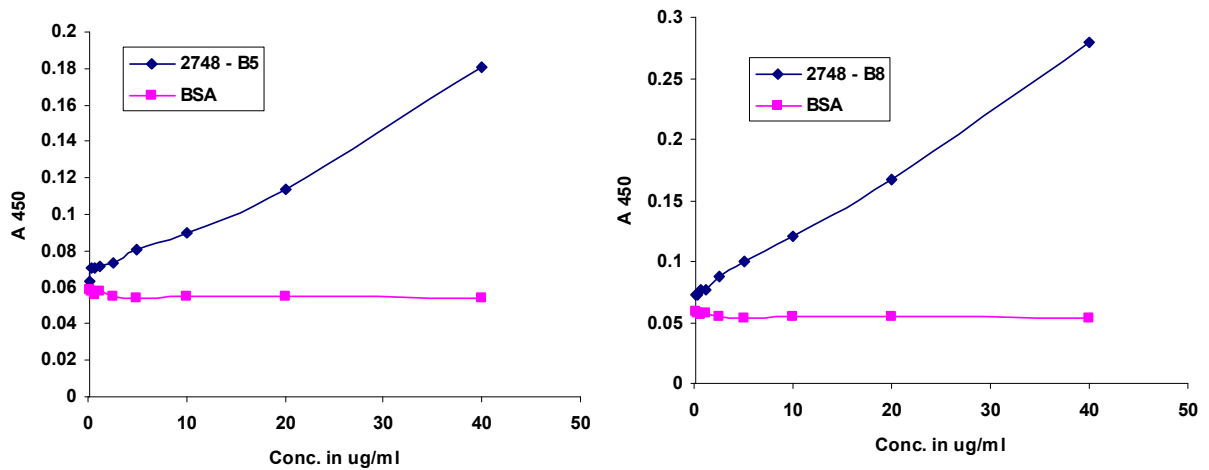


Figure 3.7: Sandwich ELISA for BPSL 2748 clones B5 AND B8
 Phage antibodies were incubated with serial dilution of BPSL 2748 protein, and specific binding was detected by anti-His antibody. BSA was used as control.

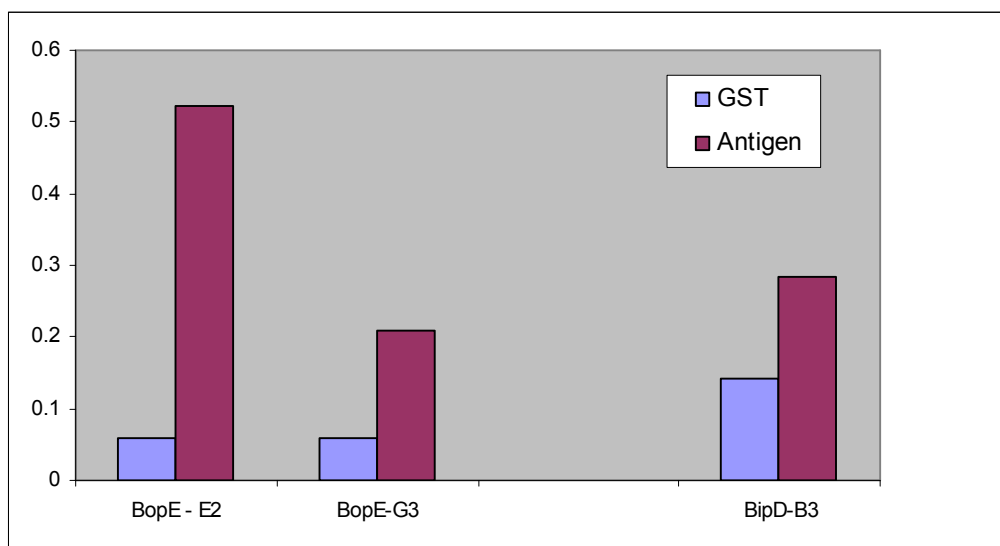


Figure 3.8: Monoclonal phage ELISA for two clones from BopE (E2 & G3) and one BipD clone (B3) exhibiting ELISA signal over control GST protein.

| | CDRH1 | CDRH2 | CDRH3 | CDRL3 |
|-----------------|--------|------------|---|------------|
| Template | FSSSSI | SISSSYGYTY | TVRGSKKPYFSGW~~~~AM | SSYS~~~LI |
| 2748-B5 | LY.YYM | ...PY..S.. | SPA W GHYWG Y APY~~~~.. | G..YGY~P. |
| 2748-B8 | LYY.YM | ...Y..S.S | SSFS.WWG.SHWYHPSY~.L | YV.YSS~.. |
| BimA-C7 | | ..Y..S.S.. | AGHYY~~~~~G. |~~~.. |
| BimA-D3 | IYY.YM | Y.YPY..... | GGYWAYPSAA.~~~~~.I | .Y.HPHPP. |
| BimA-E8 | L.Y.Y. | Y.YP...S.. | AYAPY~~~~~GL | ..SYAGG.. |
| BipD-B3 | LYYY.M | ..Y..... | GAYYPGSWSWFHPSYYW.L | HFAGYWSP. |
| BopE-E2 | | |~~~~~.. | WP.YA~~~.. |
| BopE-G3 | | |~~~~~.. | WVPYWA~.. |
| BopE-H2 | I..... | Y..PYSS... |~~~~~.. | YYSVAWPPF |

Table 3.4: CDR sequences of the clones isolated from the library in comparison with the template used for library construction.

DISCUSSION:

Monoclonal antibodies have achieved an enormous success as therapeutics in recent years for a range of conditions. However, the clinical success has been so far elusive for anti-bacterial antibodies, with major limitation being identification of suitable antigen targets. The advances in antibody engineering have made it possible to develop powerful antibody selection systems and by taking advantage of this technology to develop a high-throughput screening system for a wide array of bacterial antigens should help overcome the initial hurdles for the development of effective ant-bacterial antibodies.

Antibodies can play an important role in both diagnosis and therapeutics of melioidosis and glanders. Though several antigens have been identified as either immunogenic or pathogenic, their role in the pathogenesis of these diseases is not well understood. The aim of this study was to set up a high-throughput screening system for the selections of antibodies that can be investigated for their functionality in either diagnostics or therapeutics.

Here we describe the use of a synthetic antibody library, designed by a minimalist based approach. In this study, specific depletion steps were included in the phage panning steps to eliminate non-specific enrichment of phage. The immobilization of antigens on the immunotubes did not yield any binders for BPSL1549 and BPSL2748 indicating that these might be weak targets for this approach. However, we could isolate antibodies for BPSL2748, by using streptavidin beads approach for panning. The streptavidin beads based approach seems more favorable to isolation of antibodies, as we could isolate antibodies for 3 different antigens. This emphasizes the importance of considering

alternative selection strategies, when a particular selection strategy fails. Overall, the selection experiments were successful, in that specific antibodies were obtained for four out of five antigens from the potential bio-weapon *B. mallei* and *B. pseudomallei*. Sequence analysis of the antibodies generated against four antigens reveal highly unique CDR sequences.

Further characterization of the isolated antibodies will require assessment of their specificity and affinity in the soluble antibody format. In addition, further enrichments for each antigen will be performed and analyzed; and, if necessary, the library may be panned again by including stringent selection steps. Once highly specific antibodies are isolated, they will be tested *in vitro* for their specificity and cross reactivity by either using cell lysates or whole cells of *B. mallei* and *B. pseudomallei*.

This study demonstrates the feasibility of isolating antibodies for a wide-array of antigens through the screening of phage-displayed synthetic antibody libraries. Furthermore, the antigens used in this study were proved suitable for the selection and isolation of antibodies. Future work will focus on selection of antibodies to include antigens associated with virulence, lipopolysaccharides and whole cells.

APPENDIX 1

HIGH-LEVEL PERIPLASMIC EXPRESSION AND PRODUCTION OF AN ANTIBODY FRAGMENT (SCAB) AGAINST ANTHRAX TOXIN IN *Escherichia coli* BY HIGH CELL DENSITY FERMENTATION

INTRODUCTION:

Anthrax is an acute infectious disease that is highly lethal in most forms. It is caused by a Gram-positive bacteria *Bacillus anthracis* that forms highly resistant endospores under hostile conditions. Following the ingestion or inhalation of these spores, bacteria germinate and multiply rapidly within the body. The lethality of the anthrax disease is primarily due to the tripartite toxin released by the bacteria, that is comprised of a protective antigen (PA), edema factor (EF) and lethal factor (LF). The LF and EF exert their toxicity following PA mediated cell entry (185).

Anthrax is one of the first biological weapons to be developed, and continues to be a major threat. After October 2001 attacks with letters carrying anthrax, there have been increased efforts towards developing an effective prophylactic and therapeutic treatment, since antibiotic treatment is effective only for a brief period after exposure to the spores. Efforts have been focused on developing the anti-toxin antibodies, with PA being the major target because of its role in the pathophysiology of anthrax.

Passive immunization with polyclonal antibodies against PA provides protection against challenge with *B.anthraxis*, and antibody titers against PA correlate well with protective immunity (102, 108). Our group previously isolated an affinity-matured

antibody fragment (M18 scFv) against PA following high-throughput screening of large libraries of random mutants (57). To improve the retention of the antibody fragment in circulation we conjugated maleimide-PEG to an engineered cysteine residue at the C-terminus of the M18 scAb. The PEGylated M18 scAb showed prolonged circulation half life and conferred prophylactic protection against heavy challenge with inhalation anthrax spores (106). These results were highly significant because antibody fragments do not contain the Fc domain of IgG and hence are unable to recruit innate immune cells for the killing of the target pathogen. Consequently, protection by the PEGylated antibody fragment arises because of its ability to neutralize the toxin without which the bacteria cannot survive *in vivo*. Moreover, it enables the use of antibody fragments for therapeutics and presents a prospect of cost-effective production of the antibody fragments in bacterial hosts such as *Escherichia coli* (65, 112). If the use of PEGylated antibody fragments were to be employed in the clinic it will be necessary to produce large amounts of scAbs.

E. coli has proven to be an appropriate host for large scale production because the cells can be grown in simple inexpensive media, scale-up is relatively easy due to a short fermentation cycle. Large-scale production of recombinant proteins in *E. coli* has been effectively accomplished by high cell density cultivation (HCDC) technologies that can achieve cell densities higher than OD₆₀₀ of 100. A high volumetric productivity is achieved by the precise control of the growth medium, culture conditions and nutrient feeding strategies.

Carter et al., first reported (21) the production of 1~2 g/L of humanized F(ab)₂ in a 10 L culture. Since then, HCDC of *E. coli* has been used for the production of many

antibody fragments as well as full length IgG. (2, 25, 45, 67, 69, 123, 148, 150, 165). Horn et al. (67) performed fed-batch fermentation for the production of dimeric miniantibodies against EGF-receptor in a 10 L bioreactor, and successfully obtained more than 3 g/L of soluble antibodies, which is the best reported so far.

Single chain antibodies (scAbs) have a human constant Kappa (HuCk) domain connected to the carboxy terminus of a single chain Fv (scFv) and display improved stability and enhanced pharmacokinetic properties in comparison to scFv (18, 59, 60, 112) In spite of its significance, there have been no report of large-scale production of recombinant scAbs in *E.coli*.

In this chapter, we report the use of HCDC for large-scale production of the M18 scAb in *E. coli*. We examined four different cell densities (OD₆₀₀ of 40, 80, 120 and 150) for induction of protein expression and compared the total production yields of scAb and cell growth. We further characterized the solubility and activity of scAb purified from HCDC.

MATERIALS AND METHODS:

Bacterial strains and plasmids:

The bacterial strains used in this study are listed in Table A.1. For cloning purposes *E. coli* Jude 1 [DH10B F': Tn10 (Tet')] was used, whereas *E. coli* XL1-Blue was used for HCDC. The M18 scFv gene was cloned into pMopac16, which expresses a fusion of scFv with the human constant κ light chain to create a single chain antibody

(scAb) (106). The pMopac16 plasmid (59) has an IPTG inducible *lac* promoter and employs the PelB leader peptide for the secretion of scAb into the periplasm of *E. coli*. It also carries the gene for the *skp* chaperone for enhanced soluble expression, and a C-terminal His₆ tag with a single Cysteine residue for easy purification and site-specific PEGylation, respectively (Fig. A.1A).

| Strains | Genotypes | Ref |
|--------------------|---|------------|
| XL1-Blue | <i>recA1 endA1 gyrA96 thi-1 hsdR17 supE44 relA1 lac</i> [F' <i>proAB lacIqZΔM15 Tn10</i> (Tetr)] | Stratagene |
| Jude1 | DH10B F':Tn10 (Tet ^r) | (52) |
| BL21(DE3) | F ⁻ <i>ompT hsdS_B</i> (r _B ⁻ m _B ⁻) <i>gal dcm</i> (DE3) | Novagen |
| Rosetta2 (DE3) | F ⁻ <i>ompT hsdS_B</i> (r _B ⁻ m _B ⁻) <i>gal dcm</i> (DE3) pRARE2 (Cam ^R) | Novagen |
| HMS174 (DE3) | F ⁻ <i>recA1 hsdR</i> (r _{K12} ⁻ m _{K12} ⁺) (DE3) (Rif ^R) | Novagen |
| Rosetta gami (DE3) | F ⁻ <i>ompT hsdS_B</i> (r _B ⁻ m _B ⁻) <i>gal dcm lacY1 ahpC</i> (DE3) <i>gor522::Tn10 trxB</i> pRARE (Cam ^R , Kan ^R , Tet ^R) | Novagen |
| TG1 | Derivative of BL21(DE3), lactose permease (<i>lacY</i>) mutant | Lab stock |
| DH5α | F' Φ80 <i>dlacZ ΔM15 Δ(lacZYA-argF)U169 deoR recA1 endA1 hsdR17</i> (r _K ⁻ m _K ⁺) <i>phoA supE44 λ- thi⁻¹</i> | Lab stock |
| DHF' | DH5α F':Tn10 (Tet ^r) | Lab stock |

Table A 1: List of bacterial strains used in this study.

Shake flask cultivation:

Cells harboring pMoPac16Cys-M18 were cultivated in 125 mL flask containing 20 ml of Terrific broth (TB - Difco) medium supplemented with 100 µg/ml ampicillin (Amp) in a 37°C incubator at 200 rpm. Once the cells reached an OD₆₀₀ of 0.7, the shake flasks were transferred to 25°C for 30 min, and protein expression was induced with 1 mM IPTG. After cultivation for further 4 hr at 25°C, cells were harvested by centrifugation for further expression analysis.

High cell density cultivation³:

For preparative expression, cells were grown in R/2 medium (77) consisting of $(\text{NH}_4)_2\text{HPO}_4$, 2 g; KH_2PO_4 , 6.75 g; citric acid, 0.85 g; $\text{MgSO}_4 \cdot 7\text{H}_2\text{O}$, 0.7 g; trace metal solution [per liter of 5 M HCl: $\text{FeSO}_4 \cdot 7\text{H}_2\text{O}$, 10 g; $\text{ZnSO}_4 \cdot 7\text{H}_2\text{O}$, 2.25 g; $\text{CuSO}_4 \cdot 5\text{H}_2\text{O}$, 1 g; $\text{MnSO}_4 \cdot 5\text{H}_2\text{O}$, 0.5 g; $\text{Na}_2\text{B}_4\text{O}_7 \cdot 10\text{H}_2\text{O}$, 0.23 g; $\text{CaCl}_2 \cdot 2\text{H}_2\text{O}$, 2 g; $(\text{NH}_4)_6\text{MO}_7\text{O}_{24}$, 0.1 g)] per liter with 2% (w/v) glucose. *E.coli* XL1 Blue cells harboring pMopac16-cys M18 was cultured in 1L flasks containing 150 ml of R/2 media with 2% glucose at 37°C at 250 rpm for 6 h, and the culture was used to inoculate the fermentor. Fed-Batch fermentations were conducted in a 3.5 liter Bioflo 300 fermentor (New Brunswick Scientific Co., Edison, NJ) containing 1.5 liter of the same R/2 medium plus 2% (w/v) glucose with 10% (v/v) of inoculum (150 mL). The pH was maintained at 6.8 by the addition of 28% (v/v) ammonium hydroxide. The dissolved oxygen concentration (DOC) was controlled at 40% of air saturation by automatically increasing the agitation speed up to 1,000 rpm and then by changing the pure oxygen (O_2) percentage. Two nutrient feeding solutions were added into the fermentor by a pH-stat feeding strategy. Initially, a defined feeding nutrient solution (700 g of glucose + 20 g of $\text{MgSO}_4 \cdot 7\text{H}_2\text{O}$ per liter) was used in the pre-induction period. When the pH rose to a value greater than its set point (6.8) by 0.08 due to the depletion of glucose, the appropriate volume of feeding solution was automatically added to increase the glucose concentration in the culture broth. A complex feeding solution (500 g of glucose, 100 g of yeast extract and 20 g of $\text{MgSO}_4 \cdot 7\text{H}_2\text{O}$ per liter) was used in the post-induction period similar to above nutrient feeding strategy.

³ HCDC fermentation was performed by Dr. Ki Jun Jeong

The temperature of the culture in the pre-induction period was maintained at 30°C, and was reduced to 25°C for 30 min before inducing with 1 mM IPTG and was maintained at 25°C during the post-induction period. Cell growth was monitored by measuring the optical density (OD) at 600 nm using an Ultrospec 3000 spectrophotometer (Shimadzu, Japan). Culture samples were collected periodically by centrifugation and cell pellets and supernatants were stored at -20°C for further analysis. At the end of fermentation, cells were harvested by centrifugation (6,500 rpm, for 20 min at 4°C) and the cell paste was stored at -20°C for purification of scAb.

Purification of scAb:

For the preparation of the periplasmic fraction by osmotic shock, 2 g of wet cell paste from the fermentation culture was resuspended in 10 ml of Tris-sucrose solution (100 mM Tris (pH 8.0) + 0.75 M sucrose). Lysozyme was then added to a final concentration of 0.5 mg/ml and incubated on the rotator for 20 min at 4°C. Following incubation, 20 ml of 1 mM EDTA solution was added dropwise, and incubated for another 15 min at 4°C. Finally, 1.5 ml of 0.5 M MgCl₂ was added and incubated further for 10 minutes. Spheroplasts were centrifuged at 12,000 rpm, and supernatant periplasmic fractions were stored at 4°C for further purification. To isolate the remaining protein from the soluble fraction, the pellet from the osmotic shock procedure was homogenized in 20 ml of 1x IMAC buffer [100 mM Tris-HCl, 5 M NaCl, 0.2 M imidazole, pH 8.0], and then passed through French press (FA-078A, Thermo Electron Corporation, Waltham, MA) 3 times. Cell lysates were centrifuged at 13,000 rpm for 15

min at 4°C. The clarified supernatant along with the periplasmic fraction isolated from the osmotic shock procedure was further processed for purification of scAb.

Both the periplasmic fraction and soluble fraction from the previous procedure were combined with 1/10 volume of 10x IMAC buffer (100 mM Tris-HCl, 5 M NaCl, 0.2 M imidazole, pH 8.0) and incubated with 2 ml Ni-NTA resin (QIAGEN, Madison, WI) for 1 hour with shaking at 4°C. After washing the resin with 20 ml of 1x IMAC buffer, protein was eluted with 500 mM imidazole in 1x IMAC buffer. The purified M18 scAb was then applied to a Superdex 200 HR 10/30 column (Amersham Biosciences, Piscataway, NJ) on an Akta Fast-protein liquid chromatography (FPLC) system (Amersham Pharmacia, Piscataway, NJ). ScAb containing fractions were collected and quantified using a bicinchoninic acid (BCA) quantification kit (Pierce, Rockford, IL).

Analysis by SDS-PAGE:

For analysis of the production yield and solubility of the expressed scAb, protein samples were analyzed by electrophoresis on a pre-cast 4-20% SDS-PAGE (NuSep, Lawrenceville, GA) gel followed by western blotting. Bands on the western blots were detected by anti-His-HRP conjugated probes with 1:5000 dilutions (Sigma-Aldrich, St. Louis, MO). The band intensities on X-ray film were quantified by Quantity One gel analysis software (Bio-Rad Hercules, CA) with the purified M18 scAb as a standard.

ELISAs:

50 µl of PA83 (List Biological Laboratories) at 1 µg/ml in PBS was used to coat 96 well NUNC maxisorp plates (NUNC, Rochester, NY) overnight at 4°C. BSA at 10

$\mu\text{g/ml}$ was used as a negative control. Wells were blocked with 2% (w/v) milk in PBS for 3 hours at room temp. After washing the wells with PBS, 50 μl of purified M18 scAb with starting concentration of 5 $\mu\text{g/ml}$ was added to the wells in 1: 3 serial dilutions. The plate was placed at room temperature for 2 hours. After washing the wells 3x with PBST (PBS containing 0.05% Tween-20) and once with PBS, 50 μl of goat anti-human Kappa light chain HRP (Sigma-Aldrich) at 1:2500 dilutions were added to the wells and incubated at room temperature for 1 hour. Following washing, 50 μl of *o*-phenylenediamine substrate (Sigma-Aldrich) was added. The plate was kept for 20-30 min for the color to develop. The reaction was stopped by adding 50 μl of 4.5 N H_2SO_4 and absorbance was measured by a microplate reader (Biotek ELx808, Winooski, VT) at 490 nm.

RESULTS:

Selection of host strain for ScAb expression:

The genotypes of different *E.coli* host strains can have a great impact on protein expression levels, even under the same expression plasmid and identical culture conditions (27, 76). Therefore, choosing a suitable host strain for a high-level production of recombinant proteins in HCDC is important. In order to select the best host strain for high-level production of scAbs, we evaluated nine different *E. coli* strains that are preferred for recombinant protein production (Table A.1) in shake flask experiments. Cells were transformed with pMoPac16Cys-M18, grown under identical conditions in TB

medium and the final yield of M18 scAb after 4 hour induction was analyzed by Western blotting. While no significant difference in growth rates were observed, the level of scAb production varied greatly. *E. coli* XL1-Blue, DH5 α and DHF' strains showed higher expression levels (Fig. A.1B). We chose the *E. coli* XL1-Blue strain, since it has been successfully used before for HCDC (77).

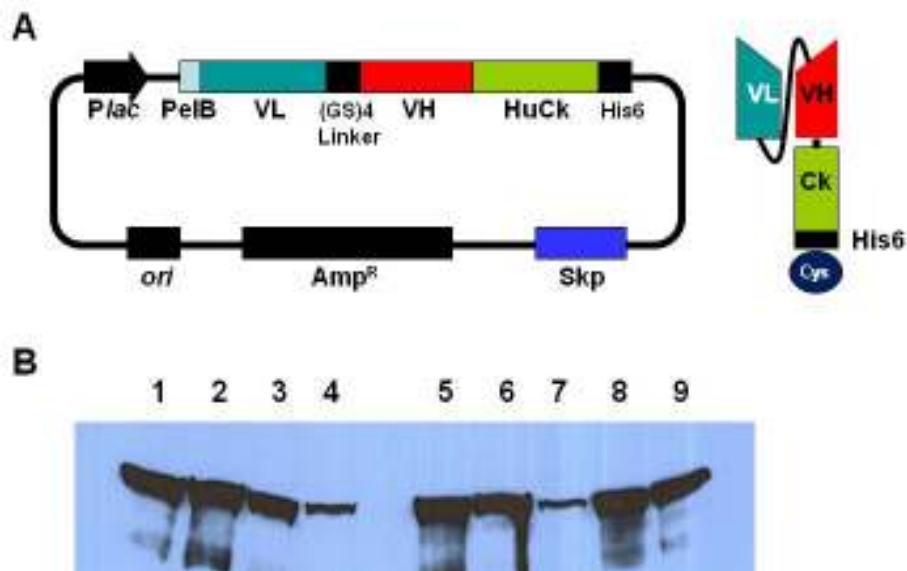


Figure A.1: Expression of M18 scAb in *E. coli*. (A) Schematic diagram of plasmid pMoPac16Cys_M18 and simple structure of scAb. HuCk region is connected to C-terminus of VH region, and His hexamer (His6) and single Cys residue were fused to Ck region for purification and PEGylation, respectively.

(B) Analysis of M18 scAb production from shake flask cultivations of nine *E. coli* strains. Lane 1, Jude1; lane 2, XL1-Blue; lane 3, BL21(DE3); lane 4, TG1; lane 5, DH5 α ; lane 6, Rosetta2(DE3); lane 7, Rosetta gami(DE3); lane 8, DHF'; lane 9, HMS174.

High Cell Density Cultivation with different induction times:

pH-stat fed-batch cultures of *E. coli* XL1-Blue harboring pMoPac16Cys-M18 were carried out as described in Materials and Methods. To examine the effect of induction time on scAb production, cells were induced with 1 mM IPTG at four different cell densities: OD₆₀₀ 40, 80, 120 and 150. During the fermentation, the temperature was maintained at 30°C in the pre induction period and a defined feeding solution (700 g/L of glucose plus 20 g/L of MgSO₄) was supplied in response to changes in the pH. In the post-induction period, the temperature was decreased to 25°C to allow correct folding of the scAb protein in the periplasm, and a yeast extract (100 g/L) mixed feeding solution was supplied for enhancing scAb production and cell growth. Figure A.2 shows the time profiles of cell density (OD₆₀₀) and antibody production yield (mg/L/OD), and data including production yields and cell growth for all runs are summarized in Table A.2.

Following low cell density (OD₆₀₀ of 40) induction, cells exhibited a good growth rate ($\mu=0.122 \text{ h}^{-1}$) and reached an OD₆₀₀ of 110, 10 hrs after induction. Production of scAb was observed immediately after induction and increased for up to 8 hrs (Fig. A.2A). The volumetric yield reached 665 mg per liter at that time point. With the induction at an intermediate cell density (OD₆₀₀ of 80), the cells grew to OD₆₀₀ of 134 in 7 hrs after induction and the final yield was 549 mg per liter (Fig. A.2B). When cells were induced at high cell densities (OD₆₀₀ of 120), they exhibited a considerable reduction in growth rate ($\mu = 0.042 \text{ h}^{-1}$) after induction in comparison to that of pre-induction ($\mu = 0.168 \text{ h}^{-1}$). In this case cell density declined after reaching OD₆₀₀ of 165 at 6 hr after induction (Fig. A.2C), and the production yield was only 378 mg per liter. Induction at another high cell

density (OD₆₀₀ of 150) also showed similar poor cell growth after induction ($\mu = 0.038 \text{ h}^{-1}$) and lower protein production (Fig. A.2D). Interestingly, in all fermentations, scAb protein was not detected in the culture medium during the fermentation (data not shown) which means neither cell lysis nor permeability increases of the outer membrane occurred during HCDC. Even though we used a *lac* promoter, which is known for its leaky expression, (67), we could not find any detectable scAbs during the pre-induction period for any of the fermentations (data not shown).

In two cultures (induction at OD₆₀₀ of 40 and 120), the solubility of M18 scAb produced was compared with end-point samples from both culture. After cell disruption by French press followed by quick centrifugation, the soluble fractions were applied to ELISA to evaluate the amount of active scAb. We found that induction at OD₆₀₀ of 120, resulted in a greater amount of soluble and active antibody fragments (77% of total scAb) compared to that (51% of total scAb) at low cell density (OD₆₀₀ of 40).

| Induction point (OD ₆₀₀) | Max cell density (OD ₆₀₀) | specific growth rate (μ) (hr ⁻¹) | | Max. production Yield (mg/L) | Max. cell specific production (mg/ L/ OD) |
|--------------------------------------|---------------------------------------|--|----------------|------------------------------|---|
| | | Pre-induction | Post-induction | | |
| 40 | 111 | 0.165 | 0.122 | 665 | 6.1 |
| 80 | 134 | 0.146 | 0.081 | 549 | 4.1 |
| 120 | 165 | 0.168 | 0.042 | 378 | 2.3 |
| 150 | 186 | 0.148 | 0.033 | 374 | 2.0 |

Table A.2: Summary of four HCDCs

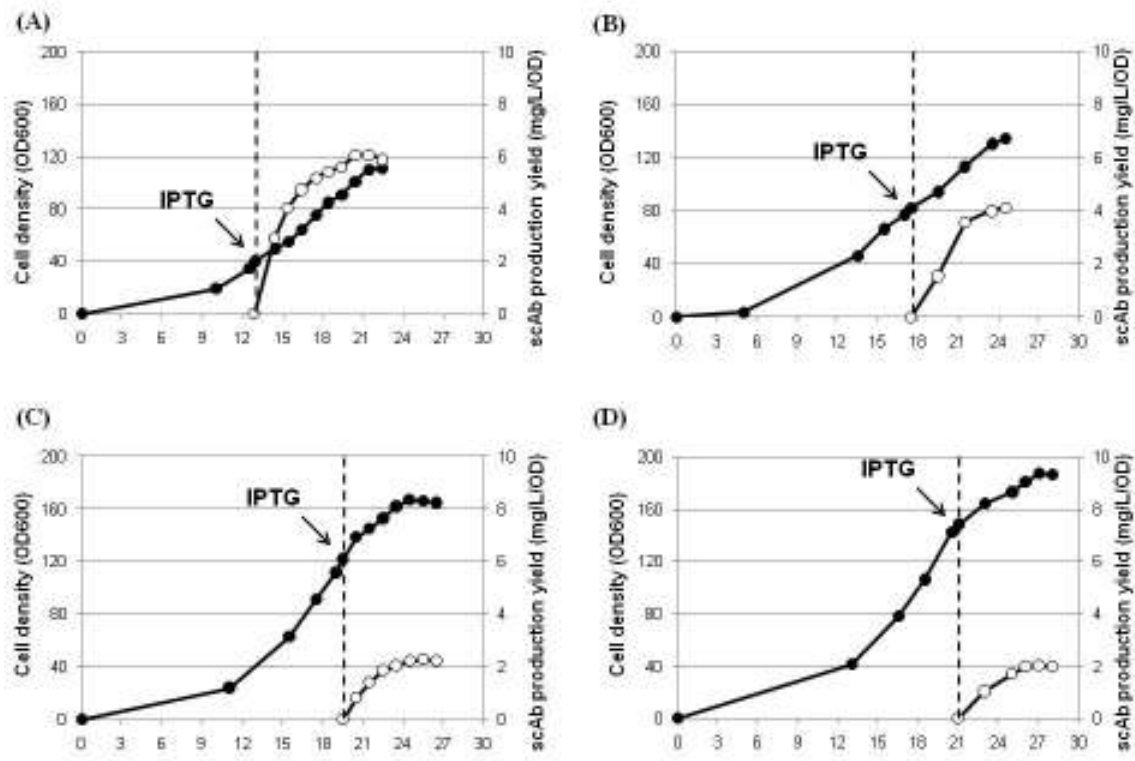


Figure A.2: Time profiles for cell density (●) and cell specific production yield (mg/L/OD) of M18 scAb (○) during HCDC with induction at four different cell densities: (A) OD₆₀₀ of 40; (B) OD₆₀₀ of 80; (C) OD₆₀₀ of 120; (D) OD₆₀₀ of 150. The dashed lines and arrows indicate the time of induction.

Purification and activity assay:

Cells were collected by centrifugation and soluble and periplasmic scAb was purified as described in Materials and Methods section. ScAbs are monomeric proteins but within the periplasm or during purification, a fraction spontaneously dimerizes, resulting in a mixture of monomeric and dimeric fragments (50). The content of monomeric scAb in eluates from Ni-NTA column was about 60%, and could be successfully separated by size exclusion column chromatography (Fig A.3). The activity of the purified scAb was analyzed by ELISA. The ELISA results verified that scAb production via HCDC did not affect the activity of the scAb, and purified scAb is biologically functional (Fig A.4).

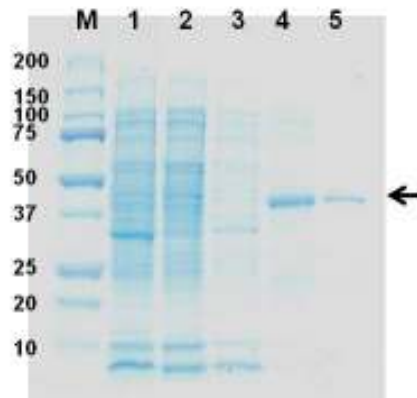


Figure A.3: SDS-PAGE analysis of samples from each purification step. Lane M, molecular mass standards; lane 1, whole cell lysate; lane 2, soluble protein fraction after spheroplast cell disruption; lane 3, periplasmic protein fraction by osmotic shock method; lane 4, eluate from Ni-NTA column ; lane 5, monomeric scAb fraction after size exclusion column . Arrow indicates the band of M18 scAb.

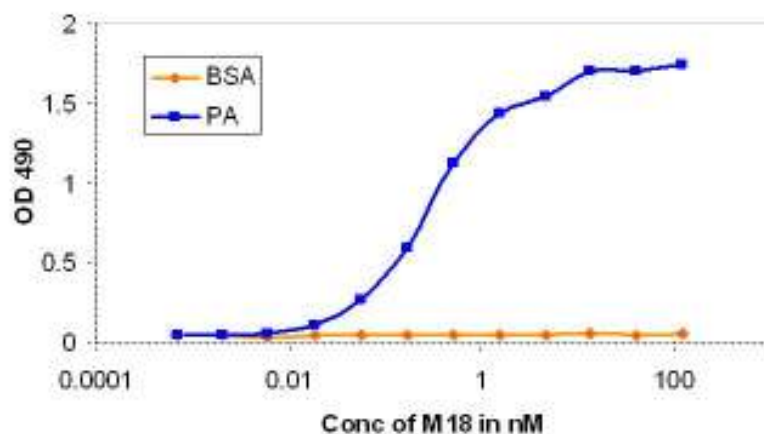


Figure A.4: Analysis of solubility and activity of M18 scAb purified from HCDC. M18 scAb was purified from HCDC cultures and its binding activity to antigen (anthrax toxin PA) was analyzed by ELISA. Bovine serum albumin (BSA) was used as a negative control in ELISA.

DISCUSSION:

HCDC techniques have been widely used for large-scale production of recombinant proteins including antibody fragments in *E. coli* (96, 146). Several factors are important for cost-effective HCDC including the composition of the growth media, the nutrient feeding strategy, oxygen transfer, temperature, and induction (inducer concentration, induction time). The culture temperature is an important factor for proper folding of scAbs as well as other antibody fragments, and generally low temperatures (30 or 25°C) are recommended even though *E. coli* cells grow better at 37°C. In all the fermentations carried out in this study, the temperature was set at 25°C after induction

based on studies with shake flask cultures (data not shown). In fed batch fermentation, cell growth and protein production can also be greatly affected by the feeding solution. However, the optimization of the nutrient feeding strategy in the pre and post induction periods can be labor-intensive and time consuming (177). In this study, as an alternative, we employed a pH-stat feeding strategy, which may not be optimal, but generally results in good protein production and cell growth.

The protein yield is affected by the time of induction (38, 77, 184). In our study, we examined four different cell densities for induction and observed that with an increase in cell density at the induction time point, both volumetric and cell specific production yields decreased inversely (Table A.2). Induction at the lowest cell density (OD_{600} of 40) resulted in the best volumetric and cell specific production yield of M18 scAb, yielding as high as 665 mg/L of total scAb and 6.1 mg/L/OD respectively, which corresponds to approx. 3.5% of total cell protein. Even though the soluble fraction of M18 scAb (51% of total) was lower compared to that observed in fermentations with induction at OD_{600} 120 (77%), the total yield of soluble and active scAb in the former case (337 mg/L) was higher than that of the latter (291 mg/L). Induction at OD_{600} of 40 also showed a much better cell growth rate in the post-induction period compared to other conditions. In the pre-induction period, all cultures showed similar growth rates ($\mu = 0.146 \sim 0.168 \text{ h}^{-1}$), however, in the post-induction period, induction at higher cell densities (OD_{600} of 120 and 150) showed a dramatic decrease in the cell growth rate (75% ~ 78% compared to those of before induction), while induction at OD_{600} 40, resulted in a slower decline (~ 26%). In conclusion, when induction was done at low cell density (early growth phase),

cells were more viable and environments were more favorable to growth and antibody production, and as a result higher amounts of scAbs could be obtained.

The overproduction of antibody fragments such as scFv or Fabs have in some cases resulted in release of the antibodies into the culture by cell lysis. This leads to a decrease in cell densities and therefore, reduced final production yields (45, 150, 151). In the present study, we could not find any detectable protein in the culture supernatant samples by Western blotting.

In summary, HCDC of recombinant M18scAb in *E. coli* was demonstrated to enable large scale production. To the best of our knowledge, this is the first report for large-scale production of scAbs in *E. coli*. Interestingly, highest level production of the M18scAb was achieved by induction at low cell density. In addition, more than 1 g of scAb could be obtained in one fed-batch cultivation of a 1.8 L culture. The information obtained in this study should be useful for the development of HCDC strategies for the efficient production of other antibody fragments including scAbs, as well as other recombinant proteins.

Acknowledgements:

I would like to thank Dr. Ki Jun Jeong (University of Texas -Austin) for conducting the fermentation experiments.

REFERENCES

1. **Aires da Silva, F., S. Corte-Real, and J. Goncalves.** 2008. Recombinant antibodies as therapeutic agents: pathways for modeling new biodrugs. *BioDrugs* **22**:301-314.
2. **Aldor, I. S., D. C. Krawitz, W. Forrest, C. Chen, J. C. Nishihara, J. C. Joly, and K. M. Champion.** 2005. Proteomic Profiling of Recombinant *Escherichia coli* in High-Cell-Density Fermentations for Improved Production of an Antibody Fragment Biopharmaceutical. *Appl. Environ. Microbiol.* **71**:1717-1728.
3. **Angal, S., D. J. King, M. W. Bodmer, A. Turner, A. D. Lawson, G. Roberts, B. Pedley, and J. R. Adair.** 1993. A single amino acid substitution abolishes the heterogeneity of chimeric mouse/human (IgG4) antibody. *Mol Immunol* **30**:105-108.
4. **Azriel-Rosenfeld, R., M. Valensi, and I. Benhar.** 2004. A human synthetic combinatorial library of arrayable single-chain antibodies based on shuffling in vivo formed CDRs into general framework regions. *Journal of molecular biology* **335**:177-192.
5. **Barbas, C. F., 3rd, D. Hu, N. Dunlop, L. Sawyer, D. Cababa, R. M. Hendry, P. L. Nara, and D. R. Burton.** 1994. In vitro evolution of a neutralizing human antibody to human immunodeficiency virus type 1 to enhance affinity and broaden strain cross-reactivity. *Proc Natl Acad Sci U S A* **91**:3809-3813.
6. **Barbas, C. F., 3rd, A. S. Kang, R. A. Lerner, and S. J. Benkovic.** 1991. Assembly of combinatorial antibody libraries on phage surfaces: the gene III site. *Proc Natl Acad Sci U S A* **88**:7978-7982.
7. **Barczak, A. K., and D. T. Hung.** 2009. Productive steps toward an antimicrobial targeting virulence. *Curr Opin Microbiol* **12**:490-496.
8. **Benhar, I.** 2007. Design of synthetic antibody libraries. *Expert Opin Biol Ther* **7**:763-779.
9. **Benhar, I., R. Azriel, L. Nahary, S. Shaky, Y. Berdichevsky, A. Tamarkin, and W. Wels.** 2000. Highly efficient selection of phage antibodies mediated by display of antigen as Lpp-OmpA' fusions on live bacteria. *Journal of molecular biology* **301**:893-904.

10. **Birtalan, S., Y. Zhang, F. A. Fellouse, L. Shao, G. Schaefer, and S. S. Sidhu.** 2008. The intrinsic contributions of tyrosine, serine, glycine and arginine to the affinity and specificity of antibodies. *Journal of molecular biology* **377**:1518-1528.
11. **Bisht, H., A. Roberts, L. Vogel, A. Bukreyev, P. L. Collins, B. R. Murphy, K. Subbarao, and B. Moss.** 2004. Severe acute respiratory syndrome coronavirus spike protein expressed by attenuated vaccinia virus protectively immunizes mice. *Proc Natl Acad Sci U S A* **101**:6641-6646.
12. **Blaise, L., A. Wehnert, M. P. Steukers, T. van den Beucken, H. R. Hoogenboom, and S. E. Hufton.** 2004. Construction and diversification of yeast cell surface displayed libraries by yeast mating: application to the affinity maturation of Fab antibody fragments. *Gene* **342**:211-218.
13. **Boder, E. T., K. S. Midelfort, and K. D. Wittrup.** 2000. Directed evolution of antibody fragments with monovalent femtomolar antigen-binding affinity. *Proc Natl Acad Sci U S A* **97**:10701-10705.
14. **Bondi, S. K., and J. B. Goldberg.** 2008. Strategies toward vaccines against *Burkholderia mallei* and *Burkholderia pseudomallei*. *Expert Rev Vaccines* **7**:1357-1365.
15. **Bosch, B. J., B. E. Martina, R. Van Der Zee, J. Lepault, B. J. Haijema, C. Versluis, A. J. Heck, R. De Groot, A. D. Osterhaus, and P. J. Rottier.** 2004. Severe acute respiratory syndrome coronavirus (SARS-CoV) infection inhibition using spike protein heptad repeat-derived peptides. *Proc Natl Acad Sci U S A* **101**:8455-8460.
16. **Burton, D. R., E. O. Saphire, and P. W. Parren.** 2001. A model for neutralization of viruses based on antibody coating of the virion surface. *Curr Top Microbiol Immunol* **260**:109-143.
17. **Butler, M.** 2005. Animal cell cultures: recent achievements and perspectives in the production of biopharmaceuticals. *Appl Microbiol Biotechnol* **68**:283-291.
18. **Byrne, F. R., S. D. Grant, A. J. Porter, and W. J. Harris.** 1996. Cloning, expression and characterization of a single-chain antibody specific for the herbicide atrazine, p. 19 - 29. vol. 8. Taylor & Francis.
19. **Cadwell, R. C., and G. F. Joyce.** 1992. Randomization of genes by PCR mutagenesis. *PCR Methods Appl* **2**:28-33.
20. **Carmen, S., and L. Jermutus.** 2002. Concepts in antibody phage display. *Brief Funct Genomic Proteomic* **1**:189-203.

21. **Carter, P., R. F. Kelley, M. L. Rodrigues, B. Snedecor, M. Covarrubias, M. D. Velligan, W. L. Wong, A. M. Rowland, C. E. Kotts, M. E. Carver, and et al.** 1992. High level *Escherichia coli* expression and production of a bivalent humanized antibody fragment. *Biotechnology (N Y)* **10**:163-167.
22. **Carter, P. J.** 2006. Potent antibody therapeutics by design. *Nat Rev Immunol* **6**:343-357.
23. **Casadevall, A.** 1998. Antibody-based therapies as anti-infective agents. *Expert Opin Investig Drugs* **7**:307-321.
24. **Charles A Janeway, P. T., Mark Walport, Mark Shlomchik.** 2001. *Immunobiology - The immune system in health and disease.*
25. **Chen, C., B. Snedecor, J. C. Nishihara, J. C. Joly, N. McFarland, D. C. Andersen, J. E. Battersby, and K. M. Champion.** 2004. High-level accumulation of a recombinant antibody fragment in the periplasm of *Escherichia coli* requires a triple-mutant (*degP prc spr*) host strain. *Biotechnol Bioeng* **85**:463-474.
26. **Choy, E. H., B. Hazleman, M. Smith, K. Moss, L. Lisi, D. G. Scott, J. Patel, M. Sopwith, and D. A. Isenberg.** 2002. Efficacy of a novel PEGylated humanized anti-TNF fragment (CDP870) in patients with rheumatoid arthritis: a phase II double-blinded, randomized, dose-escalating trial. *Rheumatology (Oxford)* **41**:1133-1137.
27. **Corisdeo, S., and B. Wang.** 2004. Functional expression and display of an antibody Fab fragment in *Escherichia coli*: study of vector designs and culture conditions. *Protein Expr Purif* **34**:270-279.
28. **Coughlin, M., G. Lou, O. Martinez, S. K. Masterman, O. A. Olsen, A. A. Moksa, M. Farzan, J. S. Babcook, and B. S. Prabhakar.** 2007. Generation and characterization of human monoclonal neutralizing antibodies with distinct binding and sequence features against SARS coronavirus using XenoMouse. *Virology* **361**:93-102.
29. **Czub, M., H. Weingartl, S. Czub, R. He, and J. Cao.** 2005. Evaluation of modified vaccinia virus Ankara based recombinant SARS vaccine in ferrets. *Vaccine* **23**:2273-2279.
30. **Daugherty, P. S.** 2007. Protein engineering with bacterial display. *Curr Opin Struct Biol* **17**:474-480.
31. **Daugherty, P. S., G. Chen, M. J. Olsen, B. L. Iverson, and G. Georgiou.** 1998. Antibody affinity maturation using bacterial surface display. *Protein Eng* **11**:825-832.

32. **de Kruif, J., E. Boel, and T. Logtenberg.** 1995. Selection and application of human single chain Fv antibody fragments from a semi-synthetic phage antibody display library with designed CDR3 regions. *Journal of molecular biology* **248**:97-105.
33. **Dimitrov, A. S.** 2009. *Therapeutic Antibodies*, vol. 525.
34. **Dorvillius, M., V. Garambois, D. Pourquier, M. Gutowski, P. Rouanet, J. C. Mani, M. Pugniere, N. E. Hynes, and A. Pelegrin.** 2002. Targeting of human breast cancer by a bispecific antibody directed against two tumour-associated antigens: ErbB-2 and carcinoembryonic antigen. *Tumour Biol* **23**:337-347.
35. **Du, L., Y. He, Y. Wang, H. Zhang, S. Ma, C. K. Wong, S. H. Wu, F. Ng, J. D. Huang, K. Y. Yuen, S. Jiang, Y. Zhou, and B. J. Zheng.** 2006. Recombinant adeno-associated virus expressing the receptor-binding domain of severe acute respiratory syndrome coronavirus S protein elicits neutralizing antibodies: Implication for developing SARS vaccines. *Virology* **353**:6-16.
36. **Du, L., Y. He, Y. Zhou, S. Liu, B. J. Zheng, and S. Jiang.** 2009. The spike protein of SARS-CoV--a target for vaccine and therapeutic development. *Nat Rev Microbiol* **7**:226-236.
37. **Du, L., G. Zhao, Y. He, Y. Guo, B. J. Zheng, S. Jiang, and Y. Zhou.** 2007. Receptor-binding domain of SARS-CoV spike protein induces long-term protective immunity in an animal model. *Vaccine* **25**:2832-2838.
38. **Durany, O., C. de Mas, and J. L?ez-Sant.** 2005. Fed-batch production of recombinant fuculose-1-phosphate aldolase in *E. coli*. *Process Biochemistry* **40**:707-716.
39. **Edwards, B. M., S. C. Barash, S. H. Main, G. H. Choi, R. Minter, S. Ullrich, E. Williams, L. Du Fou, J. Wilton, V. R. Albert, S. M. Ruben, and T. J. Vaughan.** 2003. The remarkable flexibility of the human antibody repertoire; isolation of over one thousand different antibodies to a single protein, BLYS. *Journal of molecular biology* **334**:103-118.
40. **Felgner, P. L., M. A. Kayala, A. Vigil, C. Burk, R. Nakajima-Sasaki, J. Pablo, D. M. Molina, S. Hirst, J. S. Chew, D. Wang, G. Tan, M. Duffield, R. Yang, J. Neel, N. Chantratita, G. Bancroft, G. Lertmemongkolchai, D. H. Davies, P. Baldi, S. Peacock, and R. W. Titball.** 2009. A Burkholderia pseudomallei protein microarray reveals serodiagnostic and cross-reactive antigens. *Proc Natl Acad Sci U S A* **106**:13499-13504.
41. **Fellouse, F. A., K. Esaki, S. Birtalan, D. Raptis, V. J. Cancasci, A. Koide, P. Jhurani, M. Vasser, C. Wiesmann, A. A. Kossiakoff, S. Koide, and S. S. Sidhu.** 2007. High-throughput generation of synthetic antibodies from highly

- functional minimalist phage-displayed libraries. *Journal of molecular biology* **373**:924-940.
42. **Fellouse, F. A., B. Li, D. M. Compaan, A. A. Peden, S. G. Hymowitz, and S. S. Sidhu.** 2005. Molecular recognition by a binary code. *Journal of molecular biology* **348**:1153-1162.
 43. **Fellouse, F. A., C. Wiesmann, and S. S. Sidhu.** 2004. Synthetic antibodies from a four-amino-acid code: a dominant role for tyrosine in antigen recognition. *Proc Natl Acad Sci U S A* **101**:12467-12472.
 44. **Foote, J., and G. Winter.** 1992. Antibody framework residues affecting the conformation of the hypervariable loops. *Journal of molecular biology* **224**:487-499.
 45. **Forsberg, G., M. Forsgren, M. Jaki, M. Norin, C. Sterky, A. Enhorning, K. Larsson, M. Ericsson, and P. Bjork.** 1997. Identification of Framework Residues in a Secreted Recombinant Antibody Fragment That Control Production Level and Localization in *Escherichia coli*. *J. Biol. Chem.* **272**:12430-12436.
 46. **Francisco, J. A., R. Campbell, B. L. Iverson, and G. Georgiou.** 1993. Production and fluorescence-activated cell sorting of *Escherichia coli* expressing a functional antibody fragment on the external surface. *Proc Natl Acad Sci U S A* **90**:10444-10448.
 47. **Fromant, M., S. Blanquet, and P. Plateau.** 1995. Direct random mutagenesis of gene-sized DNA fragments using polymerase chain reaction. *Anal Biochem* **224**:347-353.
 48. **Fukuda, I., K. Kojoh, N. Tabata, N. Doi, H. Takashima, E. Miyamoto-Sato, and H. Yanagawa.** 2006. In vitro evolution of single-chain antibodies using mRNA display. *Nucleic Acids Res* **34**:e127.
 49. **Godoy, D., G. Randle, A. J. Simpson, D. M. Aanensen, T. L. Pitt, R. Kinoshita, and B. G. Spratt.** 2003. Multilocus sequence typing and evolutionary relationships among the causative agents of melioidosis and glanders, *Burkholderia pseudomallei* and *Burkholderia mallei*. *J Clin Microbiol* **41**:2068-2079.
 50. **Grant, S. D., A. J. Porter, and W. J. Harris.** 1999. Comparative Sensitivity of Immunoassays for Haptens Using Monomeric and Dimeric Antibody Fragments, p. 340-345. vol. 47.
 51. **Greenough, T. C., G. J. Babcock, A. Roberts, H. J. Hernandez, W. D. Thomas, Jr., J. A. Coccia, R. F. Graziano, M. Srinivasan, I. Lowy, R. W. Finberg, K. Subbarao, L. Vogel, M. Somasundaran, K. Luzuriaga, J. L.**

- Sullivan, and D. M. Ambrosino.** 2005. Development and characterization of a severe acute respiratory syndrome-associated coronavirus-neutralizing human monoclonal antibody that provides effective immunoprophylaxis in mice. *J Infect Dis* **191**:507-514.
52. **Griswold, K. E., Y. Kawarasaki, N. Ghoneim, S. J. Benkovic, B. L. Iverson, and G. Georgiou.** 2005. Evolution of highly active enzymes by homology-independent recombination. *Proc Natl Acad Sci U S A* **102**:10082-10087.
53. **Haab, B. B.** 2005. Antibody arrays in cancer research. *Mol Cell Proteomics* **4**:377-383.
54. **Han, D. P., A. Penn-Nicholson, and M. W. Cho.** 2006. Identification of critical determinants on ACE2 for SARS-CoV entry and development of a potent entry inhibitor. *Virology* **350**:15-25.
55. **Hanes, J., L. Jermutus, S. Weber-Bornhauser, H. R. Bosshard, and A. Pluckthun.** 1998. Ribosome display efficiently selects and evolves high-affinity antibodies in vitro from immune libraries. *Proc Natl Acad Sci U S A* **95**:14130-14135.
56. **Harding, S. V., M. Sarkar-Tyson, S. J. Smither, T. P. Atkins, P. C. Oyston, K. A. Brown, Y. Liu, R. Wait, and R. W. Titball.** 2007. The identification of surface proteins of *Burkholderia pseudomallei*. *Vaccine* **25**:2664-2672.
57. **Harvey, B. R., G. Georgiou, A. Hayhurst, K. J. Jeong, B. L. Iverson, and G. K. Rogers.** 2004. Anchored periplasmic expression, a versatile technology for the isolation of high-affinity antibodies from *Escherichia coli*-expressed libraries. *Proc Natl Acad Sci U S A* **101**:9193-9198.
58. **Harvey, B. R., A. B. Shanafelt, I. Baburina, R. Hui, S. Vitone, B. L. Iverson, and G. Georgiou.** 2006. Engineering of recombinant antibody fragments to methamphetamine by anchored periplasmic expression. *J Immunol Methods* **308**:43-52.
59. **Hayhurst, A.** 2000. Improved Expression Characteristics of Single-Chain Fv Fragments When Fused Downstream of the *Escherichia coli* Maltose-Binding Protein or Upstream of a Single Immunoglobulin-Constant Domain. *Protein Expression and Purification* **18**:1-10.
60. **Hayhurst, A., S. Happe, R. Mabry, Z. Koch, B. L. Iverson, and G. Georgiou.** 2003. Isolation and expression of recombinant antibody fragments to the biological warfare pathogen *Brucella melitensis*. *J Immunol Methods* **276**:185-196.

61. **He, Y., J. Li, S. Heck, S. Lustigman, and S. Jiang.** 2006. Antigenic and immunogenic characterization of recombinant baculovirus-expressed severe acute respiratory syndrome coronavirus spike protein: implication for vaccine design. *J Virol* **80**:5757-5767.
62. **He, Y., Y. Zhou, S. Liu, Z. Kou, W. Li, M. Farzan, and S. Jiang.** 2004. Receptor-binding domain of SARS-CoV spike protein induces highly potent neutralizing antibodies: implication for developing subunit vaccine. *Biochem Biophys Res Commun* **324**:773-781.
63. **Ho, M., T. Schollaardt, M. D. Smith, M. B. Perry, P. J. Brett, W. Chaowagul, and L. E. Bryan.** 1997. Specificity and functional activity of anti-Burkholderia pseudomallei polysaccharide antibodies. *Infect Immun* **65**:3648-3653.
64. **Holden, M. T., R. W. Titball, S. J. Peacock, A. M. Cerdeno-Tarraga, T. Atkins, L. C. Crossman, T. Pitt, C. Churcher, K. Mungall, S. D. Bentley, M. Sebahia, N. R. Thomson, N. Bason, I. R. Beacham, K. Brooks, K. A. Brown, N. F. Brown, G. L. Challis, I. Cherevach, T. Chillingworth, A. Cronin, B. Crossett, P. Davis, D. DeShazer, T. Feltwell, A. Fraser, Z. Hance, H. Hauser, S. Holroyd, K. Jagels, K. E. Keith, M. Maddison, S. Moule, C. Price, M. A. Quail, E. Rabinowitsch, K. Rutherford, M. Sanders, M. Simmonds, S. Songsivilai, K. Stevens, S. Tumapa, M. Vesaratchavest, S. Whitehead, C. Yeats, B. G. Barrell, P. C. Oyston, and J. Parkhill.** 2004. Genomic plasticity of the causative agent of melioidosis, *Burkholderia pseudomallei*. *Proc Natl Acad Sci U S A* **101**:14240-14245.
65. **Holliger, P., and P. J. Hudson.** 2005. Engineered antibody fragments and the rise of single domains. *Nat Biotech* **23**:1126-1136.
66. **Hoogenboom, H. R.** 2005. Selecting and screening recombinant antibody libraries. *Nature biotechnology* **23**:1105-1116.
67. **Horn, U., W. Strittmatter, A. Krebber, U. Knüpfer, M. Kujau, R. Wenderoth, K. Müller, S. Matzku, A. Plückthun, and D. Riesenberger.** 1996. High volumetric yields of functional dimeric miniantibodies in *Escherichia coli*, using an optimized expression vector and high-cell-density fermentation under non-limited growth conditions. *Applied Microbiology and Biotechnology* **46**:524-532.
68. **Hu, H., L. Li, R. Y. Kao, B. Kou, Z. Wang, L. Zhang, H. Zhang, Z. Hao, W. H. Tsui, A. Ni, L. Cui, B. Fan, F. Guo, S. Rao, C. Jiang, Q. Li, M. Sun, W. He, and G. Liu.** 2005. Screening and identification of linear B-cell epitopes and entry-blocking peptide of severe acute respiratory syndrome (SARS)-associated coronavirus using synthetic overlapping peptide library. *J Comb Chem* **7**:648-656.

69. **Humphreys, D. P., B. Carrington, L. C. Bowering, R. Ganesh, M. Sehdev, B. J. Smith, L. M. King, D. G. Reeks, A. Lawson, and A. G. Popplewell.** 2002. A plasmid system for optimization of Fab' production in *Escherichia coli*: importance of balance of heavy chain and light chain synthesis. *Protein Expr Purif* **26**:309-320.
70. **Hwang, W. C., Y. Lin, E. Santelli, J. Sui, L. Jaroszewski, B. Stec, M. Farzan, W. A. Marasco, and R. C. Liddington.** 2006. Structural basis of neutralization by a human anti-severe acute respiratory syndrome spike protein antibody, 80R. *J Biol Chem* **281**:34610-34616.
71. **Idusogie, E. E., L. G. Presta, H. Gazzano-Santoro, K. Totpal, P. Y. Wong, M. Ultsch, Y. G. Meng, and M. G. Mulkerrin.** 2000. Mapping of the C1q binding site on rituxan, a chimeric antibody with a human IgG1 Fc. *J Immunol* **164**:4178-4184.
72. **Idusogie, E. E., P. Y. Wong, L. G. Presta, H. Gazzano-Santoro, K. Totpal, M. Ultsch, and M. G. Mulkerrin.** 2001. Engineered antibodies with increased activity to recruit complement. *J Immunol* **166**:2571-2575.
73. **Inglis, T. J., A. Merritt, G. Chidlow, M. Aravena-Roman, and G. Harnett.** 2005. Comparison of diagnostic laboratory methods for identification of *Burkholderia pseudomallei*. *J Clin Microbiol* **43**:2201-2206.
74. **Inglis, T. J., D. B. Rolim, and Q. Sousa Ade.** 2006. Melioidosis in the Americas. *Am J Trop Med Hyg* **75**:947-954.
75. **Irving, R. A., A. A. Kortt, and P. J. Hudson.** 1996. Affinity maturation of recombinant antibodies using *E. coli* mutator cells. *Immunotechnology* **2**:127-143.
76. **Jeong, K. J., J. H. Choi, W. M. Yoo, K. C. Keum, N. C. Yoo, S. Y. Lee, and M. H. Sung.** 2004. Constitutive production of human leptin by fed-batch culture of recombinant rpoS- *Escherichia coli*. *Protein Expression and Purification* **36**:150-156.
77. **Jeong, K. J., and S. Y. Lee.** 1999. High-level production of human leptin by fed-batch cultivation of recombinant *Escherichia coli* and its purification. *Appl Environ Microbiol* **65**:3027-3032.
78. **Jeong, K. J., M. J. Seo, B. L. Iverson, and G. Georgiou.** 2007. APEX 2-hybrid, a quantitative protein-protein interaction assay for antibody discovery and engineering. *Proc Natl Acad Sci U S A* **104**:8247-8252.

79. **Jermutus, L., A. Honegger, F. Schwesinger, J. Hanes, and A. Pluckthun.** 2001. Tailoring in vitro evolution for protein affinity or stability. *Proc Natl Acad Sci U S A* **98**:75-80.
80. **Jespers, L. S., A. Roberts, S. M. Mahler, G. Winter, and H. R. Hoogenboom.** 1994. Guiding the selection of human antibodies from phage display repertoires to a single epitope of an antigen. *Biotechnology (N Y)* **12**:899-903.
81. **Jirholt, P., M. Ohlin, C. A. Borrebaeck, and E. Soderlind.** 1998. Exploiting sequence space: shuffling in vivo formed complementarity determining regions into a master framework. *Gene* **215**:471-476.
82. **Jones, S. M., J. F. Ellis, P. Russell, K. F. Griffin, and P. C. Oyston.** 2002. Passive protection against *Burkholderia pseudomallei* infection in mice by monoclonal antibodies against capsular polysaccharide, lipopolysaccharide or proteins. *J Med Microbiol* **51**:1055-1062.
83. **Joosten, V., C. Lokman, C. A. Van Den Hondel, and P. J. Punt.** 2003. The production of antibody fragments and antibody fusion proteins by yeasts and filamentous fungi. *Microb Cell Fact* **2**:1.
84. **Jung, S., K. M. Arndt, K. M. Muller, and A. Pluckthun.** 1999. Selectively infective phage (SIP) technology: scope and limitations. *J Immunol Methods* **231**:93-104.
85. **Kaneko, Y., F. Nimmerjahn, and J. V. Ravetch.** 2006. Anti-inflammatory activity of immunoglobulin G resulting from Fc sialylation. *Science* **313**:670-673.
86. **Kenny, D. J., P. Russell, D. Rogers, S. M. Eley, and R. W. Titball.** 1999. In vitro susceptibilities of *Burkholderia mallei* in comparison to those of other pathogenic *Burkholderia* spp. *Antimicrob Agents Chemother* **43**:2773-2775.
87. **Kieke, M. C., B. K. Cho, E. T. Boder, D. M. Kranz, and K. D. Wittrup.** 1997. Isolation of anti-T cell receptor scFv mutants by yeast surface display. *Protein Eng* **10**:1303-1310.
88. **Knappik, A., L. Ge, A. Honegger, P. Pack, M. Fischer, G. Wellenhofer, A. Hoess, J. Wolle, A. Pluckthun, and B. Virnekas.** 2000. Fully synthetic human combinatorial antibody libraries (HuCAL) based on modular consensus frameworks and CDRs randomized with trinucleotides. *Journal of molecular biology* **296**:57-86.
89. **Koide, S., and S. S. Sidhu.** 2009. The importance of being tyrosine: lessons in molecular recognition from minimalist synthetic binding proteins. *ACS Chem Biol* **4**:325-334.

90. **Kortt, A. A., O. Dolezal, B. E. Power, and P. J. Hudson.** 2001. Dimeric and trimeric antibodies: high avidity scFvs for cancer targeting. *Biomol Eng* **18**:95-108.
91. **Krebber, C., S. Spada, D. Desplancq, A. Krebber, L. Ge, and A. Pluckthun.** 1997. Selectively-infective phage (SIP): a mechanistic dissection of a novel in vivo selection for protein-ligand interactions. *Journal of molecular biology* **268**:607-618.
92. **Kuiken, T., R. A. Fouchier, M. Schutten, G. F. Rimmelzwaan, G. van Amerongen, D. van Riel, J. D. Laman, T. de Jong, G. van Doornum, W. Lim, A. E. Ling, P. K. Chan, J. S. Tam, M. C. Zambon, R. Gopal, C. Drosten, S. van der Werf, N. Escriou, J. C. Manuguerra, K. Stohr, J. S. Peiris, and A. D. Osterhaus.** 2003. Newly discovered coronavirus as the primary cause of severe acute respiratory syndrome. *Lancet* **362**:263-270.
93. **Lamminmaki, U., S. Pauperio, A. Westerlund-Karlsson, J. Karvinen, P. L. Virtanen, T. Lovgren, and P. Saviranta.** 1999. Expanding the conformational diversity by random insertions to CDRH2 results in improved anti-estradiol antibodies. *Journal of molecular biology* **291**:589-602.
94. **Lau, Y. L., and J. S. Peiris.** 2005. Pathogenesis of severe acute respiratory syndrome. *Curr Opin Immunol* **17**:404-410.
95. **Lazar, G. A., W. Dang, S. Karki, O. Vafa, J. S. Peng, L. Hyun, C. Chan, H. S. Chung, A. Eivazi, S. C. Yoder, J. Vielmetter, D. F. Carmichael, R. J. Hayes, and B. I. Dahiyat.** 2006. Engineered antibody Fc variants with enhanced effector function. *Proc Natl Acad Sci U S A* **103**:4005-4010.
96. **Lee, S. Y.** 1996. High cell-density culture of *Escherichia coli*. *Trends Biotechnol* **14**:98-105.
97. **Lerner, R. A.** 2006. Manufacturing immunity to disease in a test tube: the magic bullet realized. *Angew Chem Int Ed Engl* **45**:8106-8125.
98. **Li, F., W. Li, M. Farzan, and S. C. Harrison.** 2005. Structure of SARS coronavirus spike receptor-binding domain complexed with receptor. *Science* **309**:1864-1868.
99. **Li, W., M. J. Moore, N. Vasilieva, J. Sui, S. K. Wong, M. A. Berne, M. Somasundaran, J. L. Sullivan, K. Luzuriaga, T. C. Greenough, H. Choe, and M. Farzan.** 2003. Angiotensin-converting enzyme 2 is a functional receptor for the SARS coronavirus. *Nature* **426**:450-454.
100. **Li, W., Z. Shi, M. Yu, W. Ren, C. Smith, J. H. Epstein, H. Wang, G. Cramer, Z. Hu, H. Zhang, J. Zhang, J. McEachern, H. Field, P. Daszak, B.**

- T. Eaton, S. Zhang, and L. F. Wang.** 2005. Bats are natural reservoirs of SARS-like coronaviruses. *Science* **310**:676-679.
101. **Liang, G., Q. Chen, J. Xu, Y. Liu, W. Lim, J. S. Peiris, L. J. Anderson, L. Ruan, H. Li, B. Kan, B. Di, P. Cheng, K. H. Chan, D. D. Erdman, S. Gu, X. Yan, W. Liang, D. Zhou, L. Haynes, S. Duan, X. Zhang, H. Zheng, Y. Gao, S. Tong, D. Li, L. Fang, P. Qin, and W. Xu.** 2004. Laboratory diagnosis of four recent sporadic cases of community-acquired SARS, Guangdong Province, China. *Emerg Infect Dis* **10**:1774-1781.
102. **Little, S. F., B. E. Ivins, P. F. Fellows, and A. M. Friedlander.** 1997. Passive protection by polyclonal antibodies against *Bacillus anthracis* infection in guinea pigs. *Infect Immun* **65**:5171-5175.
103. **Lo, B. K.** 2004. *Antibody Engineering*, vol. 248.
104. **Low, N. M., P. H. Holliger, and G. Winter.** 1996. Mimicking somatic hypermutation: affinity maturation of antibodies displayed on bacteriophage using a bacterial mutator strain. *Journal of molecular biology* **260**:359-368.
105. **Ma, J. K., A. Hiatt, M. Hein, N. D. Vine, F. Wang, P. Stabila, C. van Dolleweerd, K. Mostov, and T. Lehner.** 1995. Generation and assembly of secretory antibodies in plants. *Science* **268**:716-719.
106. **Mabry, R., M. Rani, R. Geiger, G. B. Hubbard, R. Carrion, Jr., K. Brasky, J. L. Patterson, G. Georgiou, and B. L. Iverson.** 2005. Passive protection against anthrax by using a high-affinity antitoxin antibody fragment lacking an Fc region. *Infect Immun* **73**:8362-8368.
107. **Marasco, W. A., and J. Sui.** 2007. The growth and potential of human antiviral monoclonal antibody therapeutics. *Nature biotechnology* **25**:1421-1434.
108. **Marcus, H., R. Danieli, E. Epstein, B. Velan, A. Shafferman, and S. Reuveny.** 2004. Contribution of immunological memory to protective immunity conferred by a *Bacillus anthracis* protective antigen-based vaccine. *Infect Immun* **72**:3471-3477.
109. **Marks, J. D., A. D. Griffiths, M. Malmqvist, T. P. Clackson, J. M. Bye, and G. Winter.** 1992. By-passing immunization: building high affinity human antibodies by chain shuffling. *Biotechnology (N Y)* **10**:779-783.
110. **Marra, M. A., S. J. Jones, C. R. Astell, R. A. Holt, A. Brooks-Wilson, Y. S. Butterfield, J. Khattra, J. K. Asano, S. A. Barber, S. Y. Chan, A. Cloutier, S. M. Coughlin, D. Freeman, N. Girn, O. L. Griffith, S. R. Leach, M. Mayo, H. McDonald, S. B. Montgomery, P. K. Pandoh, A. S. Petrescu, A. G. Robertson, J. E. Schein, A. Siddiqui, D. E. Smailus, J. M. Stott, G. S. Yang,**

- F. Plummer, A. Andonov, H. Artsob, N. Bastien, K. Bernard, T. F. Booth, D. Bowness, M. Czub, M. Drebot, L. Fernando, R. Flick, M. Garbutt, M. Gray, A. Grolla, S. Jones, H. Feldmann, A. Meyers, A. Kabani, Y. Li, S. Normand, U. Stroher, G. A. Tipples, S. Tyler, R. Vogrig, D. Ward, B. Watson, R. C. Brunham, M. Kraiden, M. Petric, D. M. Skowronski, C. Upton, and R. L. Roper.** 2003. The Genome sequence of the SARS-associated coronavirus. *Science* **300**:1399-1404.
111. **Mattheakis, L. C., R. R. Bhatt, and W. J. Dower.** 1994. An in vitro polysome display system for identifying ligands from very large peptide libraries. *Proc Natl Acad Sci U S A* **91**:9022-9026.
112. **Maynard, J. A., C. B. Maassen, S. H. Leppla, K. Brasky, J. L. Patterson, B. L. Iverson, and G. Georgiou.** 2002. Protection against anthrax toxin by recombinant antibody fragments correlates with antigen affinity. *Nature biotechnology* **20**:597-601.
113. **Mazor, Y., T. Van Blarcom, R. Mabry, B. L. Iverson, and G. Georgiou.** 2007. Isolation of engineered, full-length antibodies from libraries expressed in *Escherichia coli*. *Nature biotechnology* **25**:563-565.
114. **McCafferty, J., A. D. Griffiths, G. Winter, and D. J. Chiswell.** 1990. Phage antibodies: filamentous phage displaying antibody variable domains. *Nature* **348**:552-554.
115. **McGuinness, B. T., G. Walter, K. FitzGerald, P. Schuler, W. Mahoney, A. R. Duncan, and H. R. Hoogenboom.** 1996. Phage diabody repertoires for selection of large numbers of bispecific antibody fragments. *Nature biotechnology* **14**:1149-1154.
116. **Naureen, A., M. Saqib, G. Muhammad, M. H. Hussain, and M. N. Asi.** 2007. Comparative evaluation of Rose Bengal plate agglutination test, mallein test, and some conventional serological tests for diagnosis of equine glanders. *J Vet Diagn Invest* **19**:362-367.
117. **Nelson, M., J. L. Prior, M. S. Lever, H. E. Jones, T. P. Atkins, and R. W. Titball.** 2004. Evaluation of lipopolysaccharide and capsular polysaccharide as subunit vaccines against experimental melioidosis. *J Med Microbiol* **53**:1177-1182.
118. **Nie, Y., G. Wang, X. Shi, H. Zhang, Y. Qiu, Z. He, W. Wang, G. Lian, X. Yin, L. Du, L. Ren, J. Wang, X. He, T. Li, H. Deng, and M. Ding.** 2004. Neutralizing antibodies in patients with severe acute respiratory syndrome-associated coronavirus infection. *J Infect Dis* **190**:1119-1126.

119. **Nierman, W. C., D. DeShazer, H. S. Kim, H. Tettelin, K. E. Nelson, T. Feldblyum, R. L. Ulrich, C. M. Ronning, L. M. Brinkac, S. C. Daugherty, T. D. Davidsen, R. T. Deboy, G. Dimitrov, R. J. Dodson, A. S. Durkin, M. L. Gwinn, D. H. Haft, H. Khouri, J. F. Kolonay, R. Madupu, Y. Mohammoud, W. C. Nelson, D. Radune, C. M. Romero, S. Sarria, J. Selengut, C. Shamblin, S. A. Sullivan, O. White, Y. Yu, N. Zafar, L. Zhou, and C. M. Fraser.** 2004. Structural flexibility in the *Burkholderia mallei* genome. *Proc Natl Acad Sci U S A* **101**:14246-14251.
120. **Nissim, A., H. R. Hoogenboom, I. M. Tomlinson, G. Flynn, C. Midgley, D. Lane, and G. Winter.** 1994. Antibody fragments from a 'single pot' phage display library as immunochemical reagents. *Embo J* **13**:692-698.
121. **O'Connell, D., B. Becerril, A. Roy-Burman, M. Daws, and J. D. Marks.** 2002. Phage versus phagemid libraries for generation of human monoclonal antibodies. *Journal of molecular biology* **321**:49-56.
122. **Odegrip, R., D. Coomber, B. Eldridge, R. Hederer, P. A. Kuhlman, C. Ullman, K. FitzGerald, and D. McGregor.** 2004. CIS display: In vitro selection of peptides from libraries of protein-DNA complexes. *Proc Natl Acad Sci U S A* **101**:2806-2810.
123. **Pack, P., M. Kujau, V. Schroeckh, U. Knupfer, R. Wenderoth, D. Riesenberger, and A. Pluckthun.** 1993. Improved Bivalent Miniantibodies, with Identical Avidity as Whole Antibodies, Produced by High Cell Density Fermentation of *Escherichia coli*. *Nat Biotech* **11**:1271-1277.
124. **Pai, J. C., J. N. Sutherland, and J. A. Maynard.** 2009. Progress towards recombinant anti-infective antibodies. *Recent Pat Antiinfect Drug Discov* **4**:1-17.
125. **Peiris, J. S., Y. Guan, and K. Y. Yuen.** 2004. Severe acute respiratory syndrome. *Nat Med* **10**:S88-97.
126. **Pepper, L. R., Y. K. Cho, E. T. Boder, and E. V. Shusta.** 2008. A decade of yeast surface display technology: where are we now? *Comb Chem High Throughput Screen* **11**:127-134.
127. **Perez, P., R. W. Hoffman, S. Shaw, J. A. Bluestone, and D. M. Segal.** 1985. Specific targeting of cytotoxic T cells by anti-T3 linked to anti-target cell antibody. *Nature* **316**:354-356.
128. **Perlman, S., and J. Netland.** 2009. Coronaviruses post-SARS: update on replication and pathogenesis. *Nat Rev Microbiol* **7**:439-450.
129. **Pierson, T. C., Q. Xu, S. Nelson, T. Oliphant, G. E. Nybakken, D. H. Fremont, and M. S. Diamond.** 2007. The stoichiometry of antibody-mediated

- neutralization and enhancement of West Nile virus infection. *Cell Host Microbe* **1**:135-145.
130. **Pini, A., F. Viti, A. Santucci, B. Carnemolla, L. Zardi, P. Neri, and D. Neri.** 1998. Design and use of a phage display library. Human antibodies with subnanomolar affinity against a marker of angiogenesis eluted from a two-dimensional gel. *J Biol Chem* **273**:21769-21776.
 131. **Presta, L. G.** 2005. Selection, design, and engineering of therapeutic antibodies. *J Allergy Clin Immunol* **116**:731-736; quiz 737.
 132. **Ray, K., B. Marteyn, P. J. Sansonetti, and C. M. Tang.** 2009. Life on the inside: the intracellular lifestyle of cytosolic bacteria. *Nat Rev Microbiol* **7**:333-340.
 133. **Reichert, J. M.** 2009, posting date. Probabilities of success for antibody therapeutics. www.landesbioscience.com/journals/mabs/article/9031. [Online.]
 134. **Reichert, J. M., and M. C. Dewitz.** 2006. Anti-infective monoclonal antibodies: perils and promise of development. *Nat Rev Drug Discov* **5**:191-195.
 135. **Reiersen, H., I. Loberli, G. A. Loset, E. Hvattum, B. Simonsen, J. E. Stacy, D. McGregor, K. Fitzgerald, M. Welschof, O. H. Brekke, and O. J. Marvik.** 2005. Covalent antibody display--an in vitro antibody-DNA library selection system. *Nucleic Acids Res* **33**:e10.
 136. **Richard A. Goldsby, T. J. K. a. B. A. O.** Kuby Immunology 4e.
 137. **Riechmann, L., M. Clark, H. Waldmann, and G. Winter.** 1988. Reshaping human antibodies for therapy. *Nature* **332**:323-327.
 138. **Roberts, R. W., and J. W. Szostak.** 1997. RNA-peptide fusions for the in vitro selection of peptides and proteins. *Proc Natl Acad Sci U S A* **94**:12297-12302.
 139. **Roguska, M. A., J. T. Pedersen, C. A. Keddy, A. H. Henry, S. J. Searle, J. M. Lambert, V. S. Goldmacher, W. A. Blattler, A. R. Rees, and B. C. Guild.** 1994. Humanization of murine monoclonal antibodies through variable domain resurfacing. *Proc Natl Acad Sci U S A* **91**:969-973.
 140. **Rota, P. A., M. S. Oberste, S. S. Monroe, W. A. Nix, R. Campagnoli, J. P. Icenogle, S. Penaranda, B. Bankamp, K. Maher, M. H. Chen, S. Tong, A. Tamin, L. Lowe, M. Frace, J. L. DeRisi, Q. Chen, D. Wang, D. D. Erdman, T. C. Peret, C. Burns, T. G. Ksiazek, P. E. Rollin, A. Sanchez, S. Liffick, B. Holloway, J. Limor, K. McCaustland, M. Olsen-Rasmussen, R. Fouchier, S. Gunther, A. D. Osterhaus, C. Drosten, M. A. Pallansch, L. J. Anderson, and**

- W. J. Bellini.** 2003. Characterization of a novel coronavirus associated with severe acute respiratory syndrome. *Science* **300**:1394-1399.
141. **Rothe, A., R. J. Hosse, and B. E. Power.** 2006. In vitro display technologies reveal novel biopharmaceutics. *Faseb J* **20**:1599-1610.
142. **Sazinsky, S. L., R. G. Ott, N. W. Silver, B. Tidor, J. V. Ravetch, and K. D. Wittrup.** 2008. Aglycosylated immunoglobulin G1 variants productively engage activating Fc receptors. *Proc Natl Acad Sci U S A* **105**:20167-20172.
143. **Seo, M. J., K. J. Jeong, C. E. Leysath, A. D. Ellington, B. L. Iverson, and G. Georgiou.** 2009. Engineering antibody fragments to fold in the absence of disulfide bonds. *Protein Sci* **18**:259-267.
144. **Sergeeva, A., M. G. Kolonin, J. J. Mouldrem, R. Pasqualini, and W. Arap.** 2006. Display technologies: application for the discovery of drug and gene delivery agents. *Adv Drug Deliv Rev* **58**:1622-1654.
145. **Shields, R. L., J. Lai, R. Keck, L. Y. O'Connell, K. Hong, Y. G. Meng, S. H. Weikert, and L. G. Presta.** 2002. Lack of fucose on human IgG1 N-linked oligosaccharide improves binding to human FcγRIII and antibody-dependent cellular toxicity. *J Biol Chem* **277**:26733-26740.
146. **Shiloach, J., and R. Fass.** 2005. Growing *E. coli* to high cell density--A historical perspective on method development. *Biotechnology Advances* **23**:345-357.
147. **Sidhu, S. S., and F. A. Fellouse.** 2006. Synthetic therapeutic antibodies. *Nat Chem Biol* **2**:682-688.
148. **Simmons, L. C., D. Reilly, L. Klimowski, T. S. Raju, G. Meng, P. Sims, K. Hong, R. L. Shields, L. A. Damico, P. Rancatore, and D. G. Yansura.** 2002. Expression of full-length immunoglobulins in *Escherichia coli*: rapid and efficient production of aglycosylated antibodies. *J Immunol Methods* **263**:133-147.
149. **Skowronski, D. M., C. Astell, R. C. Brunham, D. E. Low, M. Petric, R. L. Roper, P. J. Talbot, T. Tam, and L. Babiuk.** 2005. Severe acute respiratory syndrome (SARS): a year in review. *Annu Rev Med* **56**:357-381.
150. **Sletta, H., A. Nedal, T. E. V. Aune, H. Hellebust, S. Hakvag, R. Aune, T. E. Ellingsen, S. Valla, and T. Brautaset.** 2004. Broad-Host-Range Plasmid pJB658 Can Be Used for Industrial-Level Production of a Secreted Host-Toxic Single-Chain Antibody Fragment in *Escherichia coli*. *Appl. Environ. Microbiol.* **70**:7033-7039.

151. **Somerville, J. E., Jr., S. C. Goshorn, H. P. Fell, and R. P. Darveau.** 1994. Bacterial aspects associated with the expression of a single-chain antibody fragment in *Escherichia coli*. *Appl Microbiol Biotechnol* **42**:595-603.
152. **Stavenhagen, J. B., S. Gorlatov, N. Tuailon, C. T. Rankin, H. Li, S. Burke, L. Huang, S. Vijh, S. Johnson, E. Bonvini, and S. Koenig.** 2007. Fc optimization of therapeutic antibodies enhances their ability to kill tumor cells in vitro and controls tumor expansion in vivo via low-affinity activating Fcγ receptors. *Cancer Res* **67**:8882-8890.
153. **Stemmer, W. P., A. Cramer, K. D. Ha, T. M. Brennan, and H. L. Heyneker.** 1995. Single-step assembly of a gene and entire plasmid from large numbers of oligodeoxyribonucleotides. *Gene* **164**:49-53.
154. **Stevens, J. M., E. E. Galyov, and M. P. Stevens.** 2006. Actin-dependent movement of bacterial pathogens. *Nat Rev Microbiol* **4**:91-101.
155. **Stevens, J. M., R. L. Ulrich, L. A. Taylor, M. W. Wood, D. Deshazer, M. P. Stevens, and E. E. Galyov.** 2005. Actin-binding proteins from *Burkholderia mallei* and *Burkholderia thailandensis* can functionally compensate for the actin-based motility defect of a *Burkholderia pseudomallei* bimA mutant. *J Bacteriol* **187**:7857-7862.
156. **Stevens, M. P., A. Friebel, L. A. Taylor, M. W. Wood, P. J. Brown, W. D. Hardt, and E. E. Galyov.** 2003. A *Burkholderia pseudomallei* type III secreted protein, BopE, facilitates bacterial invasion of epithelial cells and exhibits guanine nucleotide exchange factor activity. *J Bacteriol* **185**:4992-4996.
157. **Sui, J., D. R. Aird, A. Tamin, A. Murakami, M. Yan, A. Yammanuru, H. Jing, B. Kan, X. Liu, Q. Zhu, Q. A. Yuan, G. P. Adams, W. J. Bellini, J. Xu, L. J. Anderson, and W. A. Marasco.** 2008. Broadening of neutralization activity to directly block a dominant antibody-driven SARS-coronavirus evolution pathway. *PLoS Pathog* **4**:e1000197.
158. **Sui, J., W. Li, A. Murakami, A. Tamin, L. J. Matthews, S. K. Wong, M. J. Moore, A. S. Tallarico, M. Olurinde, H. Choe, L. J. Anderson, W. J. Bellini, M. Farzan, and W. A. Marasco.** 2004. Potent neutralization of severe acute respiratory syndrome (SARS) coronavirus by a human mAb to S1 protein that blocks receptor association. *Proc Natl Acad Sci U S A* **101**:2536-2541.
159. **Sui, J., W. Li, A. Roberts, L. J. Matthews, A. Murakami, L. Vogel, S. K. Wong, K. Subbarao, M. Farzan, and W. A. Marasco.** 2005. Evaluation of human monoclonal antibody 80R for immunoprophylaxis of severe acute respiratory syndrome by an animal study, epitope mapping, and analysis of spike variants. *J Virol* **79**:5900-5906.

160. **Swann, P. G., M. Tolnay, S. Muthukkumar, M. A. Shapiro, B. L. Rellahan, and K. A. Clouse.** 2008. Considerations for the development of therapeutic monoclonal antibodies. *Curr Opin Immunol* **20**:493-499.
161. **Swers, J. S., B. A. Kellogg, and K. D. Wittrup.** 2004. Shuffled antibody libraries created by in vivo homologous recombination and yeast surface display. *Nucleic Acids Res* **32**:e36.
162. **Takahashi, T. T., R. J. Austin, and R. W. Roberts.** 2003. mRNA display: ligand discovery, interaction analysis and beyond. *Trends Biochem Sci* **28**:159-165.
163. **Tao, M. H., and S. L. Morrison.** 1989. Studies of aglycosylated chimeric mouse-human IgG. Role of carbohydrate in the structure and effector functions mediated by the human IgG constant region. *J Immunol* **143**:2595-2601.
164. **Tessier, D. C., D. Y. Thomas, H. E. Khouri, F. Laliberte, and T. Vernet.** 1991. Enhanced secretion from insect cells of a foreign protein fused to the honeybee melittin signal peptide. *Gene* **98**:177-183.
165. **Thiel, M. A., D. J. Coster, C. Mavrangelos, H. Zola, and K. A. Williams.** 2002. An economical 20 litre bench-top fermenter. *Protein Expression and Purification* **26**:14-18.
166. **Tiyawisutsri, R., M. T. Holden, S. Tumapa, S. Rengpipat, S. R. Clarke, S. J. Foster, W. C. Nierman, N. P. Day, and S. J. Peacock.** 2007. Burkholderia Hep_Hag autotransporter (BuHA) proteins elicit a strong antibody response during experimental glanders but not human melioidosis. *BMC Microbiol* **7**:19.
167. **Traggiai, E., S. Becker, K. Subbarao, L. Kolesnikova, Y. Uematsu, M. R. Gismondo, B. R. Murphy, R. Rappuoli, and A. Lanzavecchia.** 2004. An efficient method to make human monoclonal antibodies from memory B cells: potent neutralization of SARS coronavirus. *Nat Med* **10**:871-875.
168. **Trevino, S. R., A. R. Permenter, M. J. England, N. Parthasarathy, P. H. Gibbs, D. M. Waag, and T. C. Chanh.** 2006. Monoclonal antibodies passively protect BALB/c mice against Burkholderia mallei aerosol challenge. *Infect Immun* **74**:1958-1961.
169. **Ulrich Reineke, M. S.** 2009. Epitope mapping protocols, 2 ed, vol. 524.
170. **Vaccaro, C., R. Bawdon, S. Wanjie, R. J. Ober, and E. S. Ward.** 2006. Divergent activities of an engineered antibody in murine and human systems have implications for therapeutic antibodies. *Proc Natl Acad Sci U S A* **103**:18709-18714.

171. **Visiongain.** 2009. Monoclonal Antibody therapeutics 2009-2024.
172. **von Schaewen, A., A. Sturm, J. O'Neill, and M. J. Chrispeels.** 1993. Isolation of a mutant Arabidopsis plant that lacks N-acetyl glucosaminyl transferase I and is unable to synthesize Golgi-modified complex N-linked glycans. *Plant Physiol* **102**:1109-1118.
173. **White, N. J.** 2003. Melioidosis. *Lancet* **361**:1715-1722.
174. **Whitlock, G. C., D. M. Estes, and A. G. Torres.** 2007. Glanders: off to the races with *Burkholderia mallei*. *FEMS Microbiol Lett* **277**:115-122.
175. **WHO,** posting date.
http://www.who.int/csr/sars/country/table2004_04_21/en/index.html. [Online.]
176. **Wiersinga, W. J., T. van der Poll, N. J. White, N. P. Day, and S. J. Peacock.** 2006. Melioidosis: insights into the pathogenicity of *Burkholderia pseudomallei*. *Nat Rev Microbiol* **4**:272-282.
177. **Wong, H. H., Y. C. Kim, S. Y. Lee, and H. N. Chang.** 1998. Effect of post-induction nutrient feeding strategies on the production of bioadhesive protein in *Escherichia coli*. *Biotechnol Bioeng* **60**:271-276.
178. **Wong, S. K., W. Li, M. J. Moore, H. Choe, and M. Farzan.** 2004. A 193-amino acid fragment of the SARS coronavirus S protein efficiently binds angiotensin-converting enzyme 2. *J Biol Chem* **279**:3197-3201.
179. **Wongtrakoongate, P., N. Mongkoldhumrongkul, S. Chaijan, S. Kamchonwongpaisan, and S. Tungpradabkul.** 2007. Comparative proteomic profiles and the potential markers between *Burkholderia pseudomallei* and *Burkholderia thailandensis*. *Mol Cell Probes* **21**:81-91.
180. **Wu, H., D. S. Pfarr, S. Johnson, Y. A. Brewah, R. M. Woods, N. K. Patel, W. I. White, J. F. Young, and P. A. Kiener.** 2007. Development of motavizumab, an ultra-potent antibody for the prevention of respiratory syncytial virus infection in the upper and lower respiratory tract. *Journal of molecular biology* **368**:652-665.
181. **Yan, X., and Z. Xu.** 2006. Ribosome-display technology: applications for directed evolution of functional proteins. *Drug Discov Today* **11**:911-916.
182. **Yang, W. P., K. Green, S. Pinz-Sweeney, A. T. Briones, D. R. Burton, and C. F. Barbas, 3rd.** 1995. CDR walking mutagenesis for the affinity maturation of a potent human anti-HIV-1 antibody into the picomolar range. *Journal of molecular biology* **254**:392-403.

183. **Yang, Z. Y., W. P. Kong, Y. Huang, A. Roberts, B. R. Murphy, K. Subbarao, and G. J. Nabel.** 2004. A DNA vaccine induces SARS coronavirus neutralization and protective immunity in mice. *Nature* **428**:561-564.
184. **Yim, S. C., K. J. Jeong, H. N. Chang, and S. Y. Lee.** 2001. High-level secretory production of human granulocyte-colony stimulating factor by fed-batch culture of recombinant *Escherichia coli*. *Bioprocess and Biosystems Engineering* **24**:249-254.
185. **Young, J. A., and R. J. Collier.** 2007. Anthrax toxin: receptor binding, internalization, pore formation, and translocation. *Annu Rev Biochem* **76**:243-265.
186. **Zhang, C. Y., J. F. Wei, and S. H. He.** 2006. Adaptive evolution of the spike gene of SARS coronavirus: changes in positively selected sites in different epidemic groups. *BMC Microbiol* **6**:88.
187. **Zhao, G. P.** 2007. SARS molecular epidemiology: a Chinese fairy tale of controlling an emerging zoonotic disease in the genomics era. *Philos Trans R Soc Lond B Biol Sci* **362**:1063-1081.
188. **Zheng, B. J., Y. Guan, M. L. Hez, H. Sun, L. Du, Y. Zheng, K. L. Wong, H. Chen, Y. Chen, L. Lu, J. A. Tanner, R. M. Watt, N. Niccolai, A. Bernini, O. Spiga, P. C. Woo, H. F. Kung, K. Y. Yuen, and J. D. Huang.** 2005. Synthetic peptides outside the spike protein heptad repeat regions as potent inhibitors of SARS-associated coronavirus. *Antivir Ther* **10**:393-403.
189. **Zhu, Z., S. Chakraborti, Y. He, A. Roberts, T. Sheahan, X. Xiao, L. E. Hensley, P. Prabakaran, B. Rockx, I. A. Sidorov, D. Corti, L. Vogel, Y. Feng, J. O. Kim, L. F. Wang, R. Baric, A. Lanzavecchia, K. M. Curtis, G. J. Nabel, K. Subbarao, S. Jiang, and D. S. Dimitrov.** 2007. Potent cross-reactive neutralization of SARS coronavirus isolates by human monoclonal antibodies. *Proc Natl Acad Sci U S A* **104**:12123-12128.
190. **Zysk, G., W. D. Splettstosser, and H. Neubauer.** 2000. A review on melioidosis with special respect on molecular and immunological diagnostic techniques. *Clin Lab* **46**:119-130.

VITA

Mridula Rani grew up in Udupi, India where she graduated from St. Cecily's High School in 1990. She then entered Poorna Prajna College (Mangalore University) in Udupi, India, where she graduated in 1995 with the degree of Bachelor of Sciences in Botany, Zoology and Chemistry. In 1995, she joined the Manipal Academy of Higher Education (MAHE), Manipal, India and graduated with Masters in Medical Biochemistry (M.Sc.) in 1998. She then obtained a Post-Graduate Diploma in Nutrition from National Institute of Nutrition, Hyderabad, India in 2000. She worked for Shantha Biotechnics, Hyderabad, India as a researcher from 2000 until she entered the Graduate School of The University of Texas at Austin in the fall of 2003 to pursue a doctoral degree in the Department of Cell and Molecular Biology.

Permanent address: 17, Bima Nagar, Bailoor, Udupi, Karnataka, 576101

This dissertation was typed by Mridula Rani.